Proceedings of the

FLUID AMPLIFICATION SYMPOSIUM

May 1964

Volume III

HARRY DIAMOND LABORATORIES
FORMERLY: DIAMOND ORDNANCE FUZE LABORATORIES
ARMY MATERIEL COMMAND
WASHINGTON 25, D. C.

DISCLAIMER NOTICE

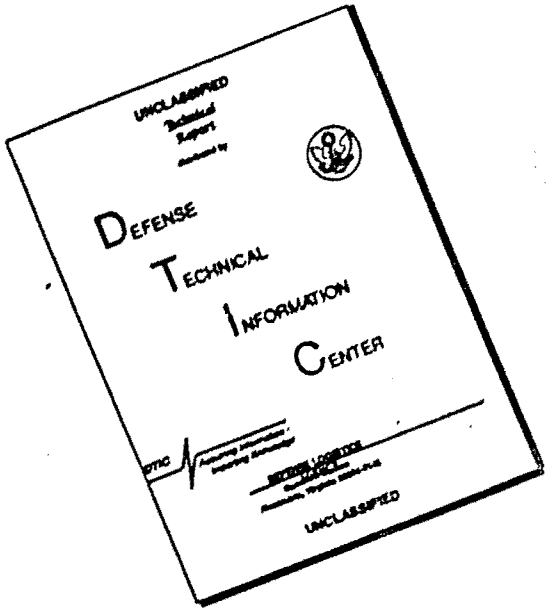

THIS DOCUMENT IS BEST QUALITY AVAILABLE. THE COPY FURNISHED TO DTIC CONTAINED A SIGNIFICANT NUMBER OF PAGES WHICH DO NOT REPRODUCE LEGIBLY.

HARRY DIAMOND LABORATORIES

Milton S. Hochmuth
Lt Col, Ord Corps
Commanding

B. M. Horton
Technical Director

MISSION

The mission of the Harry Diamond Laboratories is:

(1) To perform research and engineering on systems for detecting, locating, and evaluating targets; for accomplishing safing, arming, and munition control functions; and for providing initiation signals: these systems include, but are not limited to, radio and non-radio proximity fuzes, predictor-computer fuzes, electronic timers, electrically initiated fuzes, and related items.

(2) To perform research and engineering in fluid amplification and fluid-actuated control systems.

(3) To perform research and engineering in instrumentation and measurement in support of the above.

(4) To perform research and engineering in order to achieve maximum immunity of systems to adverse influences, including countermeasures, nuclear radiation, battlefield conditions, and high-altitude and space environments.

(5) To perform research and engineering on materials, components, and subsystems in support of above.

(6) To conduct basic research in the physical sciences in support of the above.

(7) To provide consultative services to other Government agencies when requested.

(8) To carry out special projects lying within installation competence upon approval by the Director of Research and Development, Army Materiel Command.

(9) To maintain a high degree of competence in the application of the physical sciences to the solution of military problems.

UNITED STATES ARMY MATERIEL COMMAND
HARRY DIAMOND LABORATORIES
WASHINGTON 25, D.C.

Proceedings of the
FLUID AMPLIFICATION SYMPOSIUM

Sponsored by the Harry
Diamond Laboratories
26, 27, and 28 May 1964

CONTENTS

HARRY DIAMOND LABORATORIES
Washington 25, D. C.

TRANSIENT BEHAVIOR OF BISTABLE FLUID ELEMENTS

By

Jorma R. Keto

Harry Diamond Laboratories

ABSTRACT

A qualitative study was made of the transient behavior of a bistable fluid element when subjected to a suddenly applied input. The correlation of data obtained from pressure transducers and high-speed schlieren photographs shows that the behavior is governed by reflections of pressure waves within pneumatic lines attached to the element. The splitter location, setback, and power jet pressure ratio have relatively minor effect. An oscillator based upon these findings is discussed.

INTRODUCTION

During the evolution of fluid amplification, considerable speculation has been done as to the behavior of bistable elements during switching, little of which has been reported as verified by experimentation.

It is generally believed that switching is caused by a combination of momentum flux and the buildup of static pressure in the separation bubble resulting from the accumulation of mass flow.

High speed schlieren photography coupled with helium injection permit the visualization of the switching phenomenon in detail.

Measurement of the static pressure at several critical points as a function of time synchronized with the photographs show the initiation of a rarefaction wave in the bubble which moves up to the output and is reflected.

These measurements show also that there exist certain conditions under which static pressure buildup in the bubble does not help at all in causing the stream to switch.

2. EXPERIMENTAL PROCEDURE

A conventional element was used in which the setback and splitter position could be varied. Figures 1 and 2 show details of the unit used. Crystal transducers were placed to record variations in pressure in location as follows (fig. 2)

(1) P_{LC} = left control chamber

(2) P_{RC} = right control chamber

(3) P_{LO} = left output

(4) P_{RO} = right output

(5) P_{SBL} = left separation bubble

(6) P_{SBR} = right separation bubble

(7) P_J = power jet chamber

As the work was done in the schlieren system and the transducers had to be mounted through the optical windows, only two were installed. These could be made to cover all positions, two at a time, by rotating the schlieren window. Consequently, the oscilloscope traces included here are the results of a number of separate runs. All runs were made with the left control input essentially "open", that is, with the lowest d-c impedance consistent with the requirements of the input signal generation. The right input d-c impedance was balanced with the left by throttling to obtain equal corresponding aspiration static pressures. The left and right outputs of the elements were fed into transmission lines of predetermined length, which were open to ambient at the distal end.

As the schlieren system does not visualize flow magnitude or direction, a helium tracer was used. Helium was injected into the outlet channels from nozzles in each wall of the splitter. The nozzles (Fig. 3) were 0.005 by 0.032 in. and the helium pressure used was 1 psig; consequently, the total mass flow of helium was very small compared with total mass flow of air in the unit. There was no detectable difference in the behavior of the unit and without the helium. Schlieren high-speed photographs were then taken of the switching of the unit when subjected to (1) a step function and (2) a pulsed pressure input. These photographs were correlated with the pressure measurements.

3. RESULTS

3.1 Step-Function Input

3.1.1 Transient Pressure Measurement

Figures 4 and 5 show pressures recorded during switching of the unit from left to right with a step input. These signals with the exception of the top trace were recorded at a 2 - ms/cm sweep speed and an amplitude of 4.7 psig/cm. The trace labeled Psig shows, to an arbitary amplitude scale, the output of the signal generatorused to switch the unit.

An attempt was made to correct these curves for errors in synchronization and for zero drift, by redrawing the grid, but accuracy can not be assured. The outlet transmission lines used were a total of 27 in. and 11 in., left and right respectively. The same unit was used for both sets of curves, with the splitter location and total overall setback differing as indicated.

The behavior of the output pressure is essentially identical in both sets of curves and is in agreement with that expected from transmission line theory. The behavior of the pressure in other areas can be seen to relate to the left output pressure.

The effect of setback can be seen in the right control pressure P_{RC} and the left separation bubble pressure P_{SBL}. In figure 4, P_{RC} goes negative from the increased aspiration due to the lower pressure of the left separation bubble and the shifting of the flow to the right wall by the control signal. In figure 5, however, P_{RC} goes positive due to the flow being deflected into the control orifice as a result of insufficient setback relative to the left control signal strength. The left separation bubble pressure initially increases in figure 4, but decreases sharply in figure 5. It would appear that the separation bubble pressure is influenced by the rate of expansion of the bubble due to the jet deflection which tends to reduce it and the admission of mass flow into the bubble which tends to increase it.

3.1.2 Schlieren Flash Photographs

The entire switching of the unit (with 12-w splitter position and 1.4-w setback) was covered by individual schlieren microsecond flash photographs of which 12 were picked to illustrate the action. These are reproduced in figure 6a, 6b, and 6c. The schlieren knife edge was vertical and located to the right of the picture. The oscilloscope traces below the picture show (1) left outlet pressure, and (3) time at which photograph was taken. The following analysis was made of the pictures:

A. Unit in stable equilibrium with flow attached to left wall. Air being aspirated into reaction region from right outlet.

B. Inset of signal into left control chamber. Power jet deflected toward right wall, separation bubble enlarging. Helium tracers show no reaction to flow in outlets; outlet transducers show no pressure increase.

C. Separation bubble expanded to maximum, flow "attached" (?) to right wall. Flow decreased in left outlet; flow exhausting from right outlet. Decrease in helium from nozzle in right outlet indicates increase of pressure. Transducers show pressure starting to decrease in left outlet, increase in right.

D. & E. No apparent change in separation bubble or direction of power jet. No appreciable change noted in outlet flows from picture # C. Transducers show pressure plateaus existing over interval of these pictures, negative in left outlet, positive in right.

F. No significant changes noted in separation-bubble region or location of power jet flow from previous pictures or remaining ones. Flow still exhausting from both left and

right outlets but helium flow indicates pressure has decreased in both outlets which is verified by transducers. Outgoing positive pressure wave in right outlet has suffered reflection at open end of transmission line and incoming negative wave has arrived, influencing pressure in both outlets.

G. Schlieren of flow (which has not been influenced by helium between end of splitter and helium nozzle in right outlet) indicates increase of flow extending into right outlet. No incoming flow indicated in left outlet. Left outlet pressure has reached minimum, right outlet at essentially constant pressure from here on.

H. Helium in left outlet indicates very slight outgoing flow, no significant flow change indicated in right outlet from now on. Transducer indicates outgoing negative pressure wave has reached open end of transmission line on left outlet and the reflected positive incoming pressure wave is arriving.

I. Helium shows flow starting to come into ("upstream") left outlet. Pressure transducer shows positive reflection of negative pressure of picture F is arriving. (Helium showed no apparent flow in left outlet during pressure plateau over interval between pictures H and I.)

J. K. & L. Flow appears to have completely switched flow wise in picture J, although pressure reflections continue in left outlet through picture L.

3.1.3. Schlieren High-Speed Motion Pictures

The switching sequence was also covered (for the same settings of the unit as in 3.1.2) by 8000 frame-per-second motion pictures.

During the taking of the pictures, oscillograph traces were made of the signal generator pressure, left outlet pressure, right outlet pressure, and time of each frame. The photo frames were synchronized with the oscilloscopetraces and can be located on these traces as is shown in figure 7. A definite relation of flow change to pressure change is indicated. Sources of error in correspondence can exist due to judgment and to the fact that the pressure transducers were located downstream of the schlieren area.

On a typical set of frames (not shown):

Frame No. 8: Helium in right outlet starts to show disturbance

11: Helium in right outlet shows flow outward

13: Helium in left outlet shows first decrease of flow out

25: Helium in right emerges more readily from probe nozzle indicating lessened backing pressure

28: Left helium starts forming cloud, indicating second lessening of flow out

30: Left helium indicates peak of second decrease of flow

39: Left flow starts to reverse

41: Left flow reversal complete

53: Left flow starts to increase in reverse direction

55: Flow completely switched in unit

3.2 Pulsed Input

The signal generator was adjusted to give a single pulse with about 1 - ms rise time for switching the unit. In this case the splitter was set at 12 w, and setback at 3 w: left and right outlet lines were 19 in. total and 3 in. total, respectively; and no helium was used. Pressures were recorded as shown in figure 8, and the 8000 frame-per second schlieren coverage is shown in figures 9a and 9b.

Notice on figure 8 that the input pulse P_{LC} has decayed before the reflected wave from the left output line P_{LO} has cancelled the negative pressure in the separation region. As a result, the power jet is no longer held to the right wall by the left control momentum, and the jet assumes an undeflected vertical direction. The shifting of the direction of the power jet flow to the left effects the equilibrium downstream in the region of the splitter. The difference in pressure of the right and left outputs is no longer balanced by the radial acceleration of the flow; consequently, a negative pressure wave is sent down the right outlet, and a positive wave down the left outlet. (frame 42) (A change in the momentum gives rise to a pressure change.) A knife-edge oscillation exists momentarily until the arrival of the positive reflection of the initial wave transmitted down the left output.

It is unfortunate that the right separation-region pressure was not recorded for this run. However, if one observes the curvature of flow indicated by frames 32 through 41, a low-pressure region could exist between the flow and the right wall. Frame 32 corresponds to the time when the

initial pressure disturbance (P_{RO}) in the right outlet has ceased, and a temporary equilibrium exists through frame 39 in all pressures except the left control (P_{LC}). Referring back to figure 4 shows that under identical equilibrium conditions, a negative pressure exists in the right separation (P_{SBR}). This pressure is more negative than the right control or the right outlet; therefore, the existence of a separation bubble at the right wall is plausible. If this is so, removal of the left control signal would permit expansion of the right separation bubble with a corresponding shifting of the point of attachment downstream until, as a final limit, attachment is lost and the bubble collapses with a resulting negative wave in the right output.

3.3 Quasi-static Pressure Measurements:

Separation-bubble pressure observations were made to determine if the power jet path, when influenced by a control flow, was dependent upon separation bubble pressure or upon momentum effects. The unit used in this report was set for a total setback of 1.4 w and a splitter position of 12 w. Separation-bubble pressure was observed as dependent upon control pressure for power jet pressures ranging from 1 in. H_2O to 40 psig. In all cases the separation-bubble pressure decreased when the control flow (on the same side as the separation bubble) was increased, whether suddenly or quasi-statically. Furthermore, this was true regardless of the loading of the outlet on the side opposite the separation region. These observations support the explanation in 3.1.1.

3.4 Summary of Results

The above study leads to certain conclusions as to the transient behavior of a specified type of bistable element used with open-ended outlets.

(a) The deflection of the power jet by a control signal is caused by momentum interaction in a region adjacent to the nozzles, rather than by the introduction of mass flow into the separation bubble. The deflection rate would be limited primarily by the rate of change of momentum in the input control signal relative to the power jet momentum.

(b) The deflection of the power jet (change of momentum vector) gives rise to pressure perturbations as determined by the direction of deflection.

(c) Deflection to the right causes an increase of pressure in the right outlet and a decrease of pressure in the left outlet.

(d) The pressure perturbations travel down the outlet channels, which behave as transmission lines.

(e) The change in mass flow in the outlets is determined by the transmission line characteristics and the reflection coefficients at the terminations of the line.*

(f) Final equilibrium flow (steady state) cannot exist until pressure perturbations have equalized. This means that the flow in a bistable element cannot be completely switched until reflected pressure waves have been reduced sufficiently by damping or by impedance matching.

(g) Because of the origination of a reflected wave at the terminal end of the transmission line, the flow of a unit can be switched at its outlet termination before switching is complete at the splitter region.

(h) During switching of a unit, the flow is split and goes into both outlet channels. At this time it is possible for separation bubbles and attachment points to exist on both walls.

(i) Deflection of the jet away from the attachment wall by a control causes expansion of the separation bubble (therefore, a decrease of pressure within the bubble).

(j) The separation bubble on the control signal side must collapse or rupture before the signal is removed if a clean and/or complete switch is desired.**

3.5 Electronic Analog:

The application of transmission line dependence to a bistable amplifier immediately suggests the electronic delay-line oscillator.

---

* The reflection coefficient which is a function of the terminating impedance may be a variable. An example is in the termination of a line by means of a control nozzle of a unit. In this instance a higher control jet impedance is seen with larger power jet flows.

** The bubble can be ruptured by providing a bleed passage at the proximal end of the outlet channel; or it may be collapsed by a reflection from the end of the outlet transmission line. Boundary-layer investigations show that collapse can take place in the dimension normal to the plane of the unit by a folding over due to unsymmetrical flow separation between the top and bottom cover plates of the unit.

Figure 10 is a simplified general circuit diagram of such an oscillator.* If the output and input lines are tuned to resonate at the same frequency, it is referred to as a tuned-plate/ diagonal tuned-grid circuit;however, the oscillator will work as tuned-grid if the input lines control the frequency, or as tuned-plate if the output lines control it. If the lines used for resonance are terminated in an impedance higher than the surge impedance of the line (positive reflection coefficient), it operates as a voltage oscillator with a line length equal to $\frac{2n-1}{4}$ ($n = 1,2,3...$) of a wavelength, λ. This would be the same as a closed organ pipe or a loaded output-line pneumatic oscillator. If, however, the termination impedance is lower than surge impedance (negative reflection coefficient), it will oscillate in a current mode in which the line length is $\frac{n}{2}\lambda$ This would be the case of an open-ended organ pipe.**

3.6 Pneumatic Mass-Flow Oscillator

The tuned-line oscillator used most frequently in pure fluid devices is the one in which the outlets are loaded to raise the terminal impedance. This type of system will oscillate spontaneously due to back pressures sufficient to prevent establishment of a stable attachment point. This oscillator falls in the classification of pressure output.

The other type of tuned-line oscillator possible is the one with a mass-flow output, in which the output lines are not loaded. The advantages of this system are

(1) Fundamental frequency twice that of pressure type, and high mass flow,

(2) Trippered operation.

This device behaves as an ordinary bistable amplifier unit and will only switch from side to side under ordinary use. When first turned on, the flow is stable, remaining attached to one wall unitl switched by a signal. The summary of results (paragraph 3 and 4) implies stable switching if the signal duration is longer than the time required for a reflection to a return. If the signal has a duration so short that the power jet can return to an undeflected position before the reflections have arrived, then the stability of the switch is dependent upon the reflected pressure waves. If the outlet lines are of equal length, and the input pulse duration is equal to the time for the initial output wave front to reach the end of the transmission line, then the phasing of the pressure waves result in resonance, and the system should oscillate.

The development of the oscillations is shown by wave diagrams in figure 11. The top group of diagrams shows the rarefaction wave starting

---

* This circuit may also be called coax-line, tuned-line, or transmission-line oscillator.

** Because the electronic circuit is drawn as push-pull, the true equivalent in acoustics would be two organ pipes face to face sharing a common edge.

at the proximal end of the outlet line through which stable flow exists when a control signal is applied to the same side of the unit. When this wave front has reached the end of the line, L, at a time L/C, the control signal is removed, starting a pressure wave in the outlet line. At this same time, the initial rarefaction is being reflected as a pressure wave from the open terminal end of the line, reducing the mass flow at the end to zero (assuming a perfect reflection). The two pressure waves now travel toward each other, adding as they pass, until time 2L/C when the outgoing pressure wave reaches the terminal end and reflects. At this time full flow is once again established there, and the power jet is being switched by the incoming pressure wave. (While all of this is occurring, similar waves of opposite amplitude are taking place in the other outlet line in proper phase to result in resonance.)

The pressure versus time at points located at distances L/8 and L/2 are constructed at the bottom of figure 11.

3.7 Experimental Mass-Flow Oscillator

The bistable element used in this study was left with splitter at 12 w and setback at 1.4 w and 2 3/8 in. diameter plastic lines approximately 24 in. long were attached to the outputs. The unit could be switched smoothly when the output or control inputs were blocked by hand but blocking by hand could not be used to make the unit go into oscillation. However, when a control pulse of 2 ms was introduced, the unit did go into oscillation. Pressure transducers were installed at approximately the same locations as those used for the pressure-versus-time curves constructed in figure 11. The resulting variations are shown in figure 12.

As an additional check, both outlet lines were then terminated by higher(impedances 2-in. lengths of 1/4-in. diameter plastic tubing). Now when the unit was turned on, spontaneous oscillations occured at half the previous frequency.

4. CONCLUSIONS AND RECOMMENDATIONS FOR FUTURE INVESTIGATION

(1) The decrease of pressure in the bubble on the control side during switching shows conclusively that switching can be caused purely by momentum.

(2) The behavior of a bistable element when switched by means of a fast rise time signal is dependent upon the acoustical characteristics of the associated circuits.

(3) A triggered oscillator with high flow output based upon the above conclusions has been demonstrated.

Further study should be made in determining the effects of variations in reflection coefficients at the input nozzle and at the proximal end of the output (use of bleeds). The effect of distributed resistance (viscous effects) as a limitation upon oscillations is of concern. Combined tuned-grid/tuned-plate oscillators may prove useful in achieving stability under

extreme conditions. New circuits can be developed by the addition of lumped parameters and isolators to transmission line systems (e.g., the square-wave push-pull output of the flow oscillator can be rendered sinusoidal).

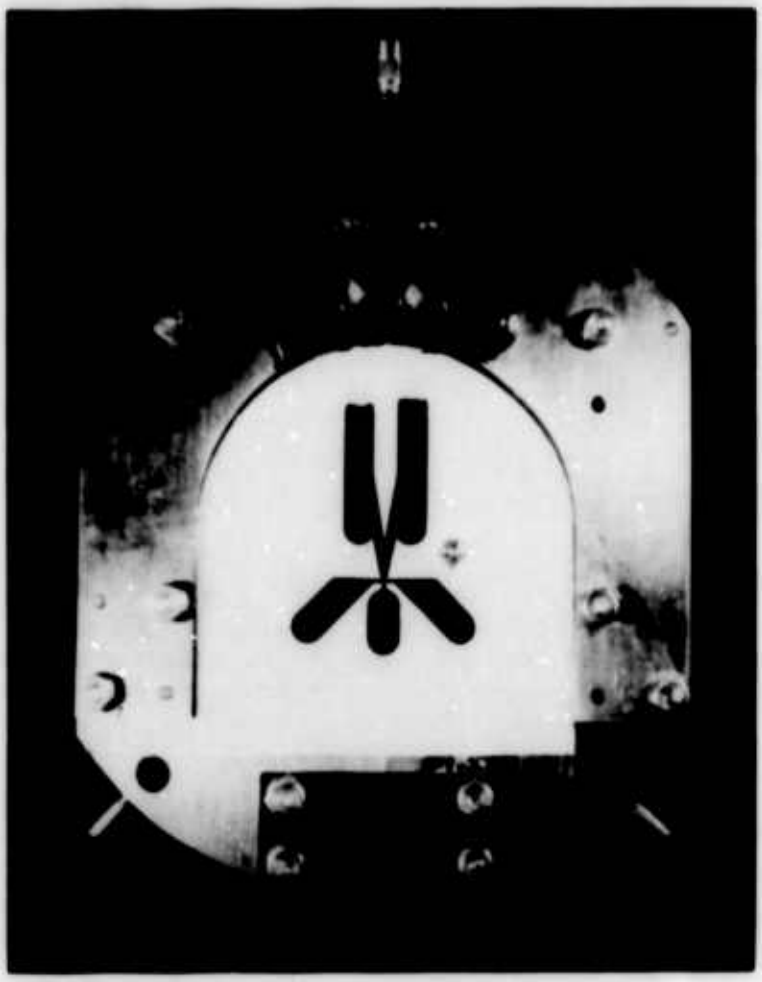

Figure 1. Photograph of test unit (bistable fluid amplifier).

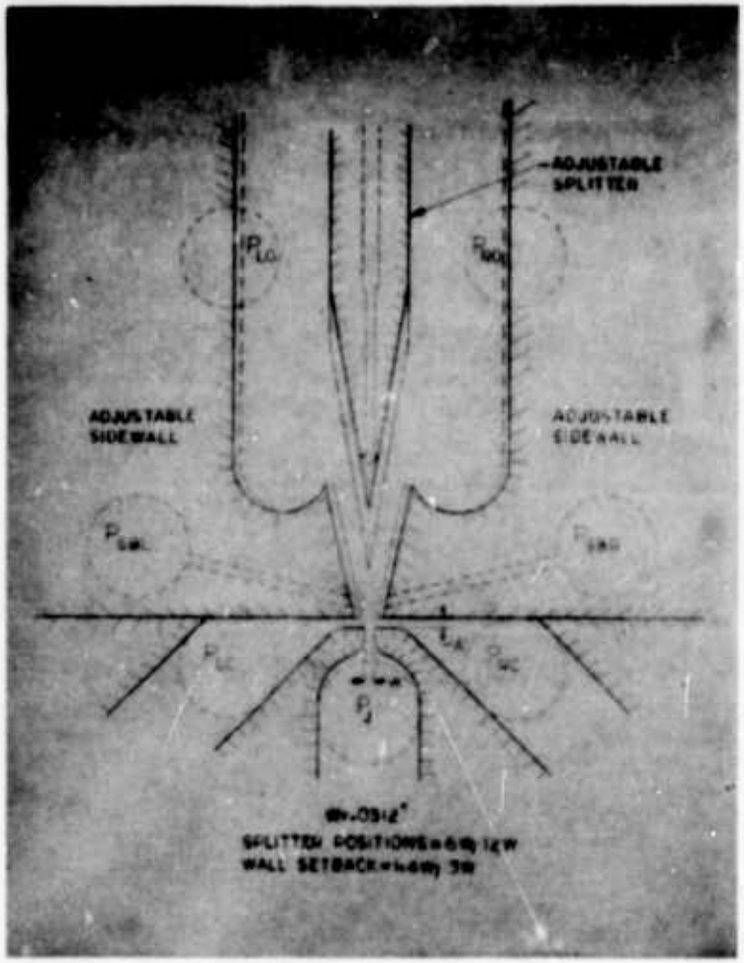

Figure 2. Scale drawing of test unit, identifying locations of pressure transducers.

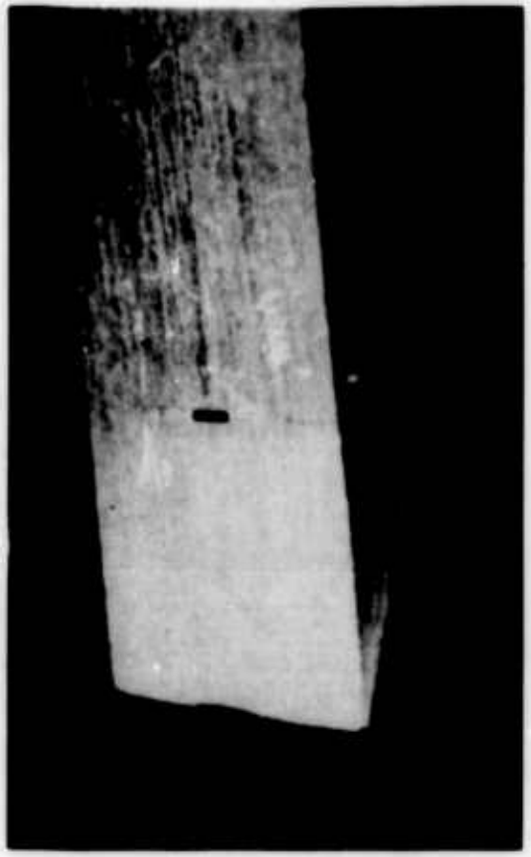

Figure 3. Nozzle in splitter for injecting helium tracer.
(Nozzle cross section, 0.005 x 0.032 in.)

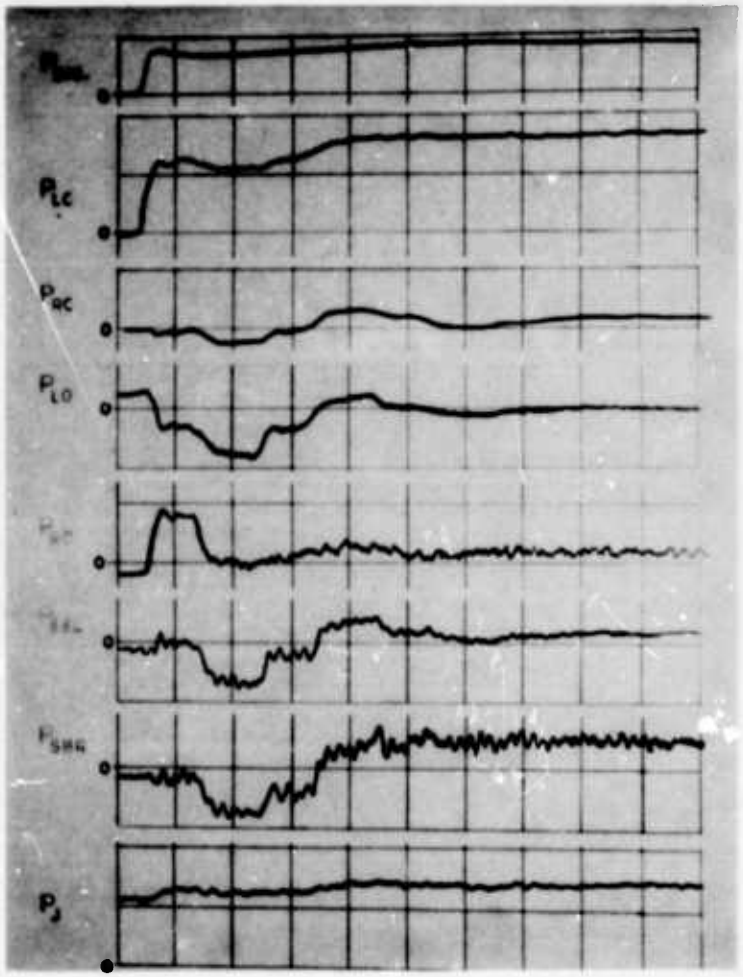

Figure 4. Pressure versus time for unit with 3-w setback, 12-w splitter position. (Pressure = 4.7 psig/div; time = 2 ms/div)

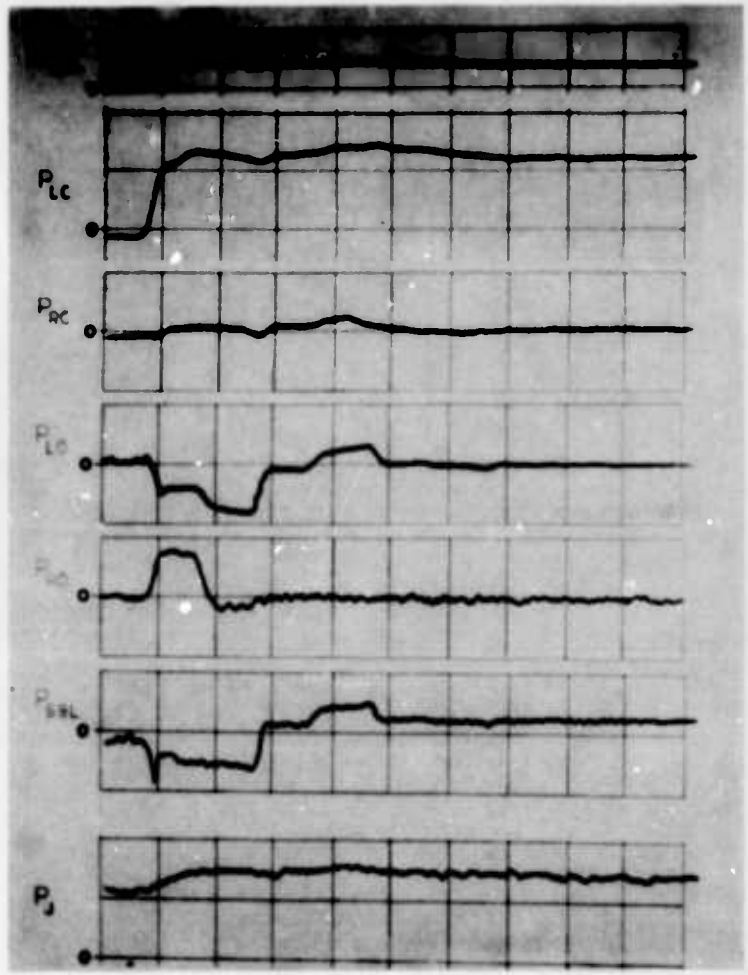

Figure 5. Pressure versus time for unit with 1.4-w setback, 6-w splitter position. (Pressure = 4.7 psig/div; time = 2 ms/div)

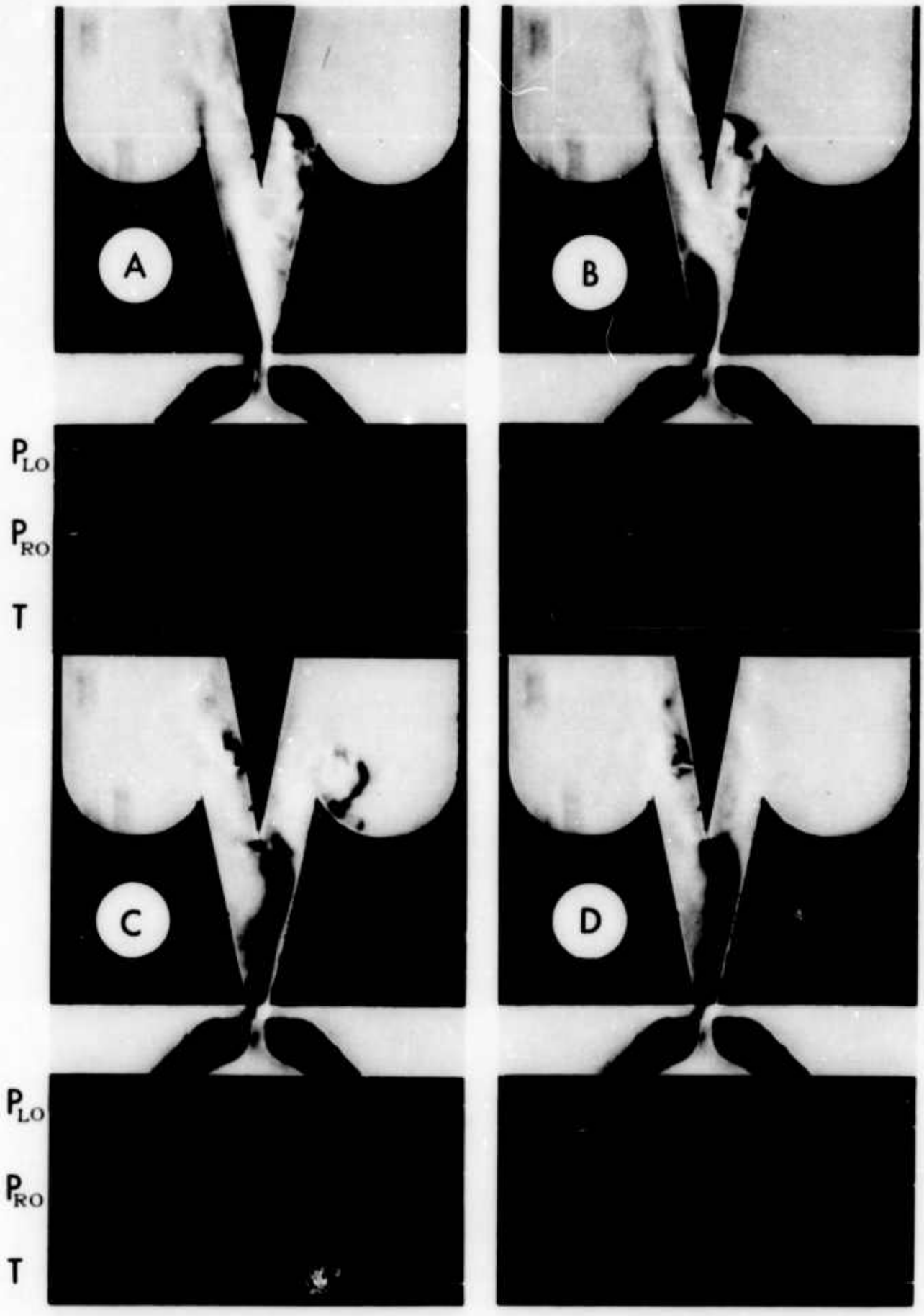

Figure 6a. Schlieren flash photographs showing switching of unit. (Setback = 1.4 w; splitter at 12 w; P_{LO} = left output pressure; P_{RO} = right outlet pressure; T = time of picture)

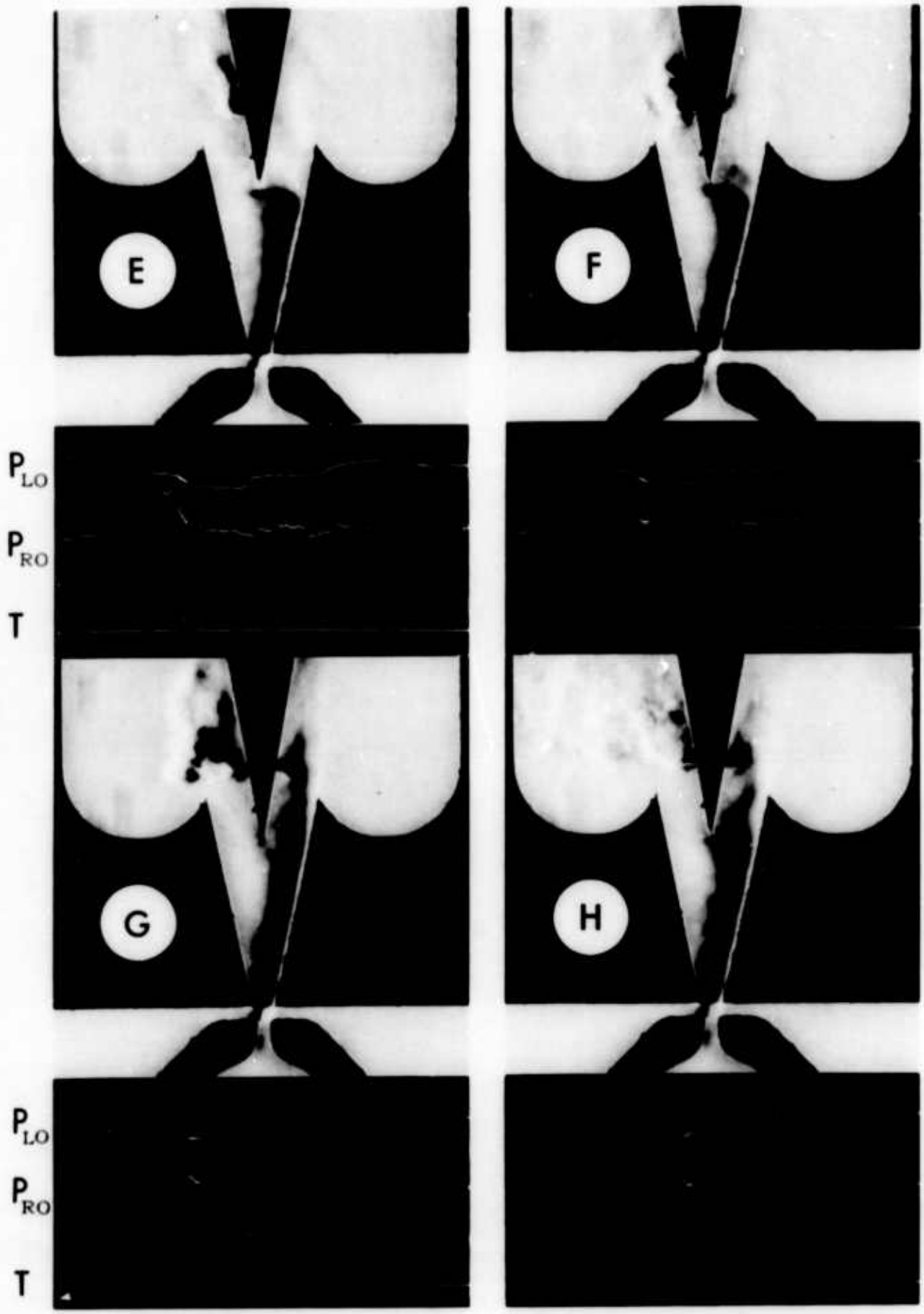

Figure 6b. Schlieren flash photographs showing switching of unit. (Setback = 1.4 w; splitter at 12 w; P_{LO} = left output pressure; P_{RO} = right outlet pressure; T = time of picture)

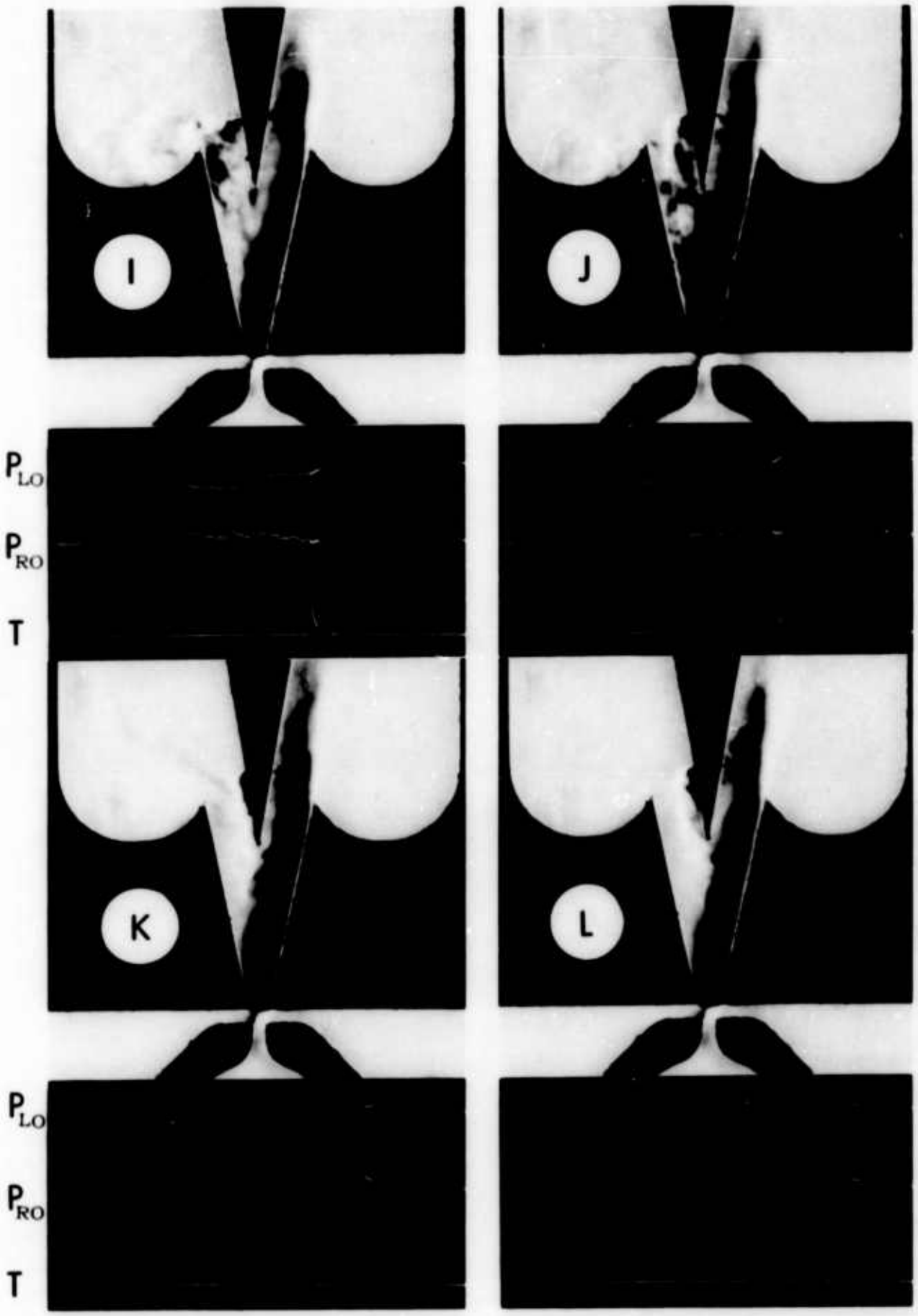

Figure 6c. Schlieren flash photographs showing switching of unit. (Setback = 1.4 w; splitter at 12 w; P_{LO} = left output pressure; P_{RO} = right outlet pressure; T = time of picture)

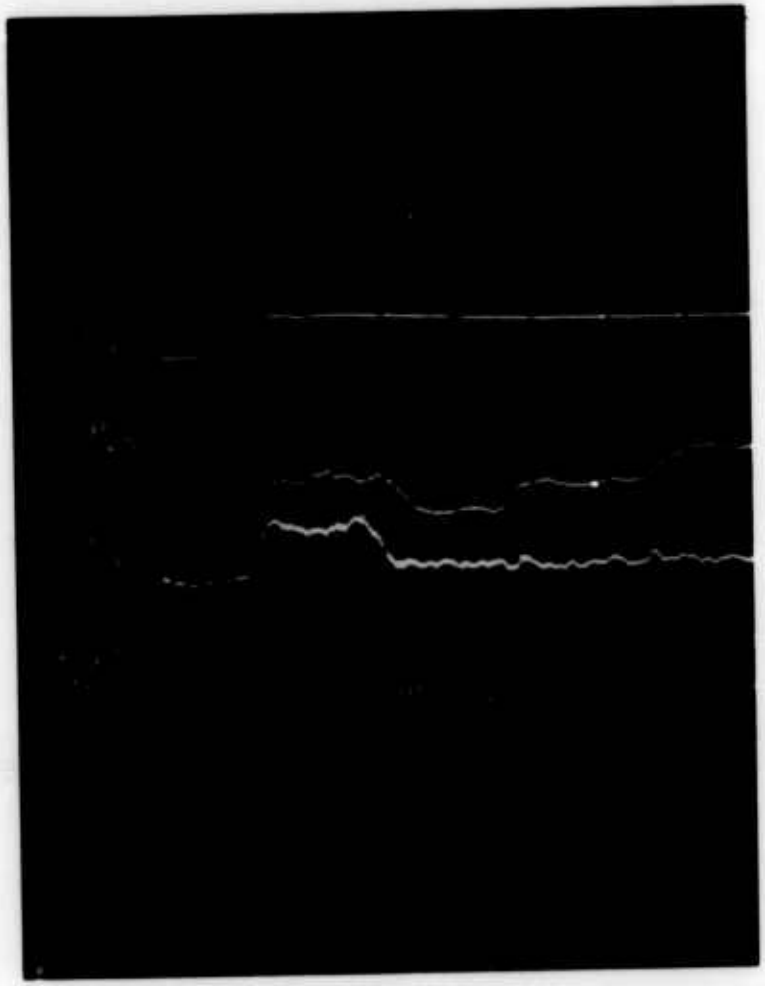

Figure 7. Correlation of pressure and high-speed schlieren movies during switching. (setback = 1.4 w; splitter at 12 w)

Figure 8. Pressure versus time for pulsed input to unit. (Setback = 3 w; splitter at 12 w)

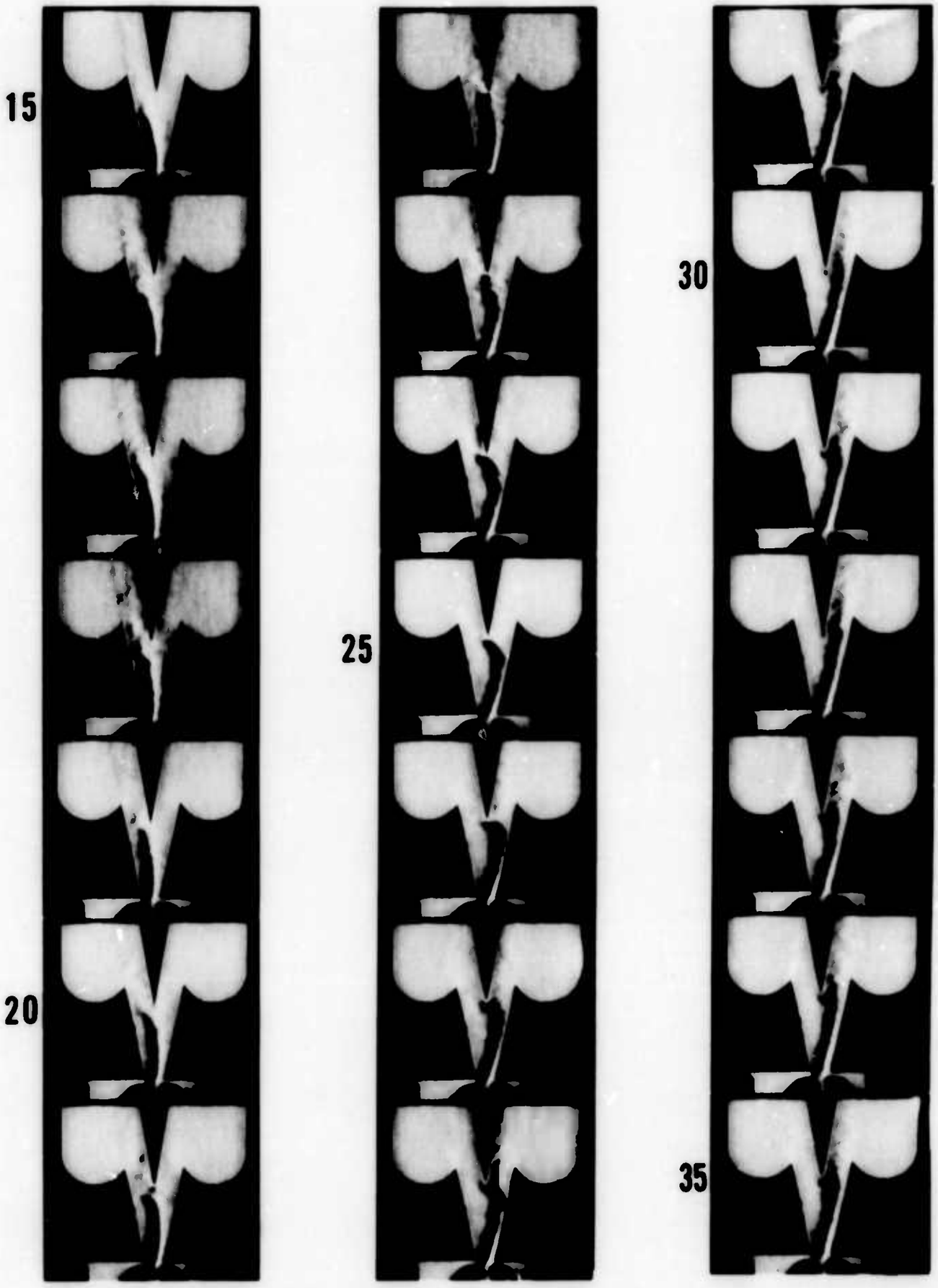

Figure 9a. High speed schlieren motion pictures of unit in figure 8. (Taken at 8000 pictures per second)

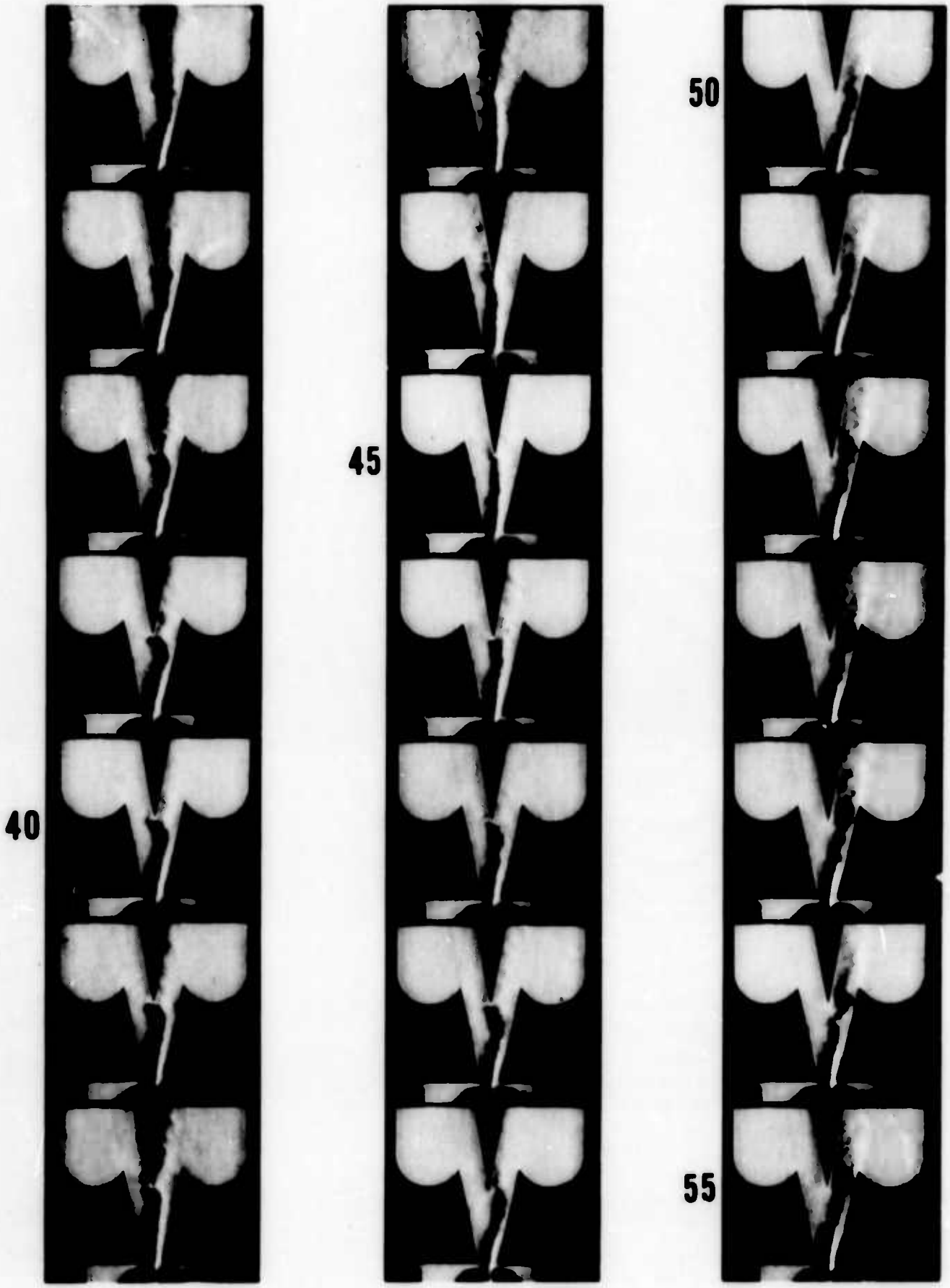

Figure 9b. High speed schlieren motion pictures of unit in figure 8. (Taken at 8000 pictures per second)

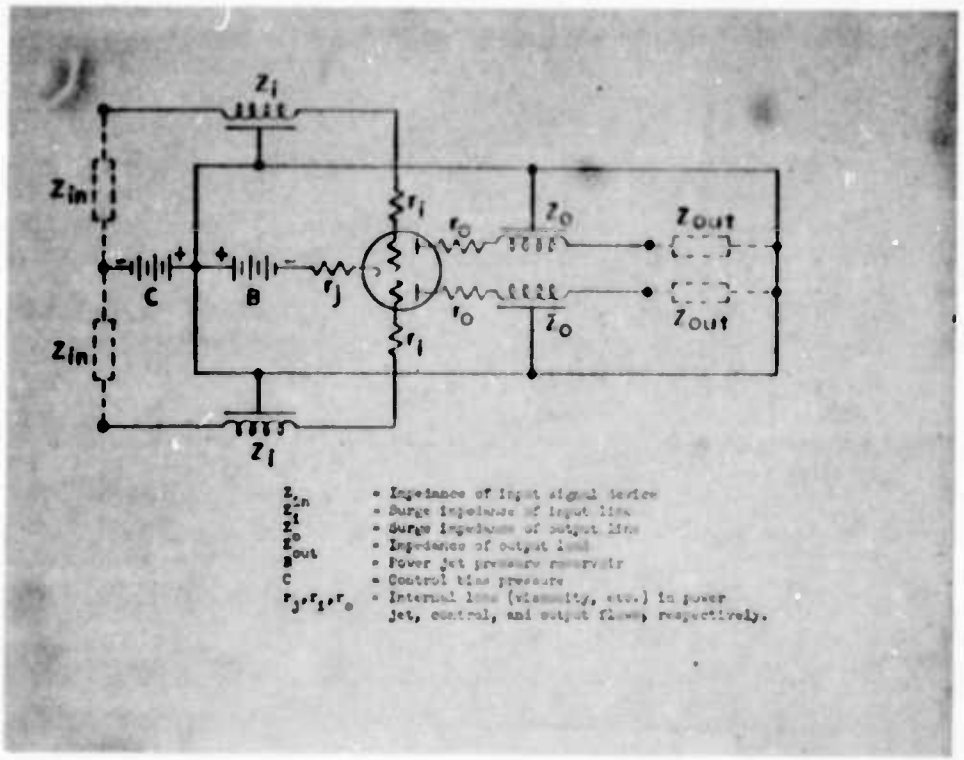

Figure 10. Delay line oscillator.

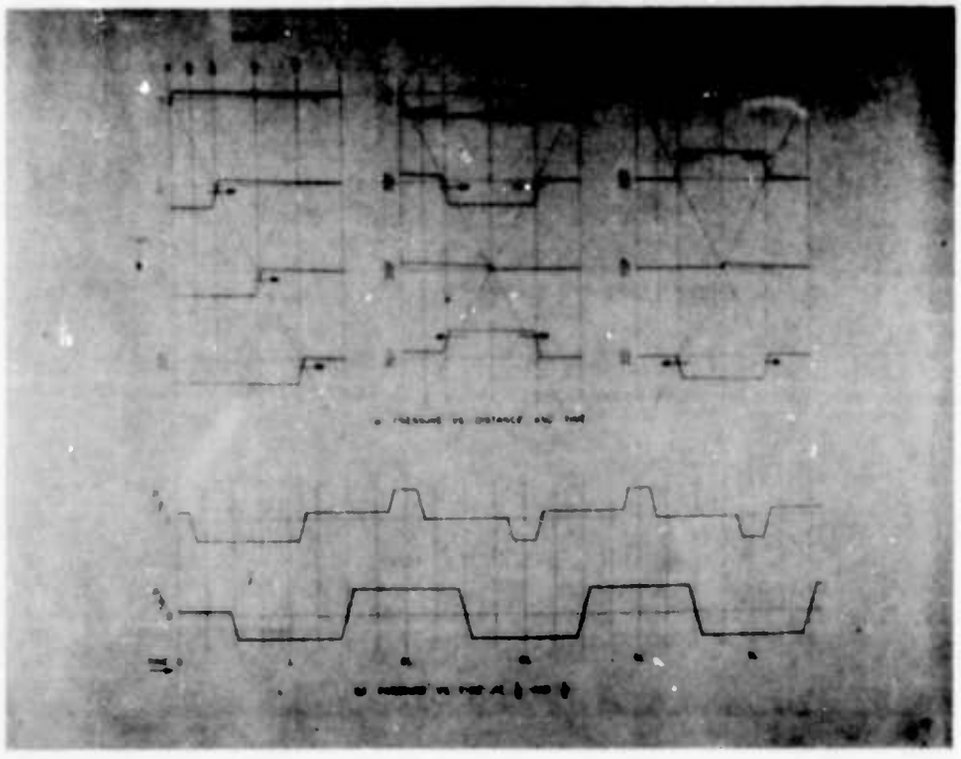

Figure 11. Wave diagram for outlet pressures of tuned-line pneumatic oscillation. Each L in the abscissa should be an L/C. L = length of transmission line; C = speed of sound in line.

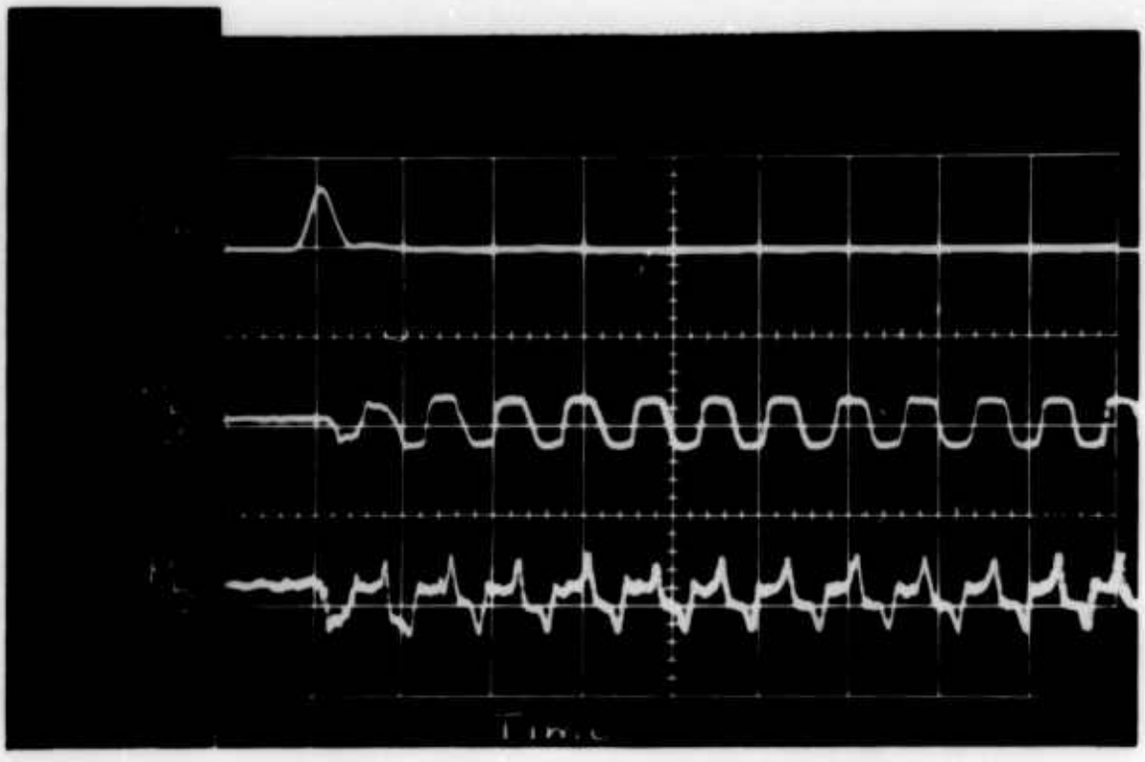

Figure 12. Transducer records of pressures in tuned-line flow oscillator.

HARRY DIAMOND LABORATORIES
Washington 25, D. C.

A SONIC OSCILLATOR

by

Chris E. Spyropoulos

ABSTRACT

A bistable pneumatic element was caused to oscillate by providing an external feedback interconnection between its two control nozzles. The effects of oscillator control interconnection length, diameter, and power-jet pressure on oscillator pulse rate were experimentally determined. These experimentally determined oscillator characteristics are compared with the theory. The oscillator control interconnection pressure wave phenomenon is also investigated.

1. INTRODUCTION

One of the basic components of all digital computers and of many control systems is a clock pulse generator. A pneumatic clock pulse generator with no mechanical moving parts has been constructed at the Harry Diamond Laboratories. This device is termed a sonic oscillator since its frequency of oscillation is dependent upon the speed of sound in a feedback loop incorporated in its design. The purpose of this report is to describe the operational principles and characteristics of a typical sonic oscillator.

A mathematical model is introduced to theoretically predict the oscillator frequency. Oscillator frequency is monitored for the complete operating range of input total pressure to the oscillator and feedback loop length. These measurements are made for three different diameters of the feedback loop. The oscillator feedback loop pressure wave phenomenon is also investigated. The theoretically predicted oscillator frequency characteristics are compared with the experimentally determined characteristics. Oscillator switching times are also determined.

2. DESCRIPTION OF OSCILLATOR

A symmetric fluid bistable element has been designed so that it switches when the flow from its output is restricted. When the controls of this element are interconnected and air is introduced into the power-jet chamber, the power jet is set into oscillation. If the oscillator unit includes a splitter and suffi-

ciently large output channels, alternate pulses from the right and left outputs result from oscillations of the power jet. The frequency of these pulses is determined primarily by the length of the channel connecting the right and left control nozzles.

Figure 1 shows the fluid bistable element used in this investigation. It has a power-jet nozzle width W of 0.32 in. and a 3 W depth. The control nozzles are 3 W wide and the splitter is located 6 W from the power jet nozzle. The control nozzles are set back 2 W from the power-jet nozzle center line. The outputs of the oscillator are circular, 5/16 in. in diameter and inclined at an angle of 12 degrees from the power-jet center line. Polyflow tubing is used to interconnect the control nozzles.

2. METHOD OF OPERATION

When air is introduced into the power-jet chamber of the oscillator, a jet is formed. The jet attaches to a wall immediately down stream from the power-jet nozzle and flows into either the right or left outlet passage.

In this discussion it is assumed that at time t = 0 the power jet has just attached to the right setback wall. At this instant there is a sharp increase in entrainment and decrease in static pressure at the right control nozzle. Consequently an expansion wave propagates away from the right control nozzle and travels along the interconnection path between the control

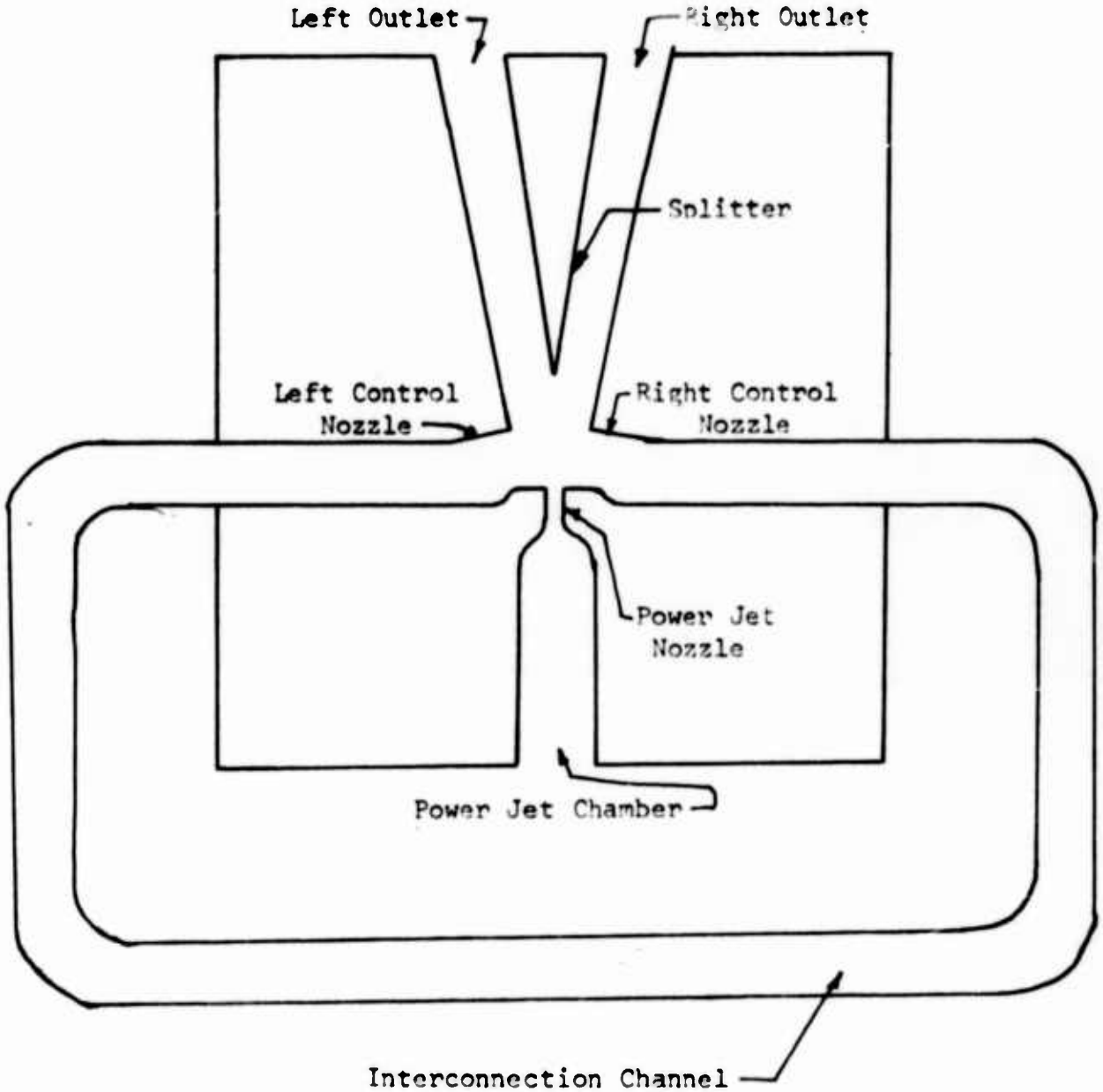

FIGURE 1: Sonic Oscillator

nozzles. The power-jet entrainment of fluid from the right control nozzle continues as the expansion wave propagates toward the left control nozzle.

The bottom trace of figure 2 shows a decrease in static pressure at the right control associated with a rise in the right output static pressure of the sonic oscillator. The shape of the drop in static pressure at the right control and the fact that the decreased pressure attained remains constant while fluid issues from the right output (a rise in static pressure) indicates that an expansion wave is being propagated at the right control.

After issuing from the right output for a finite length of time the power jet switches into the left output. The switching of the power jet from the right to left output is coincident with a drop in the right output static pressure as appears in figure 2. This drop in pressure is associated with a rise in the control chamber static pressure. The linearity and sharpness of this control pressure rise indicate that a compression wave is formed at the right control nozzle when the power jet switches into the left output. This increased pressure remains constant while the power jet issues from the left output and a compression wave propagates away from the right control toward the left control. The wave generated at the right control nozzle is caused by fluid flow into the right control from the interaction region,

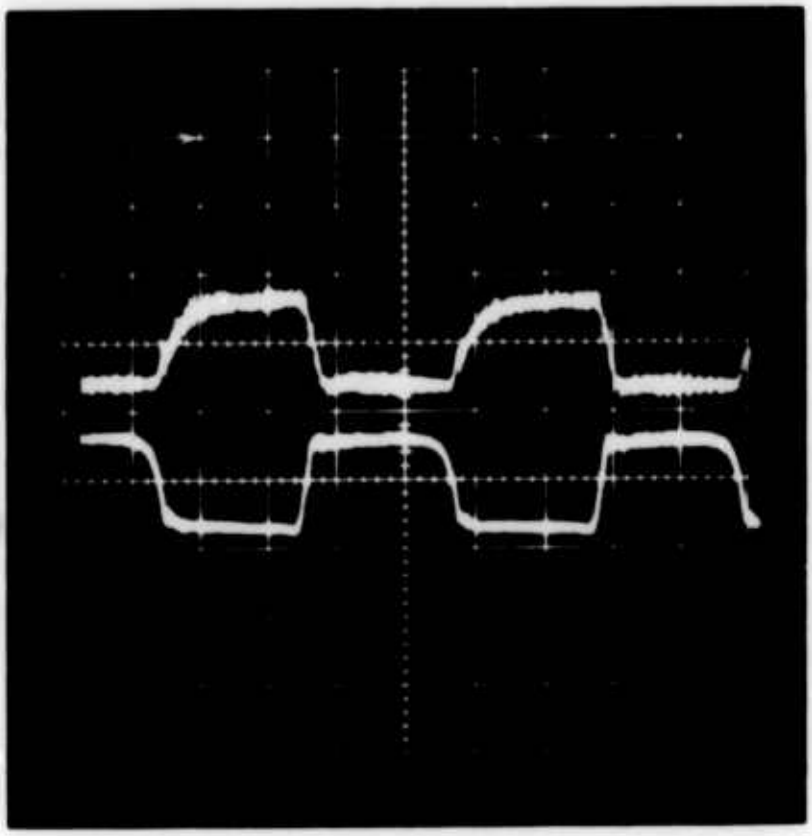

Top trace -
Right output

Bottom trace -
Right control

Figure 2. Right control and corresponding right output static pressures. Interconnection channel is 3/8 in. Polyflow tubing, 12 ft in length; P_p = 20 psig; sweep rate = 5 msec/cm.

which is at a higher absolute static pressure than that at the right control after switching.

The effect of the left control nozzle on the oscillation phenomenon is identical with that of the right control nozzle. While an expansion wave is propagating away from the right control nozzle, a compression wave propagates from the left control nozzle. This can be seen in figure 3(a), which shows the right and left control wave-forms traced at a common sweep rate. The other traces in figure 3 show the form of the pressure wave at various stations along the interconnection loop (bottom traces) compared with the pressure wave form at the left control (top traces). These pictures display the change in shape that the pressure waves undergo as they propagate through the interconnecting loop.

The traces of figure 4 give the absolute static pressure monitored at three different stations along the oscillator control nozzle interconnecting channel. The transition in shape that the pressure waves undergo is the same as that observed in figure 3. These traces verify the fact that the mean static pressure along the feedback loop is less than atmospheric.

The traces in figure 5 show the variation in the wave form and the decrease of the static pressure in the interconnecting channel with an increase in power supply pressure. This reduction in pressure is due to the increased entrainment resulting from the increase in velocity of the power jet. In addition,

Top traces taken at left control.

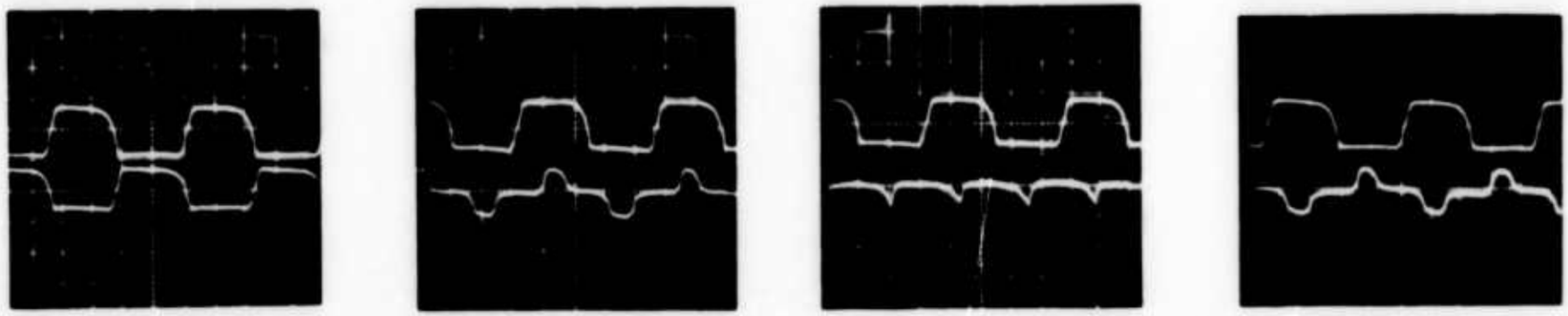

(a) Bottom trace taken at right control chamber.

(b) Bottom trace taken 4 ft from left control nozzle.

(c) Bottom trace taken at center of feedback tube.

(d) Bottom trace taken 4 ft from right control nozzle.

Figure 3: Pressure waveform along the interconnection channel compared with left control chamber waveform. Interconnection channel is 3/8 in. Polyflow tubing, 12 ft in length; P_p = 20 psig; sweep rate = 5 msec/cm.

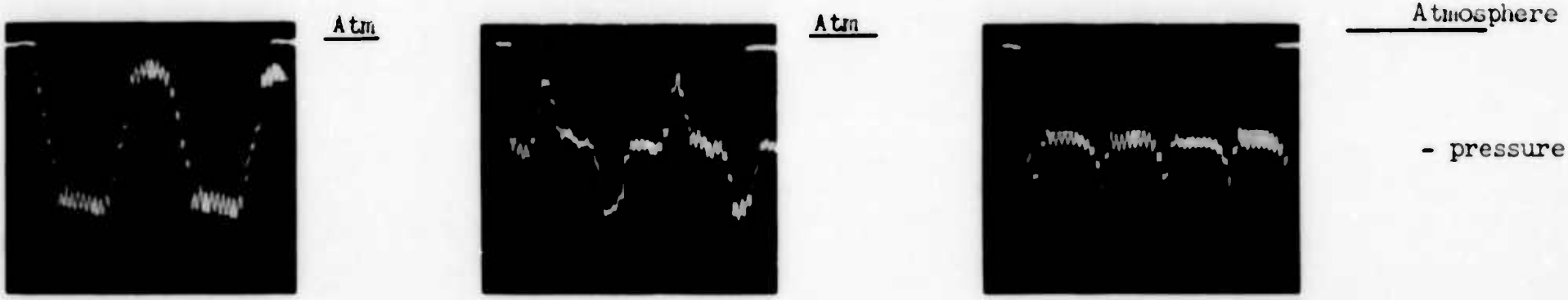

(a) Transducer set 6 in. from right control.

(b) Transducer set 3 1/3 ft from right control.

(c) Transducer set at center of interconnection channel.

Figure 4: Static pressure traces taken at three different locations along the interconnection channel. 1/2 in. Polyflow tubing, 12 ft. in length; P_p = 15 psig; sweep rate = 5 msec/cm; vertical scale graduation = 0.7 in. Hg/cm.

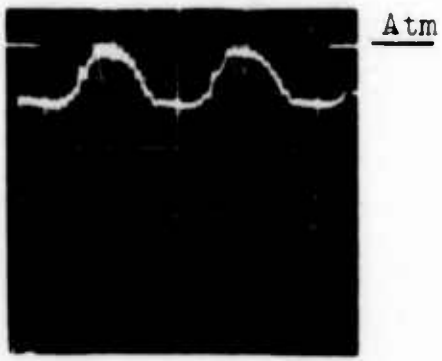

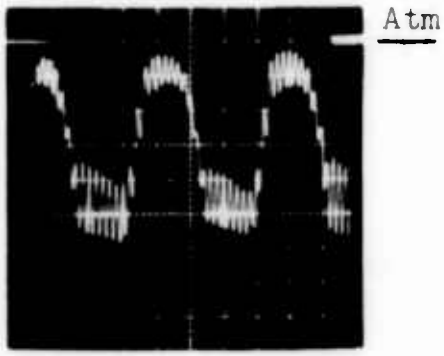

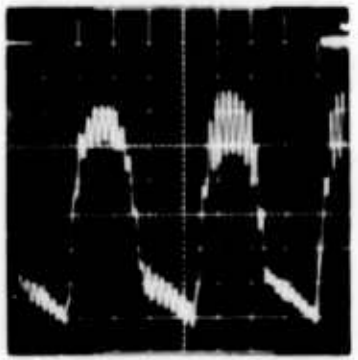

P_p = 3.8 psig P_p = 13.0 psig P_p = 22.5 psig

Figure 5: Feedback static pressure traces obtained by varying power jet pressure (P_p). Traces are obtained with a transducer set 6 in. from the right control nozzle. 1/2 in. Polyflow tubing, 10 ft in length; sweep rate = 5 msec/cm; vertical scale graduation = 0.7 in. Hg/cm.

with the increase of power-jet pressure the amplitudes of the waves in the interconnection tube increase.

As was previously mentioned, when the power jet attaches to the right setback wall, an expansion wave is propagated at the right control nozzle and a compression wave is propagated at the left control nozzle. When these pressure waves reach the opposite control nozzles the unit switches. At switching, an expansion wave is set up at the left control nozzle and propagates toward the right control nozzle and a compression wave is set up at the right control nozzle and propagates toward the left control nozzle. This mode of operation continues as the unit oscillates.

The period of the oscillation is equal to the time required for two traverses of waves through the channel, plus twice the time required for the impacting waves to switch the jet. The period T may be expressed as

$$T = 2t_c + 2t_s \qquad (1)$$

where t_c is the time required for a wave to traverse the channel and t_s is the time for the impacting wave to switch the jet.

Assuming that the flow phenomenon in the interconnection loop is isentropic, then the speed at which the expansion wave propagates is the local speed of sound a_o. The velocity of a shock wave for an ideal gas c_s is given by the following equation (ref 2)

$$C_s = a_o \left(\frac{\gamma - 1}{2\gamma} + \frac{\gamma + 1}{2\gamma} \frac{p_1}{p_o} \right)^{\frac{1}{2}} \qquad (2)$$

where a_o is the speed of sound in the medium into which the shock wave propagates, p_1 is the pressure behind the shock wave, p_o is the pressure of the medium into which the shock wave is propagating and γ is the gas isentropic constant. Expanding equation (2) in series and retaining only the first terms in $\frac{p_1 - p_o}{p_o}$ gives

$$C_s \doteq a_o \left(1 + \frac{\gamma + 1}{4\gamma} \frac{p_1 - p_o}{p_o} \right) \qquad (3)$$

If the normalized pressure jump ($\frac{p_1 - p_o}{p_o}$) of a shock wave is very small, then the speed of the shock wave is nearly equal to the local speed of sound a_o.

In this discussion it is assumed that the normalized pressure jump of the shock waves occurring in the interconnection of the oscillator is small so that the wave velocity can be assumed to be sonic. The time required for the waves to traverse the cahnnel t_c is given by

$$t_c = \frac{L}{a_o} \tag{4}$$

where L is the length of the interconnection channel.

The period T may now be expressed as

$$T = \frac{2L}{a_o} + 2t_s \tag{5}$$

The switching time t_s may be expected to depend on the amplitude, shape, and flow associated with the waves developed at the oscillator control nozzles, as well as the attenuation that these waves undergo while traversing the interconnection channel. These effects are dependent on the internal dimensions of the oscillator as well as the thermodynamic state of the fluid which is fed into the oscillator.

If the oscillator switching time t_s is considered negligible compared with the wave travel time t_c, the oscillator frequency f_t becomes

$$f_t = \frac{a_o}{2L} \tag{6}$$

The sonic velocity in the interconnection loop is given by the following isentropic expression

$$a_o = 49.0 \sqrt{T_o} \qquad (7)$$

where a_o is in ft/sec and T_o is in degrees Rankine. The relation of frequency to channel length as given by equation (6) is plotted in figure 6, assuming that the wave velocity in the interconnection channel is ambient sonic velocity for T = 530° R.

4. INSTRUMENTATION

Experiments were conducted to investigate the fundamental characteristics of the sonic oscillator. A block diagram of the instrumentation employed is shown in figure 7. The power jet is supplied from a stagnation tank where the total pressure is measured with a Bourdon gauge of ± 0.2 per cent accuracy. A pressure regulator is used to control the input pressure. Air flows from the stagnation tank to the power jet chamber of the oscillator through a short section of 1/2 in. pipe. Transducers are located in the controls and outputs of the oscillator as shown in the figure. The sensing area of the transducers is located on the inside wall of the oscillator cover plate. The outputs of the transducers are fed into calibrators and then into an oscilloscope and a counter.

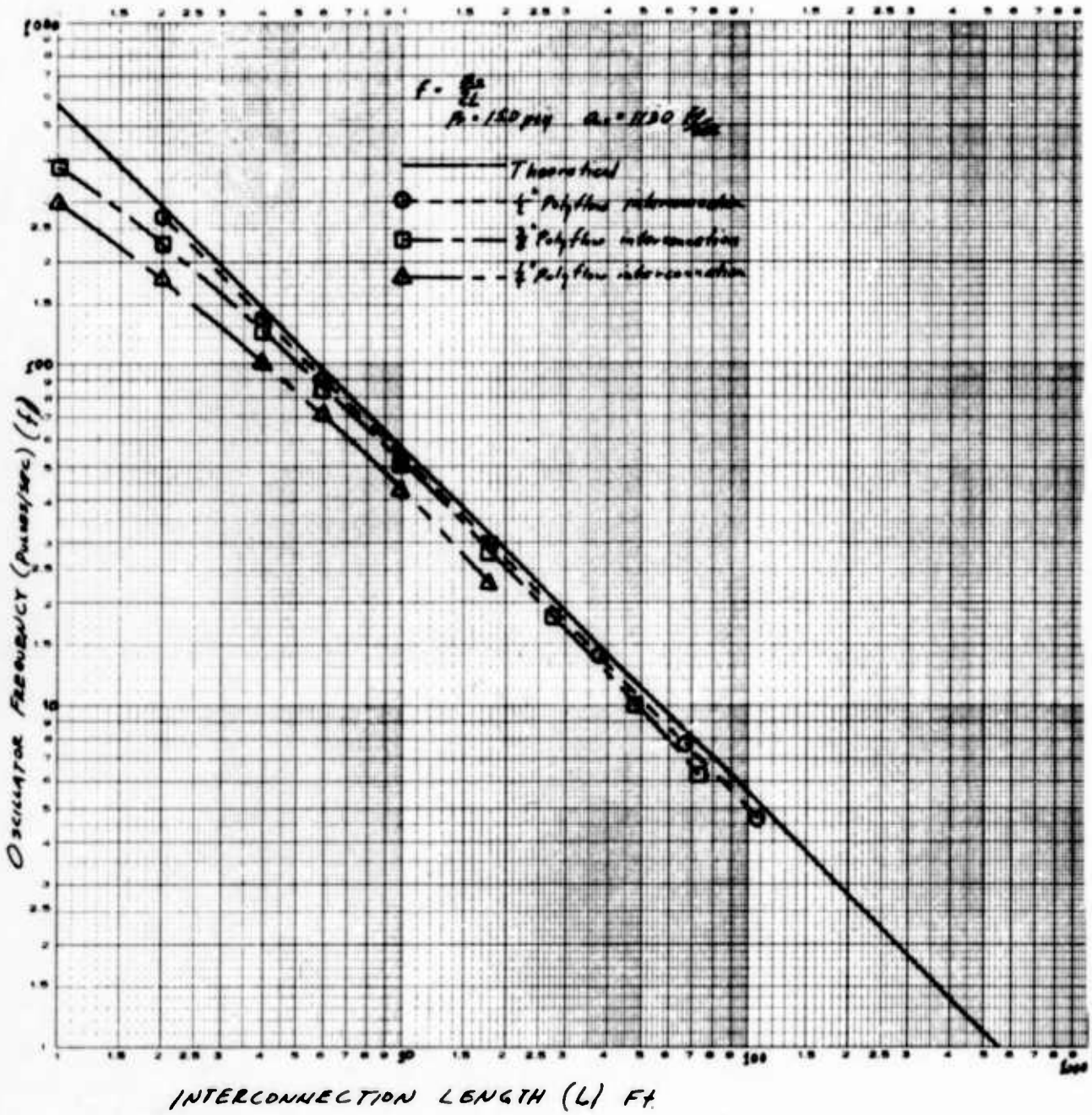

Figure 6: Oscillator Frequency versus
Interconnection Channel Length

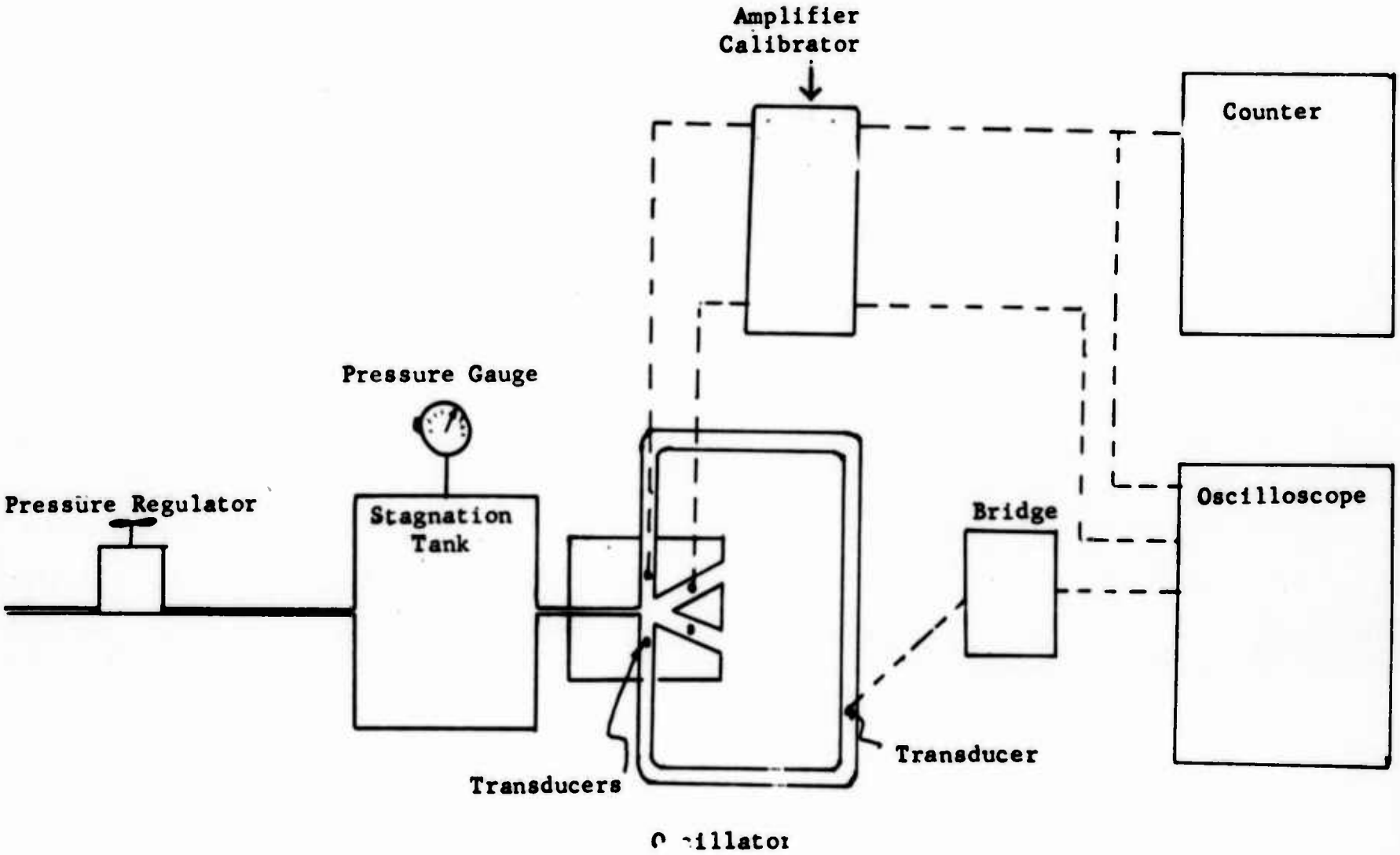

Figure 7. Instrumentation Diagram

Pressure in the interconnection channel is monitored with a strain-gage transducer. This transducer is calibrated with a ± 0.2 per cent laboratory test gauge and is used to measure absolute static pressures in the oscillator interconnection. Transducers are also used to observe wave forms in the various stations mentioned as well as at various points along the feedback interconnection. The output of a transducer located at a control chamber is used to trigger the counter for pulse rate measurement.

5. EXPERIMENTAL RESULTS

In figure 6 the oscillator frequency is plotted against the lengths of the interconnection channel for the theoretical frequency equation and for experimental results obtained with channels having different diameters. The power supply pressure is held at 15.0 psig in all cases. For the different channel lengths, the experimental frequencies approach the theoretical frequency as the diameter is increased. These results indicate that switching time becomes of greater significance with respect to the wave traverse time as the diameter decreases. With decreasing diameter the attenuation of the waves increases. The waves reach the control nozzles with decreased amplitude and attain the amplitude required to switch at a later point of phase.

Figure 8 shows curves of oscillator frequency versus power-jet supply pressure for various lengths and diameters of inter-

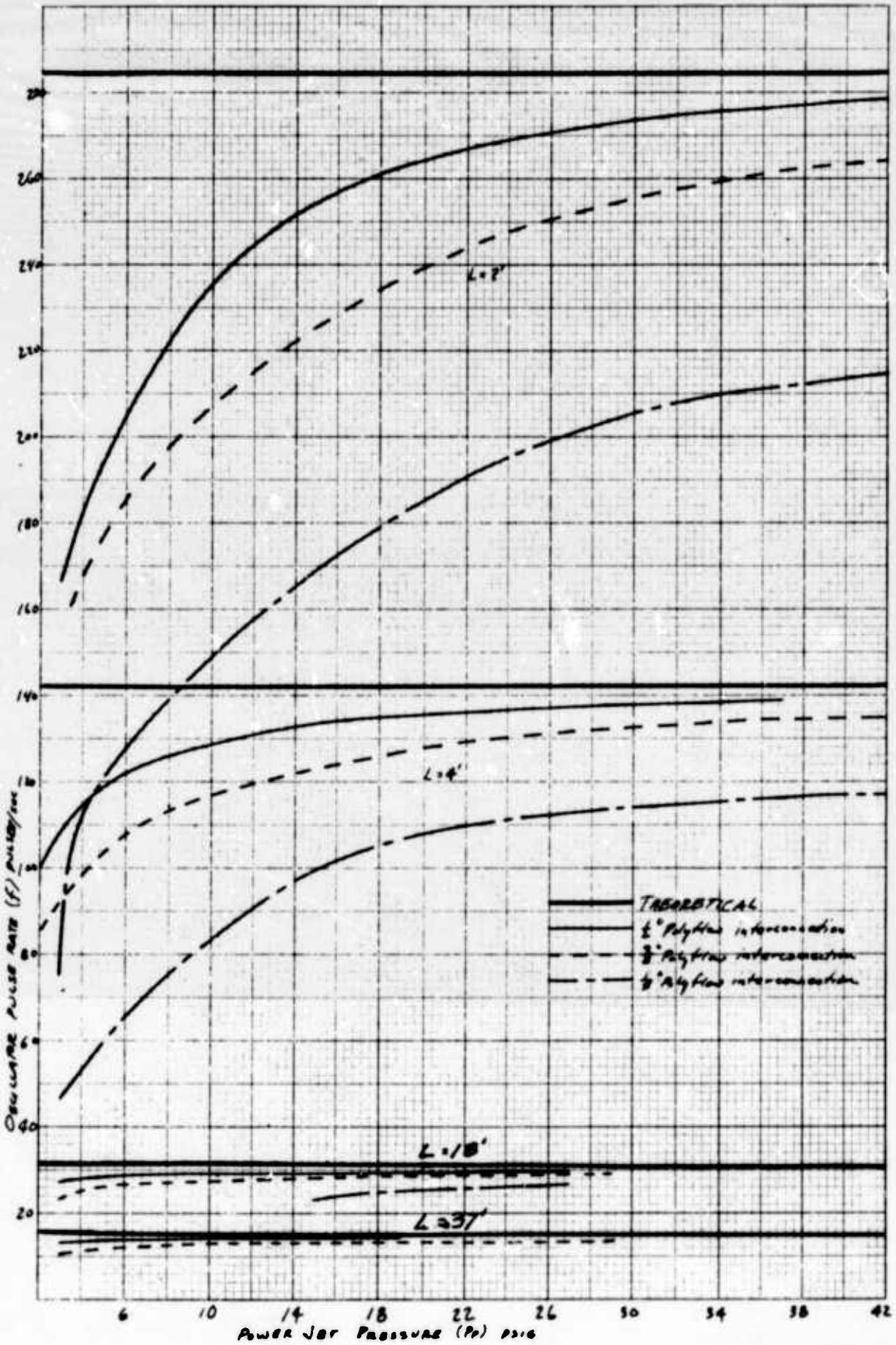

Figure 8: Oscillator Frequency versus
Power-jet Supply Pressure

connection channel. For all diameters, the discrepancy from the theoretical frequency decreases as the power supply pressure increases. The increase of frequency with power supply pressure may indicate both increased amplitude and faster rise times for the compression waves and faster pressure drop times for the expansion waves formed at the control nozzles. These phenomena would tend to decrease the switching time of the oscillator. Another cause of increase of frequency with power-jet pressure that should be considered as a possibility is the increase of velocity of the compression waves formed at high amplitudes as given by equation (3).

Experiments were conducted to measure directly the speed of the waves in the interconnection channel. Two pressure transducers were located in the interconnection channel a known distance apart. The transducer outputs were connected to a dual-beam oscilloscope and to a counter. The output from one transducer started the counter, the output from the other stopped it. The counter started and stopped at definite voltage levels of the transducer outputs. The triggering points were monitored on the oscilloscope.

Typical oscilloscope traces are shown in figure 9. For this particular case the starting and stopping transducers are located 0.5 and 14.5 ft, respectively, from the right control nozzle. On the bottom curve of (a) a dot on the increasing pressure slope

(a) Positive pressure wave velocity determination. Counter triggered on increasing slope of traces (points indicate triggering level). Lower trace starts counter, upper trace stops counter.

(b) Expansion wave velocity determination. Counter triggered on decreasing slope of traces (points indicate triggering level). Lower trace starts counter, upper trace stops counter.

Figure 9: Wave Velocity Determination. 3/8 in. Polyflow tubing, 36 ft in length; P = 15 psig; sweep rate = 10 msec/cm; bottom trace monitored 6 in. from right control nozzle; top trace monitored 14 ft from bottom trace pickup.

of a shock wave shows when the counter was started; on the top curve a dot on the increasing pressure slope shows when the counter was stopped. The traces of (b) show similar starting and stopping points on the decreasing slopes of expansion waves. For both pressure and expansion waves, the velocities were determined by dividing the distance between the transducers by the counter time reading. The wave velocities for both the shock and expansion for this particular case were $\bar{1111}$ fps.

The mean static pressure in the interconnection channel p_o for this particular case was measured and, assuming an isentropic change of state, the mean temperature in the channel was computed with the following equation

$$T_o = T \left(\frac{p_o}{p} \right)^{\frac{\gamma - 1}{\gamma}} \tag{8}$$

where T and p are room temperature and pressure. Substituting T_o of the above equation into equation (7), a_o becomes

$$a_o = 769\ p_o^{.143} \tag{9}$$

where a_o is in fps and p_o is in psia.

The velocity of sound determined by equation (9) for the particular case under consideration is $\bar{1117}$ fps.

Similar procedures were followed for other channel lengths and diameters for the measurements conducted to obtain the data shown on figure 6. The measured velocities showed close agreement with the computed velocity in the interconnection channel.

Taking the velocity in the channel as given by these experiments, and the measured oscillator frequency f_a, it is possible to determine the switching time t_s by means of equation (5). When this equation is solved for t_s, there results

$$t_s = \frac{1}{2}\left(\frac{1}{f_a} - \frac{1}{f_t}\right) \qquad (10)$$

This equation is used to compute t_s for the data of the experiments of figure 6. The results are plotted on figure 10, which indicates that the switching time as computed by equation (10) increases with increase of length and decrease of diameter of the interconnection channel. Both the increase in length and decrease in diameter may be expected to increase the attenuation of the waves and thus increase the time necessary for the flow rate and pressure difference at the control nozzles to build up sufficiently to switch the jet.

6. CONCLUSIONS

A mathematical model was introduced to theoretically predict the frequency of a sonic oscillator. Theoretically predicted oscillator frequency characteristics compared with experimentally determined characteristics are presented in figure 6. These graphs as well as oscilloscope traces of pressure monitored in the oscillator outputs and interconnection channel during oscillator operation lend support to the validity of

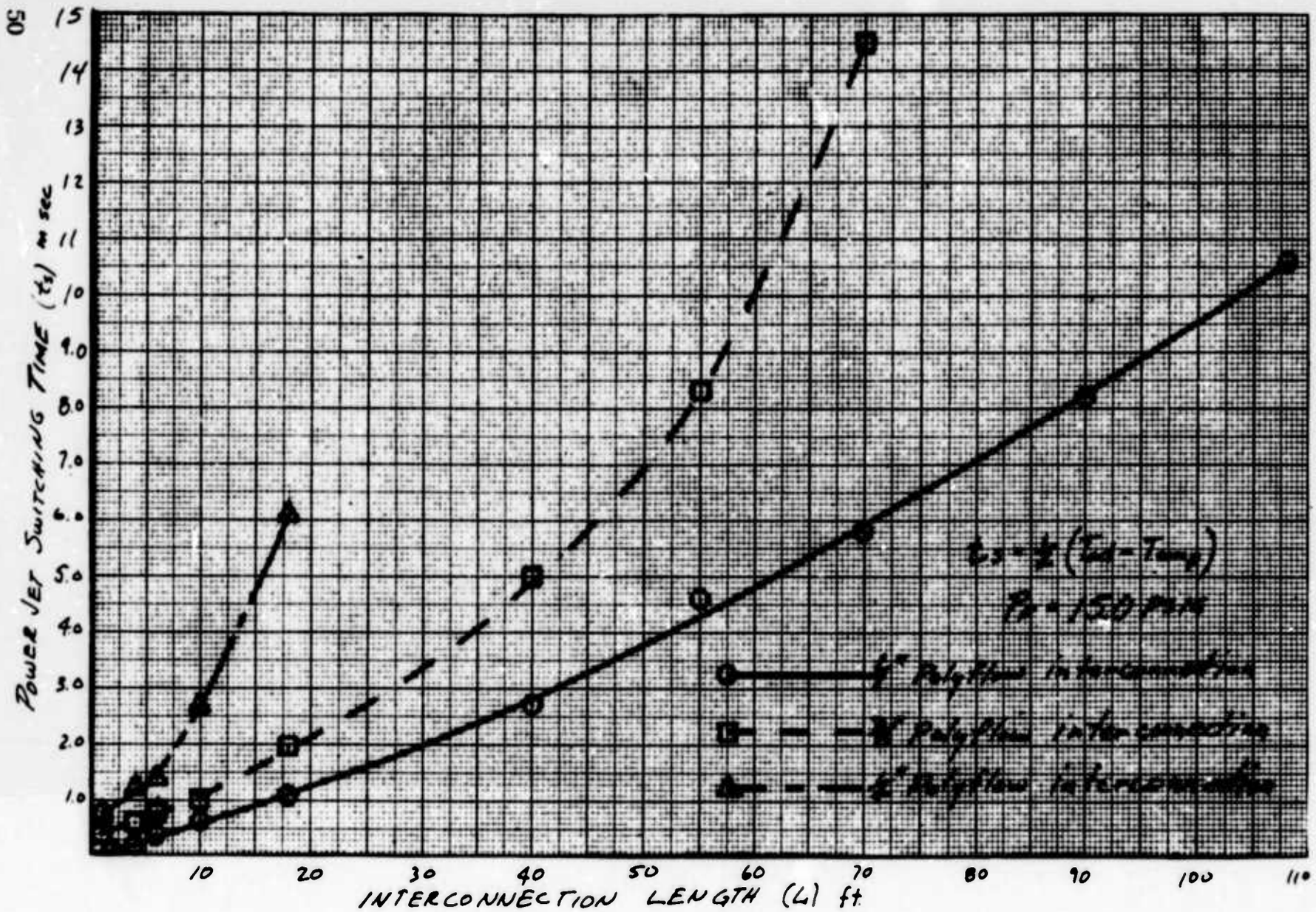

Figure 10: Power Jet Switching Time versus Interconnection Channel Length

the mathematical model. The mathematical model in conjunction with experimental data determines the oscillator switching time. Typical switching time characteristics are given in figure 10.

REFERENCES

1. Warren, Raymond, "Wall Effect and Binary Devices," Proceedings of the Fluid Amplification Symposium, October 1962, Vol. I

2. Liepman, H. W., and Roshko, A., "Elements of Gasdynamics," New York, John Wiley and Sons, 1957

INTERCONNECTION OF
FLUID AMPLIFICATION ELEMENTS

by

Raymond W. Warren

of the

Harry Diamond Laboratories

ABSTRACT

The interconnection of fluid logic elements necessitates that both flow and wave effects be considered. Practical considerations impose additional limitations on the system. Some approaches to the problem of operating within these limitations are discussed.

The operation of a wall-interaction fluid amplifier with open controls and with a minimum setback between the stream and the walls is discussed. It is shown that a decrease in flow in the control on the side of the stream opposite the separation bubble is very effective in switching the stream. Characteristics of the output waves are reported.

Techniques used to solve interconnection problems are discussed.

1. INTRODUCTION

There are several fluid amplification techniques that can be used in logic systems. This discussion is concerned with fluid elements using the technique of attaching a stream to a wall. In designing logic systems from such elements, there are two methods of connecting the elements to accommodate the flow. These are sometimes called the closed system and the bleed system.

In the closed system, the successive elements are made larger and larger to accommodate all the flow of the previous stages. This type of system is employed for multistage flow and pressure amplifiers. All the fluid supplied at the inputs is available at the output for efficient use of power. Because the size of each unit must be adjusted to that of the preceding one, such a design is not practical for the more complex logic systems.

When the bleed method is adapted to logic systems, it is desirable from the standpoint of simplicity that the fluid elements have the following characteristics: (1) same size, (2) same pressure source, and (3) equal pressure drop across nozzle, i.e., equal flow.

If a system is to have these characteristics, it is necessary to remove as much flow from each unit as is put into it after it has accomplished its assigned task. Thus in a digital system, the flow can be exhausted after it has properly switched the next bistable element.

Additional desirable characteristics are as follows:

(1) Stability with respect to downstream effects, loading, etc.

(2) Stability with respect to transients.

(3) High instantaneous gain, and consequent ability to feed several units, i.e., to "fan out".

(4) High speed of response.

(5) No flow in nonactive output.

2. BLEEDS

An approach to maintaining the same flow from all power-jet nozzles is the introduction of directional bleeds into the interaction region to maintain all the interaction regions essentially at ambient pressure. The bleeds are located in both boundary walls downstream of the high pressure region associated with the point of reattachment.

Figure 1 is an example of a flip-flop with bleeds at right angles to the power stream; In 1A, the flow is shown with no load on the output, and in 1B, the right output is loaded by a nozzle, and there is no flow in the left output.

The bleeds are located in as high velocity a region as practicable, consistent with being downstream of the separation bubble and region of attachment. The bleeds being downstream of the region of attachment tend to isolate the unit from downstream loading effects.

As shown in figure 1A, with no load or when the stream is initially switched into an outlet, the high-velocity fluid passes the bleed without leakage and attaches to the farther wall, which is set back. When the flow encounters a load, such as the next control nozzle, the dynamic pressure converts to static pressure, which readily induces flow out of the right and left bleeds. The left bleed must be located and sized to prevent flow into the left output, which would constitute a false signal. It is necessary to locate the bleeds downstream of the area in which the stream attaches to the wall to prevent atmospheric flow into the separation bubble, which would decrease the ability to remain attached to the wall.

The bleeds must be shaped to avoid organ-pipe type oscillation. This is done in figure 1B by inducing a vortex to match the bleed flow into the atmosphere. The passage could be made diverging to impedance-match the flow into the atmosphere instead of using the vortex. In other designs the essentially right-angle bleeds are placed in the covers instead of as shown in figure 1. In these instances the holes are tapered to avoid oscillation and to facilitate matching.

3. OPEN CONTROLS

Open controls (1) reduce the ability to attach firmly to either wall, (2) move reattachment region downstream, (3) require more flow to switch (lower gain), and (4) are receptive to any transients in the system. These effects are fairly obvious except that normally, as the stability is decreased, the gain is increased; whereas in the case of open controls, both the stability and gain are decreased. The open controls reduce the pressure differential across the stream, reducing the force holding the stream against the wall so the stream is less stable. The reduction in gain is due to the increased control-flow requirements needed to switch. Even though the power jet is attached to one wall, it is entraining from both controls. The control flow to switch must exceed the opposing entrained control flow by the required differential before the power jet will attach to the opposite wall.

If the resistance to flow in the opposing control is increased by additional length of passage or passive elements, it will reduce the control flow necessary to switch toward the opposing control. Unequal loading of the controls can thus serve as a bias, decreasing stability on one side and increasing it on the other. This decreases the allowable fan out.

4. REDUCTION OF FLOW

It is generally desirable to accomplish logic or control functions at as low an energy level as practicable and then to amplify the signal to the required power level. While reduction in the stream velocity reduces the ability to remain attached to the wall under load, it does not result in a corresponding reduction in the control flow required to switch; that is, the instantaneous gain is reduced.

As the velocity is reduced so that laminar flow is approached, the entrainment is reduced and a longer time is required to attach to the wall. in one test using a setback of 1W (unity orifice width) and a boundary wall inclined at an angle of 12 deg. to the stream, a stream of air attached to the wall at a power-jet pressure of 0.2 in. H2O. The Reynolds number was 30. There was considerable variation in the time required for the stream to attach to a wall without a control stream. However, in general, the time was 1 sec. or more with closed controls, and it did not attach with open controls at this low flow.

Reducing the setback of the boundary wall reduces the time for a stream to attach to the wall without a control stream. The reduced setback also enables a stream to attach to an inclined wall with open controls at a lower flow.

At very low power-jet velocities, a pulse in one control jet may appear in the opposite control jet. To minimize this effect, the control orifices can be at an angle to each other. There appears to be no effect on operation for small angles, such as 15 deg. from perpendicular to the power-jet stream.

Figure 2 is an instantaneous photogrammetric picture of the surface of a flip-flop in the water table taken at the University of Maryland with equipment developed at Aberdeen Proving Ground. This gives a visual impression of the waves present in a subsonic bistable element with the stream attached to the right wall. The difference in the heights between adjacent contour lines is 0.1 mm H_2O. The average pressure pattern in the flip-flop is almost obscured by the effect of the waves.

When a bistable element is switched, both pressure and rarefaction waves are created. In addition, the vortex in the separation bubble is disturbed and may move downstream. If a pressure wave arrives at the separation bubble of a second unit at the same time a rarefaction wave arrives at the opposite side of the stream, the element will switch if it has high enough gain. Higher gain elements can be switched by either the pressure or rarefaction wave alone.

A pressure wave will reflect as a pressure wave from a closed-end tube or a right-angle turn. It will reflect as a rarefaction wave from an open-end tube. Rarefaction waves act similarly with regard to like and unlike reflection.

To conserve energy, logic systems must be operated at pressures producing only a low subsonic flow. To achieve fast system response under these conditions, it is necessary to utilize the forward-wave traveling at the local speed of sound, rather than to wait for the subsonic flow to switch an element.

This necessitates the use of fluid devices with high instantaneous gain, which, like all high-gain systems containing feedback tend to oscillate. A vortex, rotating in the direction of flow, has been the most effective means of passing the forward wave unimpeded and inhibiting the reflected waves. As shown in figure 1B, a cusp induces a fixed vortex in the bleed. A reflected wave moving upstream is divided at the cusp. A portion of the wave enters the interaction region. The remainder of the wave is expanded, reduced in amplitude, and sent out the bleed. If no bleed is present, the wave is rotated 90 deg. and moves back and forth across the passage perpendicular to its former direction of travel. The portion of the energy of the wave removed from the main wave front by the vortex aids in preventing oscillations.

The direction of flow of the vortex in the interaction region is such as to resist flow attempting to enter the boundary layer between the power stream and the boundary wall. If fluid could enter this boundary layer with sufficient energy to surmount the pressure hump at the point of stream attachment, it could enter the separation region and decrease stability.

The vortex in the interaction region and smaller vortices in the separation bubble and controls have a stabilizing effect on the stream as long as they are fixed in position. A cusp shape at the end of the splitter enhances and assists in maintaining the vortex fixed in the interaction region, but requires close tolerances to prevent biasing the unit.

Where it is desired to utilize wave effects to achieve a high rate-of-response system, it is essential to connect the elements with smooth contours. Right-angle turns, open-ended passages, and dead-end passages reflect waves and sustain oscillation in a high-gain system.

5. OPERATIONAL CHARACTERISTICS

The operational characteristics of a bistable fluid amplifier that are of primary importance are as follows:

(1) Instantaneous gain

(2) Stability

(3) Impedance

(4) Efficiency

(5) Speed of response

Associated with each of these are a flow, a pressure, and a total energy. Variation of each of these results in considerable data, which can be presented in many ways. There are also many physical parameters that can be changed in the bistable element. Changing one physical parameter frequently affects several operational characteristics and other physical parameters as well. It is a time-consuming task to take and analyse large amounts of data for the many variables involved. The water table is of considerable assistance in visualizing the flows and determining promising physical configurations. From the water table and measurements with air, it is apparent that high instantaneous gains are associated with low stability and high output impedance with low efficiency and vice versa.

There are primarily two mechanisms by which a boundary wall amplifier can be switched. The first is predominant when the walls are relatively far apart. As flow is introduced into the separation bubble, the point of attachment moves downstream. When sufficient fluid enters the separation bubble to satisfy the entrainment, the stream moves to the center, entrainment on the opposite side lowers the pressure, and the stream moves to the opposite wall. Moving the walls farther apart increases the gain and lowers the stability. Moving the bleed upstream also increases the gain and lowers the stability as it provides readier access to the separation bubble.

The second mechanism of switching is predominant when the amplifier walls are relatively close together. As control fluid enters, its momentum causes the stream to contact the opposite boundary wall forming a second separation bubble. The stream is now in contact with both walls. As more control fluid enters the original separation bubble, fluid is entrained from the new separation bubble. The new point of attachment moves downstream and the stream progressively attaches to the new boundary wall as it leaves the old.

In this mechanism of shifting, the gain and stability increase as the walls are moved closer together until the stream attaches to both walls, then stability decreases.

It appears that between the two extremes there are two boundary-wall positions where gain is a maximum and stability is sufficient for the particular output impedance. Between the two maximum gain positions there is an operating range of less gain and greater stability.

The entire range is of interest; however, the less energy the stream loses by entrainment the higher is the efficiency. With the walls closer to the stream, the attachment point is closer to the power-jet nozzle; and the splitters can be kept the same distance from the attachment point and be closer to the power-jet nozzle, thereby conserving energy and raising efficiency.

Response time should also be reduced with decreased distance for the stream to travel from one wall to the other.

The above factors favor having the walls close to the stream. However, as the power-jet pressure increases, the stream spreads, which limits the useful range of power-jet pressure. This range is smaller for small setbacks than for large ones.

This indicates that for constant-pressure operation, such as in logic systems, there may be advantages in increasing gain by moving the walls close to the stream. For operation over a wide range of pressures, the instantaneous gain should be increased by moving the walls farther apart.

To investigate the effects of moving the walls close together, a unit was constructed as shown in figure 1. The efficiency is shown in figure 6 for the same conditions as those in figures 3 and 4, where the area of the outputs are the same as the area of the power jet.

To impedance match the outputs to the succeeding controls when all the power jets are at the same pressure, fan out is used--the output of one unit is used to switch more than one unit.

Families of curves can be plotted to optimize the fan-out ratio, the number of units that can be switched by one unit. A 1-psig power-jet level was selected from figure 4 as assuring a reasonable fan-out at a low power. Larger fan-out could have been obtained at higher power-jet pressures. The pressure and flow in the right control during switching is shown in figure 7. The pressure was gradually increased above atmospheric until the stream switched. The dotted line indicates the impedance of the control after switching.[1] Lowering the pressure and flow in the same control produced another switch point below atmosphere. The area between the lines represents the hysteresis loop.

The condition of the controls open to atmosphere is indicated for both the control on the side to which the stream is attached and the control at which the stream is not attached. The diagram indicates that if the flow to the non-attached control is reduced very slightly below the conditions prevailing when open to atmosphere, the left switch point is reached and the unit switches.

The entrainment of flow in the controls shown in figure 4 appears to be enough to switch a second unit if one of the controls of each of the two units is connected to the upper arms of a Y flow divider, the opposite controls are open, and the lower leg of the Y has sufficient resistance.

A signal in the lower leg of the Y switchs the two units. When the signal is removed the units switch back because of mutual entrainment.

This forms a very effective decision circuit, which produces an output when a signal is present above a certain threshold but no output when the signal is below the threshold. It can also be used as an inverter, which produces an output only when no control signal is present. In effect the two units are slaved together.

Placing bleeds in the Y as shown in figure 8 eliminates the effect of drawing the streams toward the Y by providing an additional source of the fluid required for entrainment in bistable action.

To obtain gain information from the impedance curves of figure 7, the reciprocal of the plotted ratios must be taken. For the 1-psig power jet, this indicates a flow gain of 10 and a pressure gain of 7, similar to the gain figures for 1 psig on figure 5.

In operation with attendant losses, a fan out of 8 was too great for a unit to switch under steady-state conditions. Under dynamic conditions 8 units switched readily.

Traces of the waves were desired, but, since there was insufficient gain with the available pressure sensors to obtain measurable traces with a fan out of 8, the arrangement in figure 9 was used.

The trace in figure 10A shows that when the driving unit is switched, a pressure wave appears in the first sensor with a rise time of 1/2 ms. This is immediately followed by a smaller rarefaction wave, most probably reflected from the open leg of the stream divider. When the driving unit is switched to the left, the sudden cessation of flow causes a rarefaction or expansion wave with the same rise time as that of the pressure wave. This is immediately followed by a reflected compression wave. The pressure does not return to atmospheric due to the entrainment of the control flow similar to that shown in figure 4. The pressure trace at the second sensor located after the divider is similar to that at the first sensor except that the wave peaks are not so high and the rise time is 1 ms.

Attaching the unit in a system affected the control impedances and biased the unit. The bleeds added to the Y as shown in figure 8 helped to equalize the control impedances. However, the bleeds also lower the pressure of the output of the driving unit as shown in traces C and D of figure 10 and, therefore, lower the gain. The bleeds also eliminated the effect of the driven unit switching on the rarefaction wave and the effect of the units switching on mutual entrainment when two controls were connected to the Y.

6. CONCLUSIONS

Available techniques indicate that fluid elements can be assembled into reliable bleed-type systems. When the outputs are stable, the impedance of the controls in this type of bleed unit determines most of the operating characteristics of the system. The interaction of the controls in a fan-out system affects operation. The wave effects are appreciable but can be controlled to produce the slaving of units and fast responses.

Boundary-wall-type units with small setbacks exhibit high gains and fast responses.

Acknowledgement is made of the careful work of E. Swartz and W. Kehres in taking and reducing the data employed in the preparation of this paper.

References:

1. Norwood, R. E. "A Performance Criterion for Fluid Jet Amplifiers" ASME Symposium, November 1962, Fluid Jet Control Devices

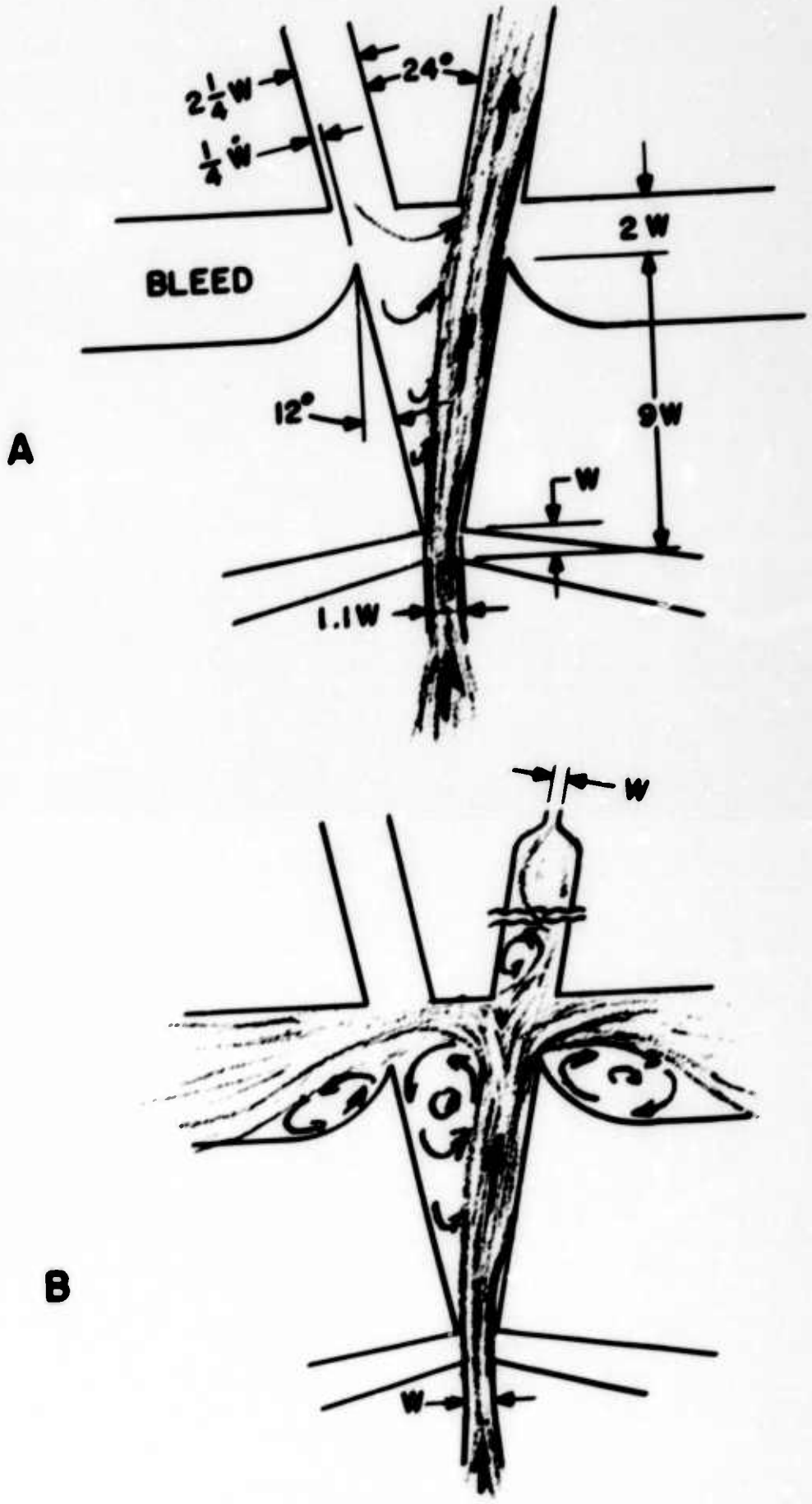

Figure 1. Wall interaction fluid amplifier.

Contourlines: unit 0.1 mm

778-62

Figure 2. Water table surface bistable fluid amplifier.

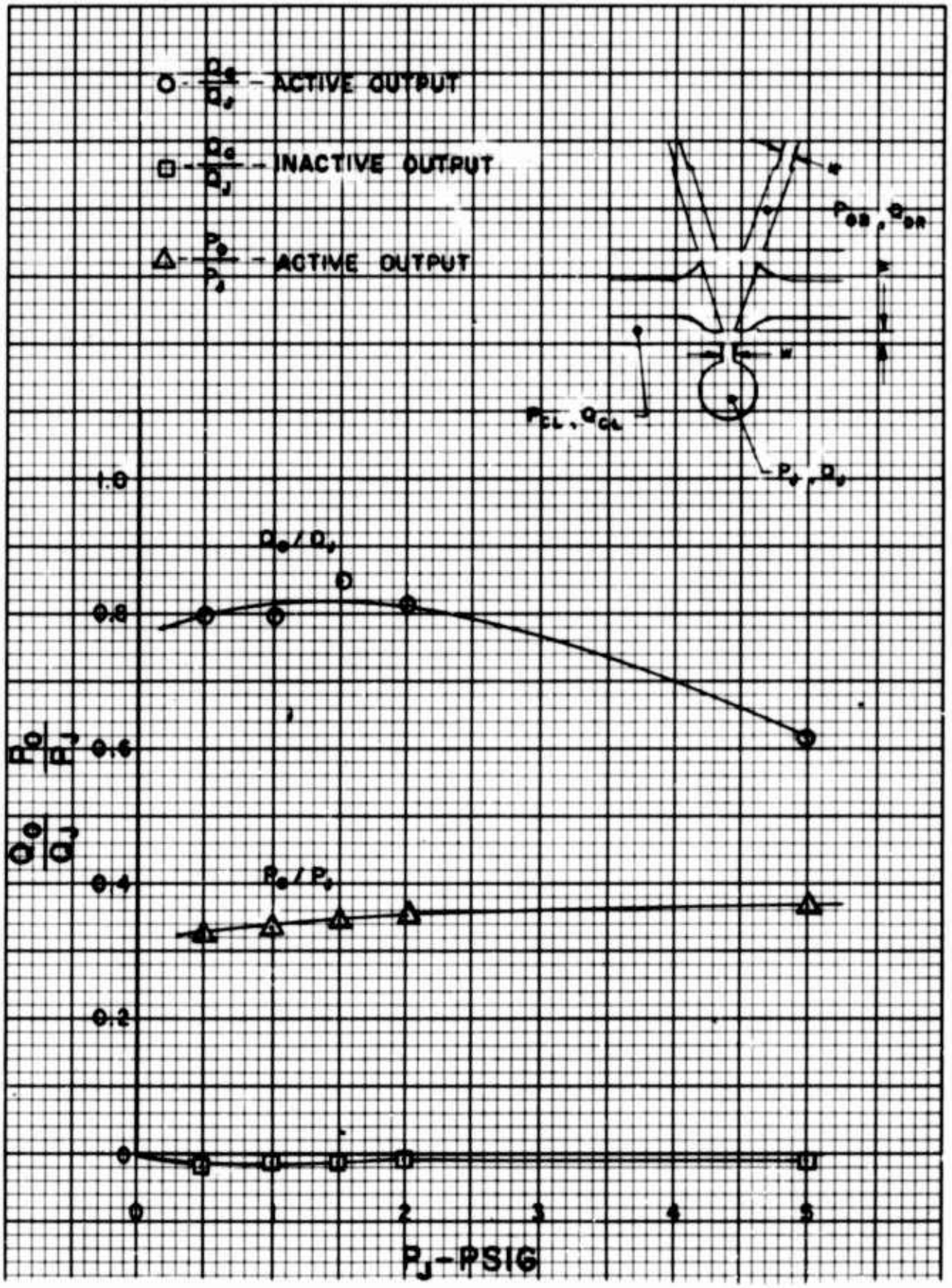

Figure 3. Flow and pressure at outputs with open controls.

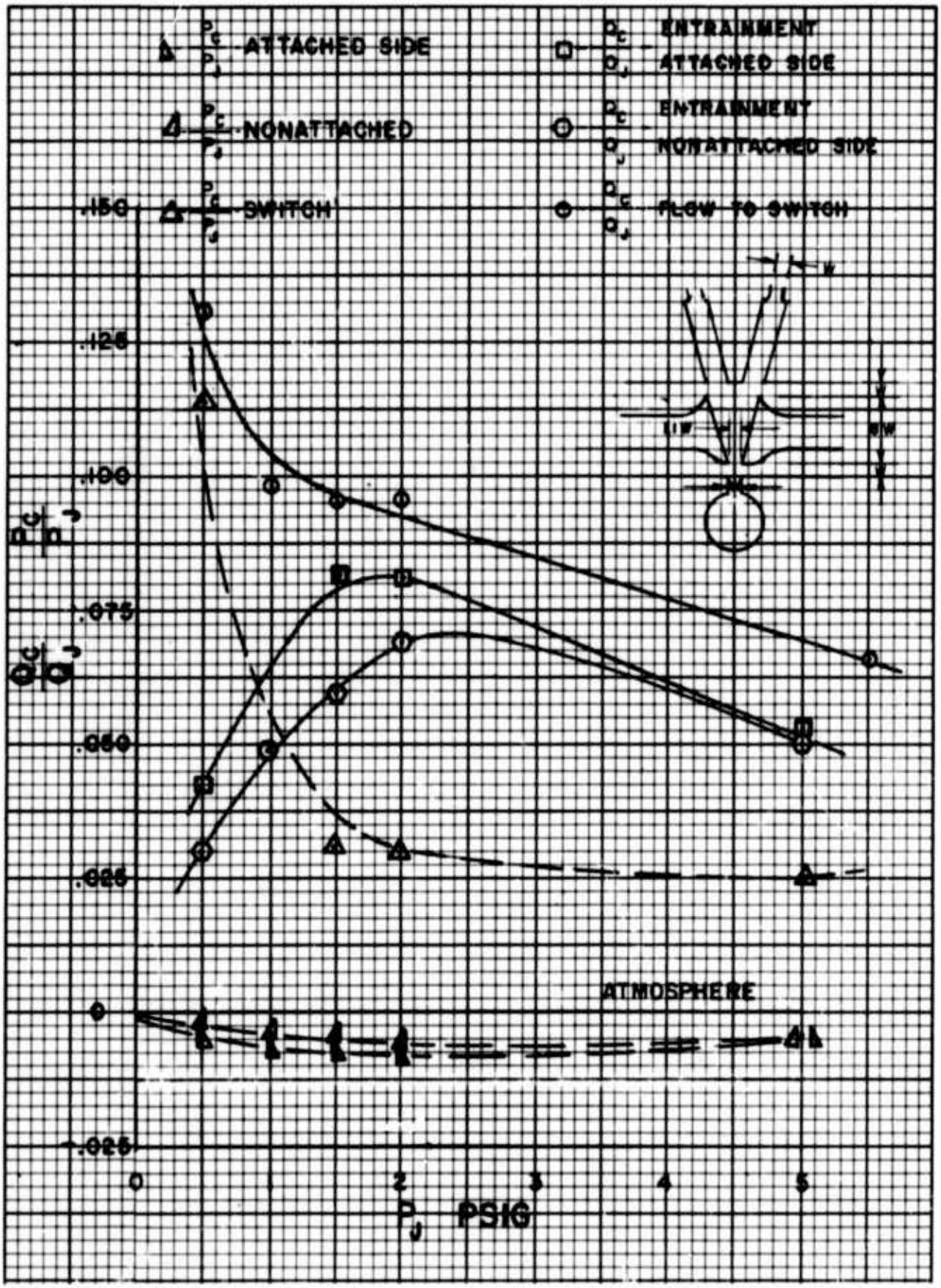

Figure 4. Flow and pressure in controls at steady state and switching conditions.

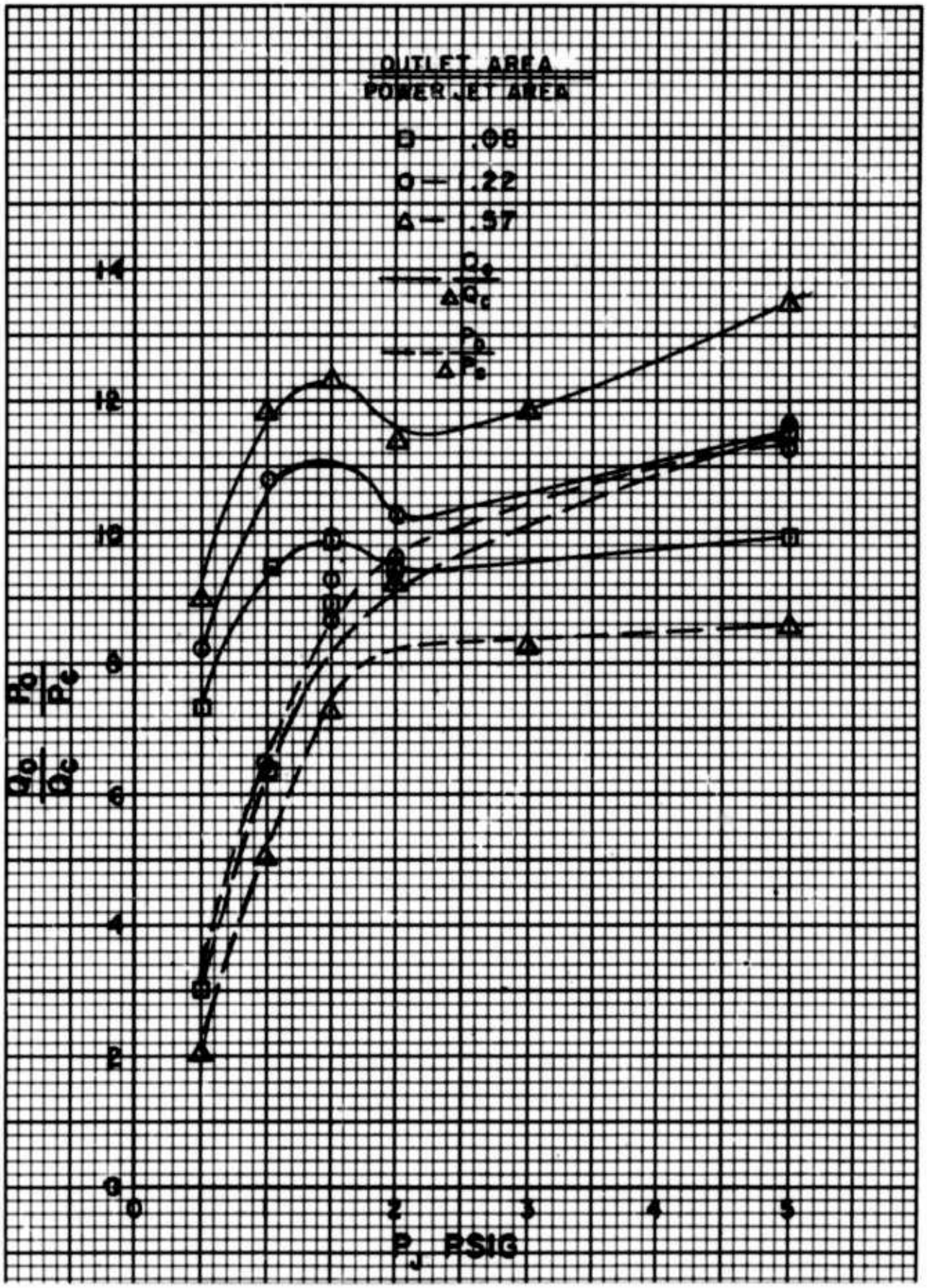

Figure 5. Ratio of control flow and pressure at switching to output flow and pressure.

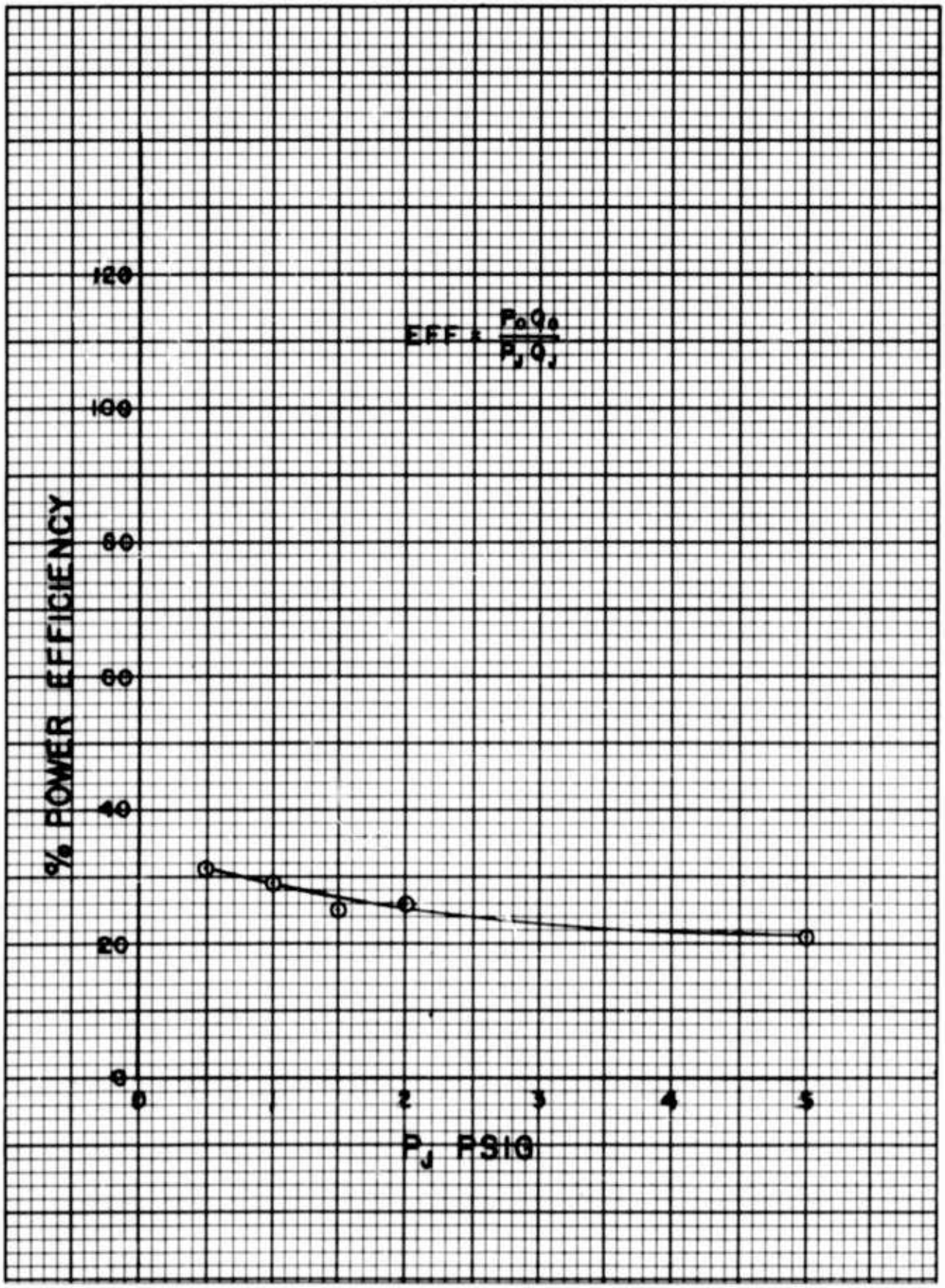

Figure 6. Efficiency.

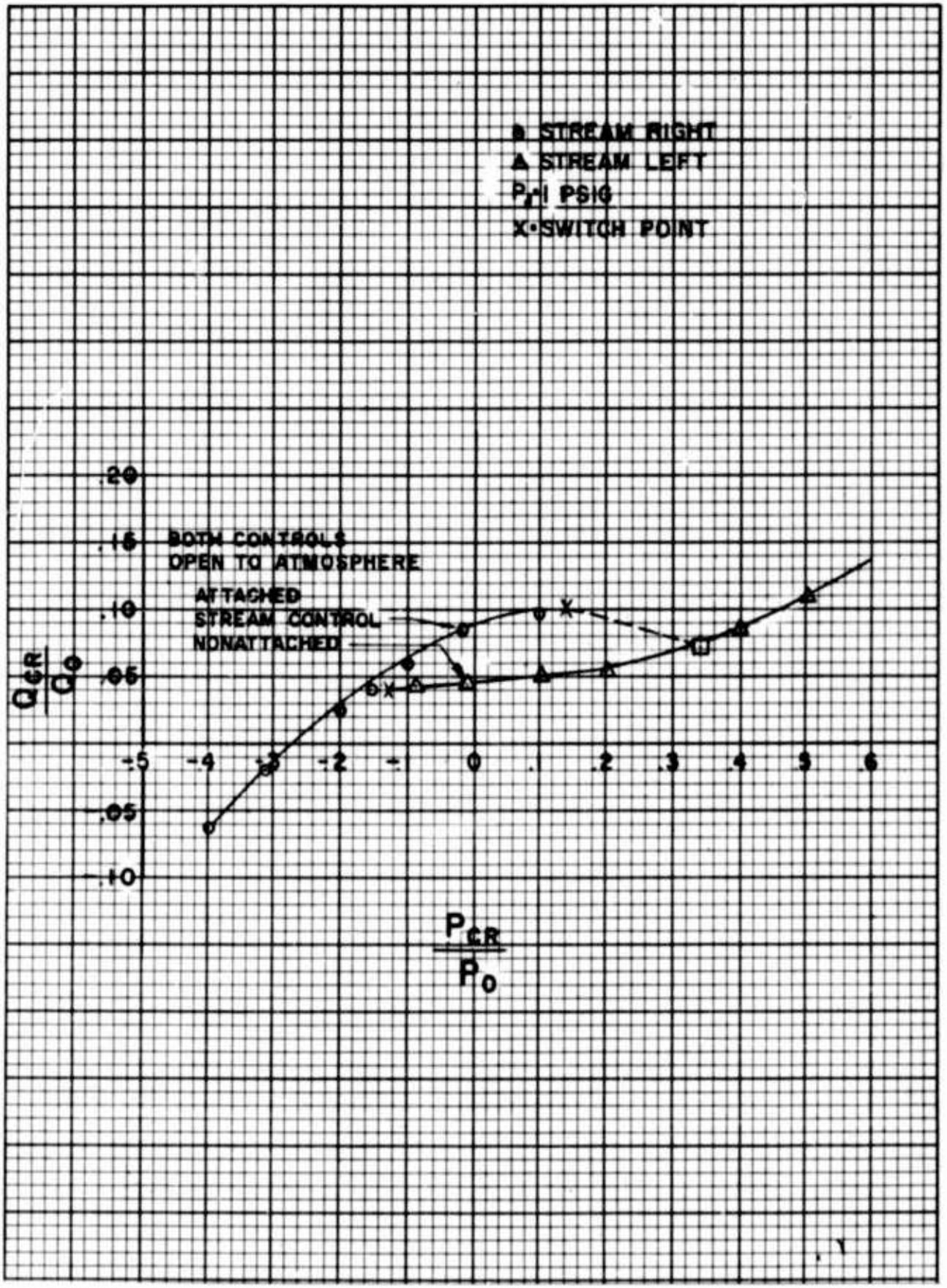

Figure 7. Impedance of control with opposite control open to atmosphere.

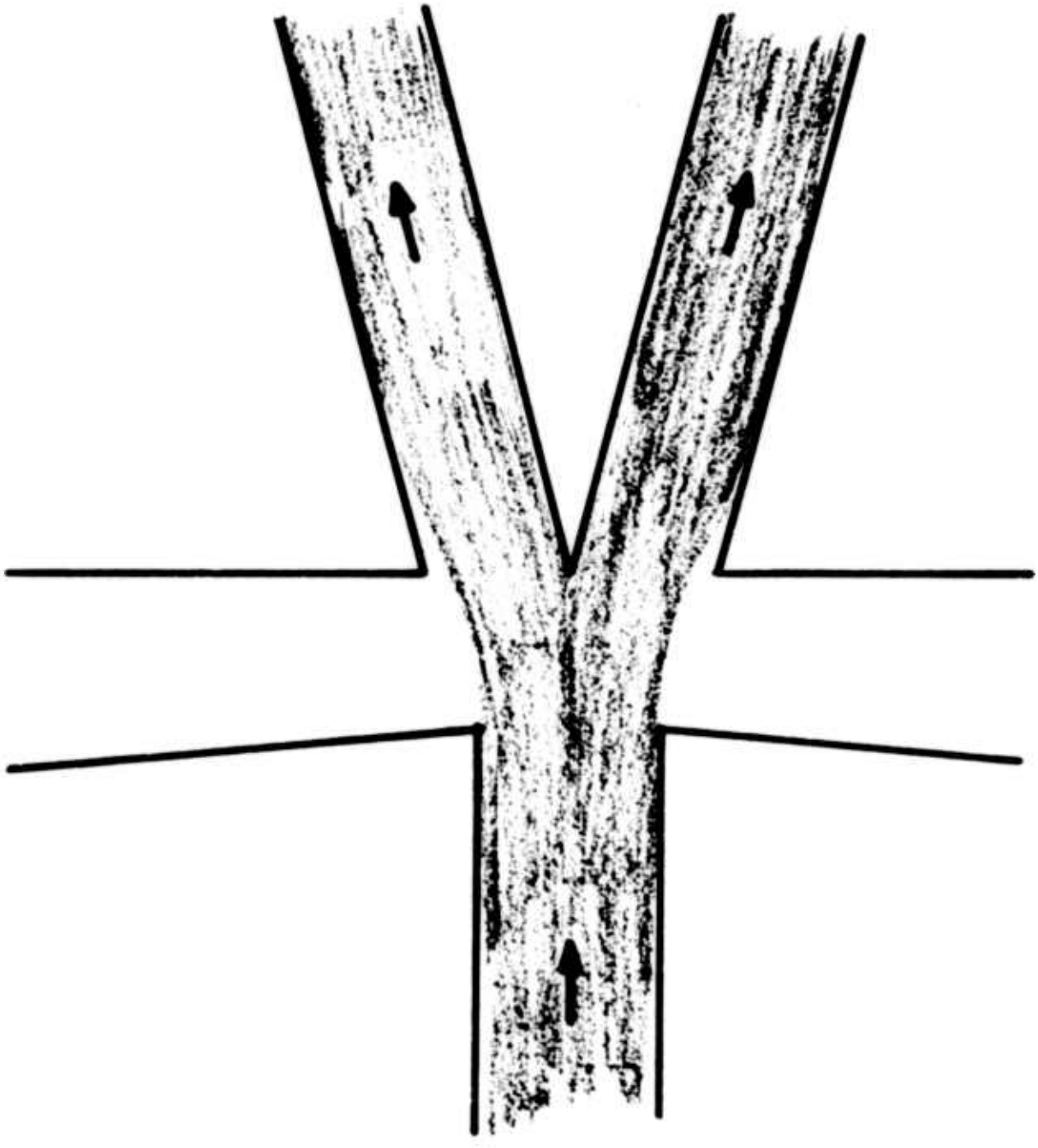

Figure 8. "Y" stream divider with bleeds.

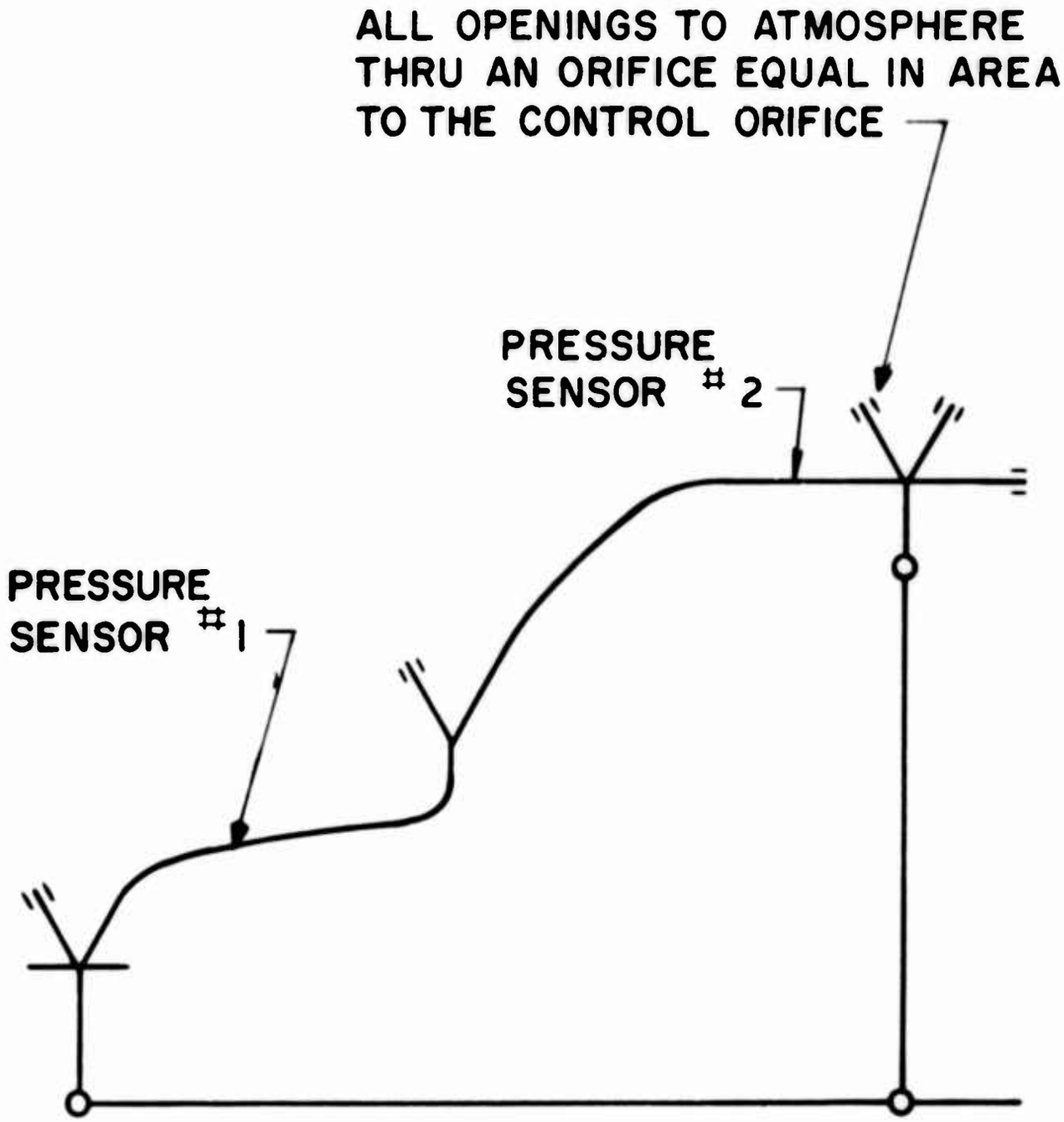

Figure 9. Pressure sensor arrangement.

Fig 10 Output Pressure Traces

Without Bleeds in Stream Divider

With Bleeds in Stream Divider

HARRY DIAMOND LABORATORIES
WASHINGTON 25, D. C.

STAGING OF CLOSED PROPORTIONAL FLUID AMPLIFIERS

by

GARY L. ROFFMAN

ARMY MATERIEL COMMAND DEPARTMENT OF THE ARMY

ABSTRACT

A method of staging a closed proportional fluid amplifier for large flow gain is discussed. The amplifier, of which all stages are similar, was designed by considering momentum and continuity of the fluid between stages. The gain of each stage, which is equal to the ratio of the power nozzle area of a stage to the power nozzle area of the previous stage, is calculated to be 5.7.

INTRODUCTION

To demonstrate the feasibility of high gain proportional fluid amplification, a five stage fluid amplifier was designed and built at HDL. The design of the amplifier required many simplifying assumptions because of the complexity of the flow in the amplifier. B. M. Horton designed the amplifier, and he and S. J. Peperone built and tested the model. This paper is based on their work.

The following criteria were used in the design:

(1) The unit must be entirely self-inclosed except for power inputs, first stage control inputs, and last stage outputs.

(2) All power nozzles should be at the same pressure. This is not, of course, necessary but is convenient.

(3) All stages must be geometrically similar.

(4) Stages must be matched in terms of deflection, that is when one stage is fully deflected, all stages are fully deflected. Thus, no stage is overdriven and the full output of the amplifier can be used. If the actual gain per stage is less than the calculated gain, the last stage can be only partially deflected when the first stage is completely deflected, which is, of course, highly undesirable. On the other hand if the true gain is greater than the calculated gain, the last stage can be fully deflected. Therefore, it is better to overestimate rather than underestimate losses.

(5) The diffuser apertures (collectors) are chosen to pass all the flow of the power and control nozzles when the power jet is fully deflected.

An aperture width to just pass the flow was chosen, since a larger aperture would produce frictional losses and a smaller one would cause loss of gain because of flow leaving from the other aperture.

The following assumptions were used in the design:

(1) Incompressible flow is assumed.

(2) The static pressure throughout all the stages is assumed to be ambient pressure so that the total pressure in terms of gage pressure is the same as the dynamic pressure. This is a convenient assumption, which should be approximately correct as long as wall friction is neglible and flow is subsonic.

(3) A pressure loss of one-half from the power nozzle to the collection aperture is assumed when the stream is fully deflected. Horton measured pressure losses of this order for splitter to power nozzle distances.

(4) The distance from the splitter to the power nozzle is chosen as six nozzle widths for the following reasons:

If the deflected power stream were to retain all of its energy regardless of distance, then the longer the distance the stream travels, the more its deflection when it reaches the output apertures and consequently the higher the gain. On the other hand the power stream profile changes, which tends to decrease the energy with increasing splitter distance. It follows that there must be some optimum splitter distance for which gain is a maximum. Horton estimated a distance of about six nozzle widths as the optimum distance.

(5) The diffuser (i.e., the passage from the collecting aperture of one stage to the control of the next) is of constant area and is assumed lossless. This assumption is not quite accurate, because aside from the loss due to wall friction, which is probably

small, there may be an appreciable loss due to the fact that the velocity profile continues to change within the diffuser. A more accurate analysis should divide the 50 percent loss between the interaction region and the diffuser.

THEORETICAL DEVELOPMENT

When the power stream is deflected by the control stream, the tangent of the deflection angle is given approximately by the ratio of the momentum flux difference of the two control nozzles to the momentum flux of the power nozzle. For a fully deflected stream, the momentum flux ratio, or deflection angle for complete deflection when the deflection is small, is defined as r_m. The momentum ratio, which is the same for all stages, can be written as

$$r_m = \frac{\rho A_2 V_2^2}{\rho A_1 V_1^2} , \tag{1}$$

where ρ is the fluid density, V is the fluid velocity, A is the nozzle area, and the subscripts 1 and 2 refer to the power and control nozzles, respectively. Since the velocity equals the volume flow u divided by the nozzle area A for incompressible flow, r_m becomes

$$r_m = \frac{A_1}{A_2}\left(\frac{u_2}{u_1}\right)^2 . \tag{2}$$

Since the areas of the control and power nozzles are fixed, the ratio of the power nozzle flow to the control nozzle flow, when the power stream is fully deflected, is fixed and is defined as

$$r_f = \frac{u_2}{u_1} . \tag{3}$$

Substituting equation (3) into equation (2) gives

$$r_m = \frac{A_1 r_f^2}{A_2} \tag{4}$$

or $$a \equiv \frac{A_2}{A_1} = \frac{r_f^2}{r_m} \, .$$

The flow in any stage is referred to by the subscript j. . The next stage is referred to by the subscript j+1. In referring to the j-stage power nozzle, the subscripts 1,j are used. In referring to the j-stage control nozzles, the subscripts 2,j are used. Continuity requires that the power and control nozzle flow of the j-stage is the control nozzle flow of the j+1 stage, when the j-stage is fully deflected. Using the notation given above, the continuity equation for flow between stages is

$$u_{2,j+1} = u_{1,j} + u_{2,j} \, , \tag{5}$$

where u is the volume flow. Using equation (3), equation (5) becomes

$$u_{1,j+1} r_f = u_{1,j} + u_{1,j} r_f \tag{6}$$

or $$\frac{u_{1,j+1}}{u_{1,j}} = \frac{1+r_f}{r_f} \, .$$

The ratio of power outputs of two adjacent stages is defined as

$$G = \frac{u_{1,j+1} \, p_{1,j+1}}{u_{1,j} \, p_{1,j}} \, , \tag{7}$$

where p_1 is the power nozzle pressure. Substituting equation (6) into equation (7) gives

$$G = \left(\frac{1+r_f}{r_f}\right) r_p \, , \tag{8}$$

where r_p is the ratio of power nozzle pressures of adjacent stages. If we assume that power nozzle pressures are the same, r_p is equal to unity and solving equation (8) for r_f gives

$$r_f = \frac{1}{G-1} \quad . \tag{9}$$

Bernoulli's equation can be written as $P = \frac{\rho V^2}{2}$ according to assumption 2. Using Bernoulli's equation and letting $r_p = 1$, equation (7) becomes

$$G = \frac{A_{1,j+1}}{A_{1,j}} \quad . \tag{10}$$

Again using Bernoulli's equation (7) becomes

$$r_m = \frac{P_2 A_2}{P_1 A_1} \quad . \tag{11}$$

Now the control pressure p_2 of any stage is equal to the pressure recovered in the aperture of the previous stage. Since a pressure recovery of one half is assumed and since the power jet pressure of the previous stage is also p_1, it follows that:

$$r_m = \frac{P_1/2\, A_2}{P_1 A_1} \tag{12}$$

or $$r_m = \frac{a}{2} \quad .$$

Let the aperture width be b times the power nozzle width. Then, since the height of the aperture in any stage is the same as the height of the power nozzle for that stage, the aperture area for any stage is also b times the power nozzle area for that stage.

Thus

$$a = \frac{A_{2,j+1}}{A_{1,j+1}} = \frac{b A_{1,j}}{A_{1,j+1}} \tag{13}$$

or using equation (10)

$$G = \frac{A_{1,j+1}}{A_{1,j}} = \frac{b}{a} .$$

If the stages are scaled in three dimensions, using the linear scaling factor s, then:

$$S = \sqrt{\frac{b}{a}} = \sqrt{G} . \tag{14}$$

It is seen that fixing the diffuser to power nozzle area ratio fixes the scaling factor. From figure (1) it can be seen that the angle for complete deflection for small deflection angles is

$$\gamma_M = \frac{b W_{1,j}}{2L} , \tag{15}$$

where $W_{1,j}$ is the width of the power nozzle, L is the length from interaction area to the splitter, and b is the ratio of the diffuser area to power nozzle area. The value of L depends on the width of the control nozzle, since L is usually defined as the distance from the power nozzle to the splitter minus half the width of the control nozzle. Therefore, L can be written as

$$L = 6 W_{i,j} - \frac{a W_{1,j}}{2} . \tag{16}$$

Combining equations (15) and (16)

$$\gamma_M = \frac{b}{2\left(6 - \frac{a}{2}\right)} . \tag{17}$$

Equations (4), (9), (12), (13) and (17) are five independent equations with five unknowns. Solving for the variables in interest gives:

$$a = \frac{A_2}{A_1} \cong 0.3$$

$$b \cong 1.7$$

$$G \cong 5.7 \ ,$$

and the scale factor from equation (15) is

$$S = \sqrt{G} \cong 2.4 \ .$$

CONCLUSION

The calculations are based on a number of assumptions. The extent to which these assumptions are valid in a fluid amplifier determines the performance characteristics of the amplifier.

The effect of the staging method is to allow the greatest increase in area between stages and thus the greatest gain. This is accomplished by using all the fluid of one stage to completely deflect the next stage. Because of this assumption, the diffuser must be large enough to pass all the fluid entering a stage into the next stage.

If assumed losses are overestimated, the area scaling factor will be reduced and thus gain for large deflections will be lowered. The partial deflection of the first stage will not completely deflect the last stage. If the assumed losses are underestimated, the area scaling factor will be increased. The full deflection of the first stage will not completely deflect the last stage. Therefore, it is best to overestimate losses since full deflection of the last stage is desired.

One must not lose sight of the individual stages in a multi-stage amplifier. Unless each stage is properly designed, there is little chance of the amplifier working. One important design feature used by Horton in a five-stage amplifier consists of connecting both sides of the interaction region with a channel (figure 2). This channel increases the gain of the amplifier because it reduces negative feedback,

by preventing the buildup of pressure on the side of the amplifier toward which the power jet stream is being deflected, and provides a positive feedback path in the amplifier. The measured gain of the five-stage proportional amplifier is greater than the calculated gain by a factor of about 2 due to the effect of this positive feedback path. Because of this extra gain, the last stage is fully deflected by a partial deflection of the first stage.

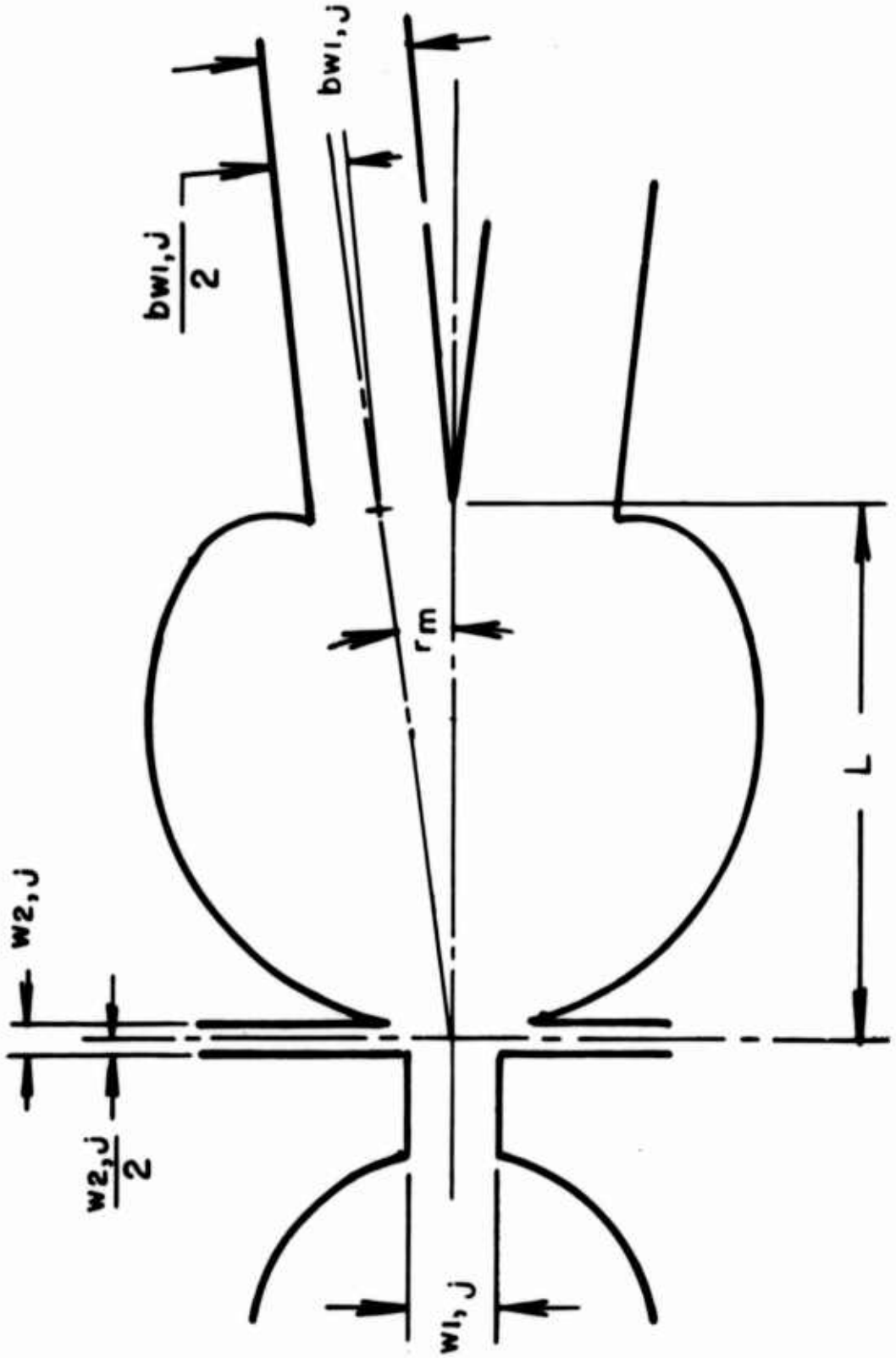

Figure 1: Angle for complete deflection of proportional fluid amplifier.

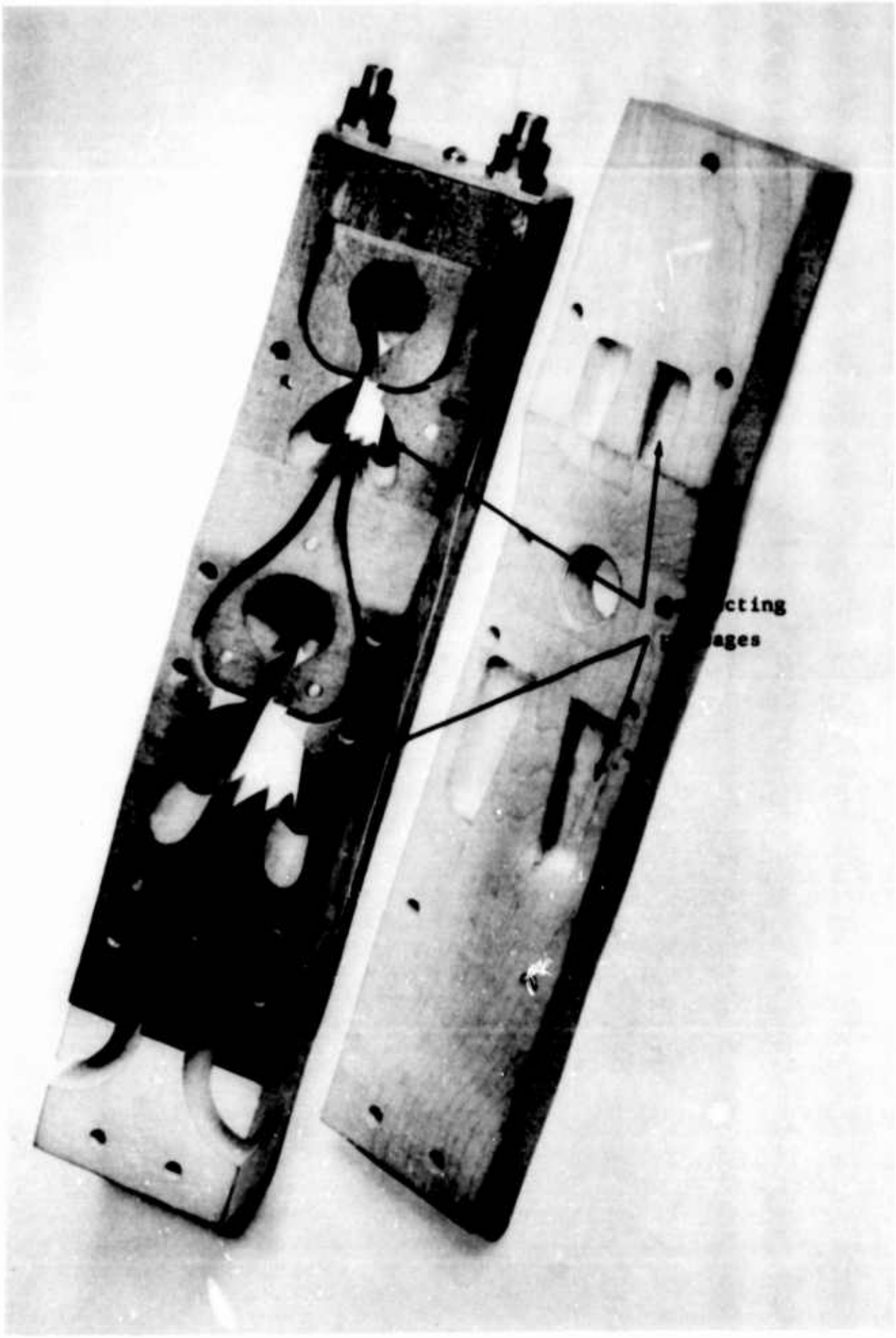

Figure 2. Interaction region connecting passages of proportional amplifier.

HARRY DIAMOND LABORATORIES
WASHINGTON, D. C. 20438

ANGULAR VELOCITY REGULATION WITH A FLUID INTERACTION SYSTEM

by

JOSEPH M. ISEMAN

ARMY MATERIEL COMMAND DEPARTMENT OF THE ARMY

PREFACE

This paper describes a portion of the work sponsored under MIPR No. 33-657-2-R&D-105 by the Air Force Propulsion Laboratory of the Aeronautical Systems Division at Wright-Patterson Air Force Base (WPAFB), Ohio, and investigated by the Harry Diamond Laboratories. The general objective of this work is to provide basic technology in the control of advanced turbo-compressor jet engines with pneumatic (or fluid) techniques using no moving parts. The general guidance and review of the objectives and progress by C. Bentz and other Air Force staff members is gratefully acknowledged.

This method of speed regulation was conceived by Silas Katz, who worked together with the author on the initial phases of this project.

ABSTRACT

A two-position control system using no moving parts to regulate the angular velocity of a turbine has been constructed and evaluated. The experimental model uses the two outputs of a bistable fluid amplifier as correction jets, one tending to drive (speed up) a turbine, one tending to load (slow down) the turbine. The amplifier is appropriately switched by the outputs of a pneumatic angular velocity sensor, so that the turbine speed is varied continuously between speeds 2 percent faster and 2 percent slower than a nominal, desired speed. The switching characteristics of the bistable fluid amplifier, and design and operation of the sensor and transmission lines are described and analyzed.

NOMENCLATURE

		Units
a	Velocity of sound	ft/sec
$A(t)$	Illuminated area function	ft^2
c_s	Velocity of propagation of pressure shock front	ft/sec
L	Length of the delay line	ft
L_f	Length of the delay line for the fast pulse	ft
L_s	Length of the delay line for the slow pulse	ft
$\dot{m}$	Mass flow	lbm/sec
$\dot{m}_c$	Mass flow through control nozzle	lbm/sec
$\dot{m}_e$	Mass flow entrained by the power jet	lbm/sec
$\dot{m}_f$	Mass flow in the fast collector	lbm/sec
$\dot{m}_r$	Returned mass flow	lbm/sec
$\dot{m}_s$	Mass flow in the slow collector	lbm/sec
M_{min}	Minimum mass of one control pulse required to switch the bistable amplifier	lbm
p_B	Bubble pressure	psig
p_∞	Ambient pressure	psig
p_o	Stagnation pressure of the signal in the fast collector	psig
p_1	Pressure behind diaphragm (supply pressure)	psig
p^+	Pressure of the air source	psig
Δp	Change of pressure inside the low pressure bubble	psig
ΔP	Change in power to the turbine wheel	ft-lbf/sec
R	Gas constant for air	53.3 $lbm\text{-}ft^2/sec^2/°R$

t	Time	sec
t_p	Width of the generated pulse	sec
t_r	Pulse rise time	sec
T	Absolute temperature	^{o}R
U	Volume of the low pressure bubble	ft^3
v	Velocity of the fluid pulse in the delay line	ft/sec
$v(t)$	Velocity at the end of the delay line	ft/sec
γ	Ratio of specific heats	
θ	Angle or angular displacement	deg
θ_A	Angular width of slot illuminating the emitters	deg
θ_C	Angular width of the fast and slow collectors	deg
θ_E	Angular width of the emitters	deg
θ_f	Angular width of slot illuminating fast collectors	deg
θ_s	Angular width of slot illuminating slow collectors	deg
θ_1	Angular displacement of slow slot	deg
θ_2	Angular displacement of fast slot	deg
ρ	Density	lbm/ft^3
τ	Delay time due to delay line	sec
ω	Angular velocity	deg/sec
ω_a	Angular velocity equivalent to beginning of slow pulse	deg/sec
ω_b	Angular velocity equivalent to beginning of fast pulse	deg/sec
ω_d	Set-point angular velocity	deg/sec

ω_f	Angular velocity equivalent to threshold of bistable amplifier for fast control	deg/sec
ω_ℓ	Lower angular velocity	deg/sec
ω_s	Angular velocity equivalent to threshold of bistable amplifier for slow control	deg/sec
ω_u	Upper angular velocity	deg/sec

Subscripts

d	Desired
f	Fast
ℓ	Lower
m	Maximum
s	Slow
u	Upper

1. INTRODUCTION

A two-position system (fig. 1) using a bistable fluid amplifier to control the angular velocity of a turbine wheel was designed and tested. One output of the amplifier is used as a correction jet tending to drive the turbine; the other, tending to load it. When the turbine reaches a velocity ω_u, while being driven, the amplifier is switched to the other output, which loads the turbine. When the velocity decreases to the lower velocity ω_ℓ, while under load, the amplifier is switched to the output driving the turbine. A pneumatic angular velocity sensor (fig. 2) supplies the necessary switching pulses. Operation continues in this fashion as long as air is

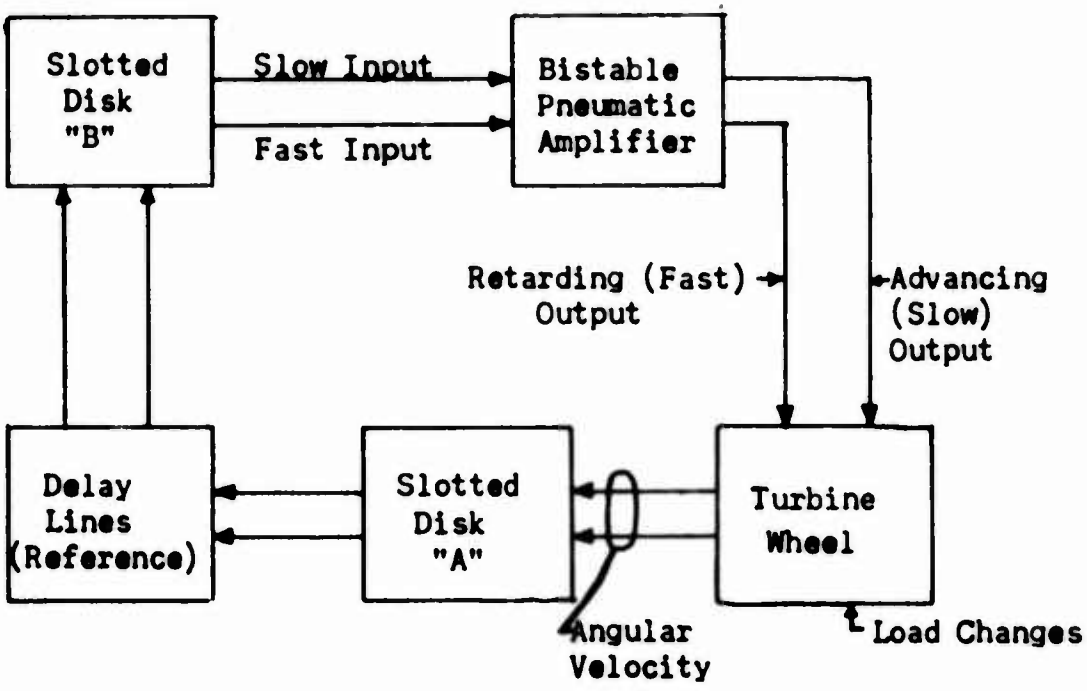

FIGURE 1: SYSTEM BLOCK DIAGRAM

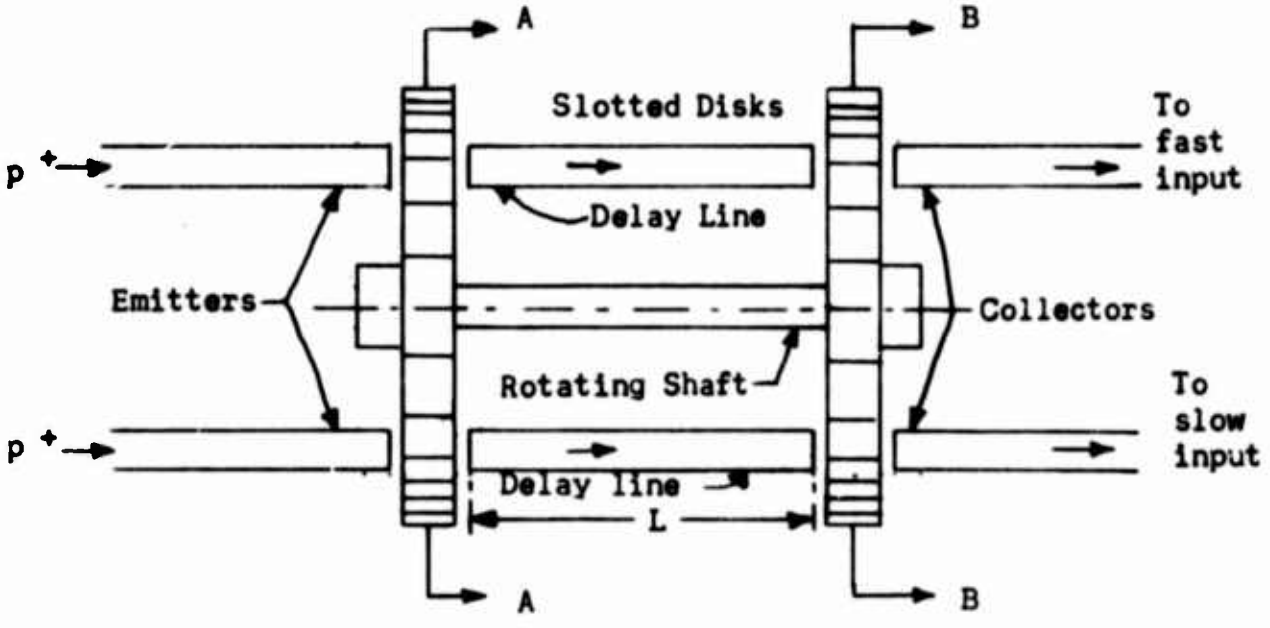

FIGURE 2: ANGULAR VELOCITY SENSOR

supplied to the control system so that velocity varies about a nominal, desired set-point ω_d.

The idealized responses of the unloaded turbine to a step change in power ΔP, and to step regulation $\pm \Delta P$, are shown in figure 3. Comparison of figures 3a and 3b shows the effect of an increase in the differential gap $(\omega_u - \omega_\ell)$. Comparison of figures 3a and 3c shows that the effect of an increase in ΔP is merely to increase the regulating frequency, leaving the differential gap unchanged.

In principle, the angular velocity sensor (fig. 2) comprises two disks A and B, with a slot in each, rigidly attached to the turbine shaft. Two jets of air (emitters) continuously impinge on disk A and a pulse enters each delay line whenever the slot in disk A permits. The pulse passes through the delay line and arrives at disk B after a delay characteristic of the length of the delay line and the pulse velocity. The distance that the slot in disk B moves from the moment the pulse enters the delay line to the moment it reaches the end of the line depends on the angular velocity of the disk. Obviously, a pulse appears in the collector only when a pulse and a slot arrive simultaneously at the end of the delay line. Hence, the length of the delay lines, the pulse velocity, or the position of the slots can be adjusted to obtain pulses of flow in the collectors, sufficient to actuate control; in this case, at two angular velocities, $\omega_s \geq \omega_\ell$ and $\omega_f \leq \omega_u$. The greater-than and lesser-than signs represent any delay from the time the pulse

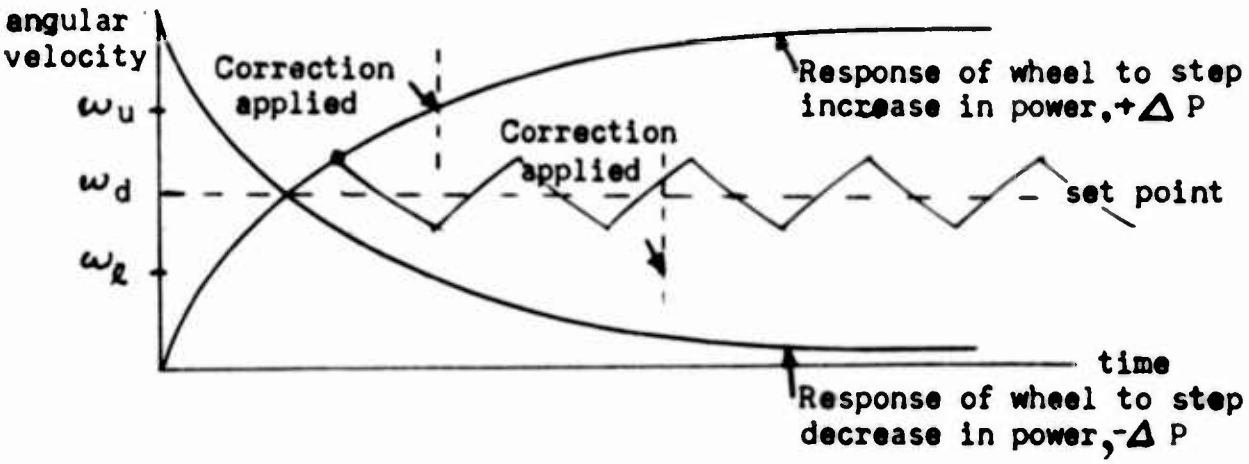

Figure 3a) Turbine wheel response for ω_u, ω_ℓ, and ΔP

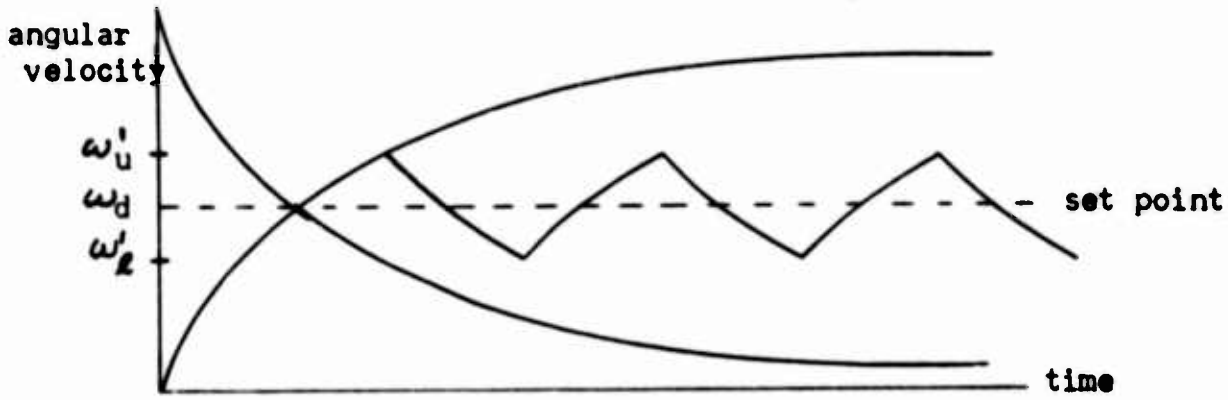

Figure 3b) Response for $\omega'_u > \omega_u$, $\omega'_\ell < \omega_\ell$ and $\Delta P' = \Delta 1$

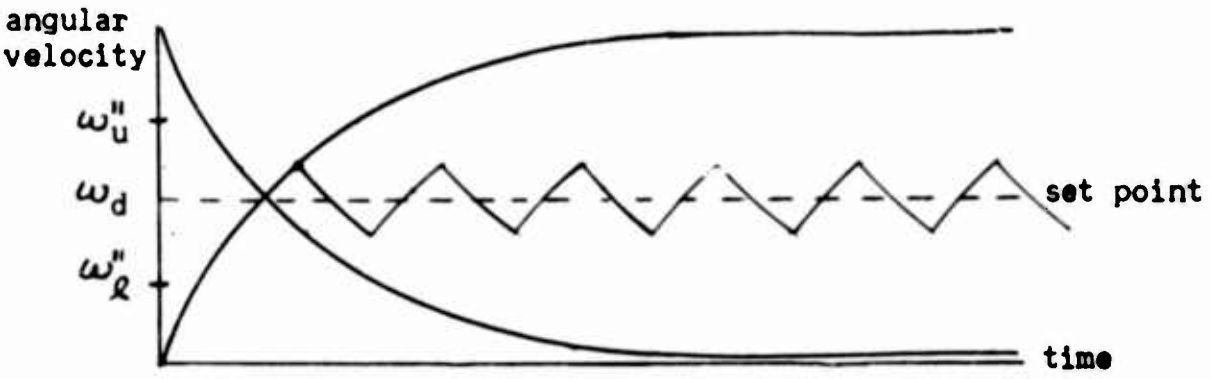

Figure 3c) Response for $\omega''_u = \omega_u$, $\omega''_\ell = \omega_\ell$ and $\Delta P'' > \Delta P$

FIGURE 3: IDEALIZED TURBINE WHEEL RESPONSE FOR TWO POSITION CONTROL SYSTEM

is supplied into the collector to the time power at the turbine is reversed. These principles may be applied in an angular velocity sensor using only one slotted disk with both emitters and both collectors on one side, and with delay lines looped 180 deg on the other side (fig. 4). In this case, the pulse must pass through the same disk twice before being supplied to the bistable fluid amplifier.

The system with a turbine was constructed merely to demonstrate the feasibility of the control system and to provide a model adequate for analysis and experimentation. These analyses and results of experiments are presented in this report. The sensor used was designed with a single disk, and its operation is described in section 2 with particular emphasis on the pulse characteristics. The bistable fluid amplifier was used rather than a proportional amplifier because it can provide at least one order of magnitude more power gain per stage than a proportional amplifier. Also, it is difficult to generate a sizeable pneumatic signal that is proportional to angular velocity, which makes it difficult to apply proportional amplifiers in a system of this type.

2. SYSTEM OPERATION

2.1 Bistable Amplifier

When the bistable element (fig. 5) is in one of its equilibrium positions, a low pressure ($p_B < p_\infty$) bubble is formed. Under

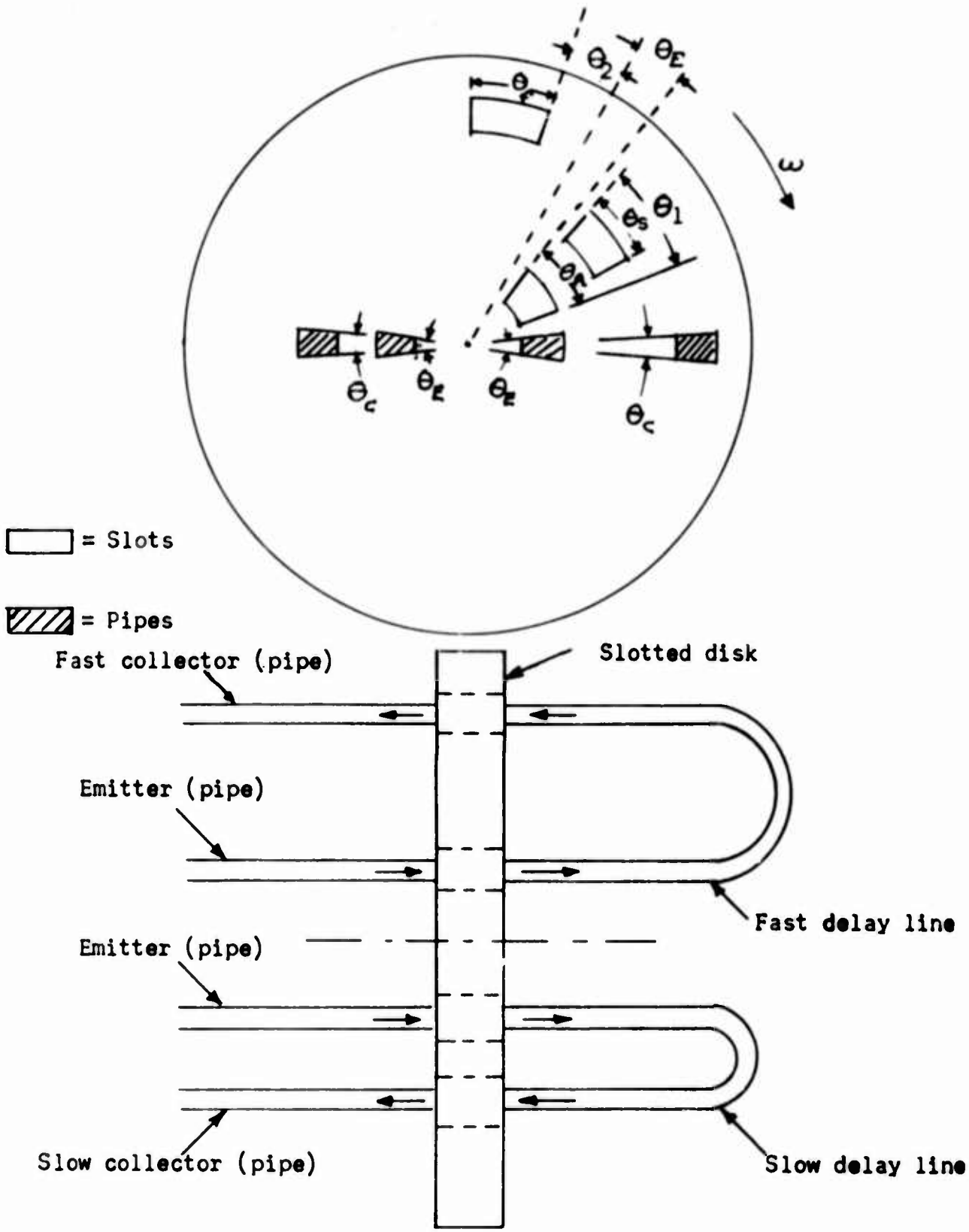

FIGURE 4 PHYSICAL LAYOUT OF SLOTTED DISK, EMITTERS, DELAY LINES, AND COLLECTORS

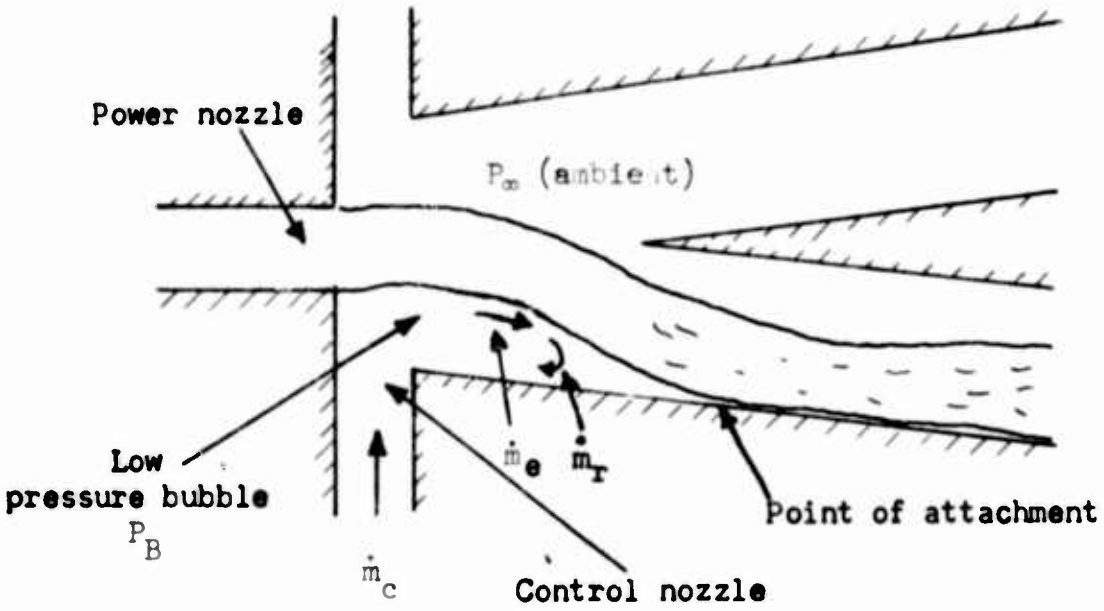

FIGURE 5: BISTABLE FLUID AMPLIFIER

equilibrium conditions, the mass flow into the bubble is equal to the mass flow out of it. The mass flow out of the bubble $\dot{m}_e$ is the flow entrained by the power jet as it moves downstream. The mass flow in consists of fluid drawn in through the control nozzle $\dot{m}_c$ and a portion of the entrained fluid $\dot{m}_r$ being returned.

When the pressure due to the signal pulse into the low pressure bubble increases the bubble pressure above the ambient pressure, the jet switches to the second equilibrium position. The amount of flow necessary to switch may be determined as follows: The pressure change required is

$$p_\infty - p_B = \Delta p \ ,$$

which may be expressed by the equation of state as

$$\Delta p = \left(\int \dot{m}\, dt \right) RT/U \,, \qquad (1)$$

where R = the gas constant

T = the absolute temperature

U = the volume of the low pressure bubble

By making the simplifying assumption for the volume,

$$U = \text{constant}$$

then equation (1) may be written as

$$M_{min} = \int \dot{m}\, dt = \text{constant} \,, \qquad (2)$$

where M_{min} is the minimum mass needed to switch the amplifier of fixed geometry, power jet, and loading conditions. Test data (fig. 6) shows mass required to switch the bistable amplifier remains approximately constant.

In figure 7a, the two angular velocities ω_c and ω_s are shown as the intersections of the curves of mass flow into the controls of the bistable amplifier and the curve M_{min}, the threshold mass for switching the amplifier. To reduce the differential gap, $(\omega_u - \omega_l)$, more switching mass can be introduced into the system to give the ω versus mass steeper slopes. Also the curves may be shifted (fig. 7b) so that pulses below the threshold for the slow signal begin at ω_a and pulses below the threshold for the fast signal begin at ω_b. Thus for smaller changes in ω, the threshold M_{min} is achieved. If the two mass curves of figure 7b intersect above the threshold level, there is sufficient mass entering the control region from both controls (180 deg apart) to cause the bistable element to oscillate

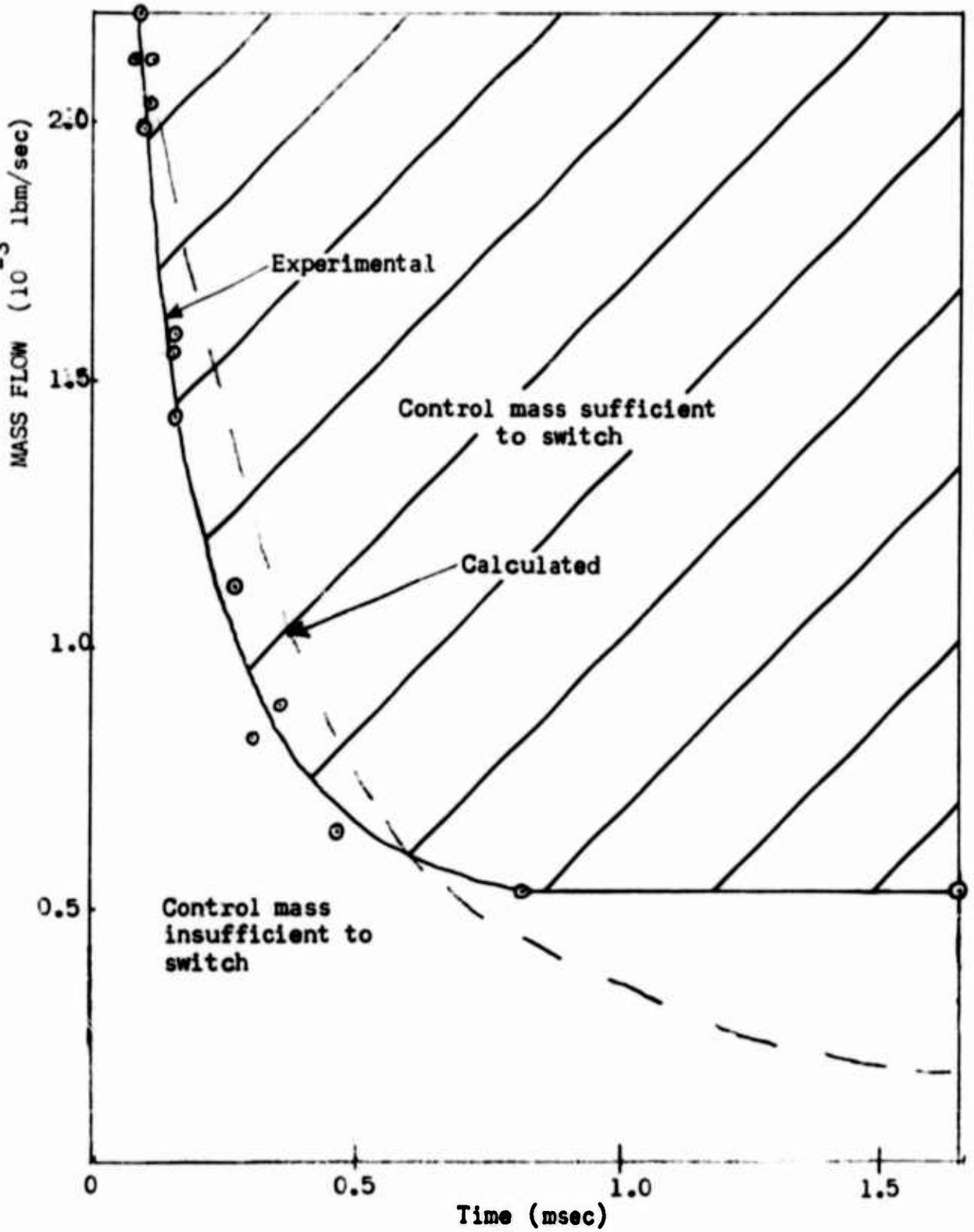

FIGURE 6: MASS FLOW REQUIRED TO SWITCH BISTABLE FLUID AMPLIFIER

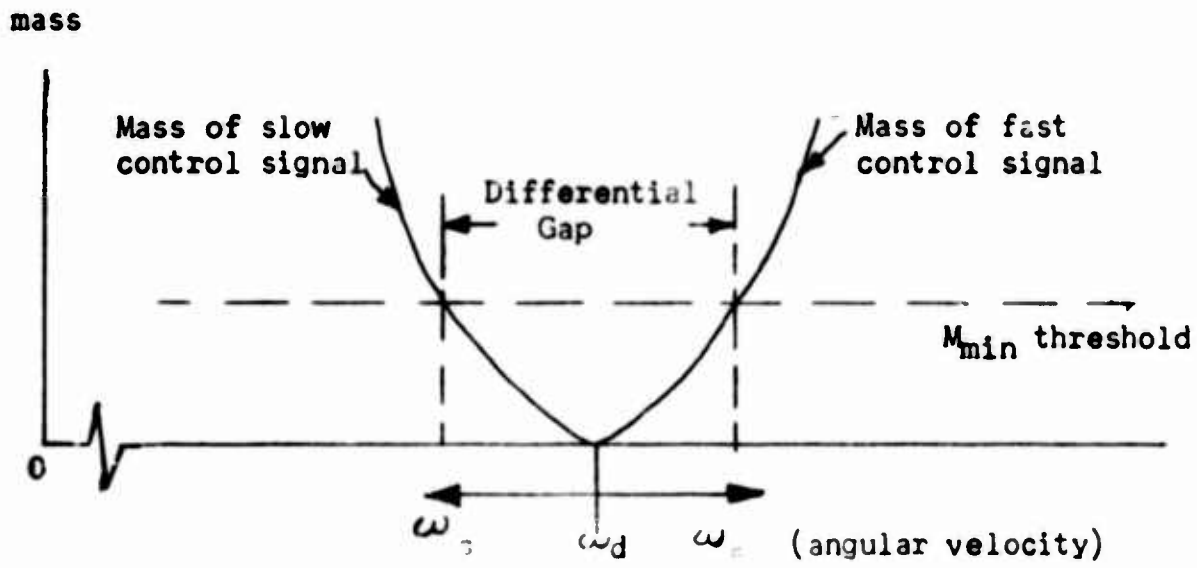

Figure 7a: Differential gap for mass flows of zero at ω_d

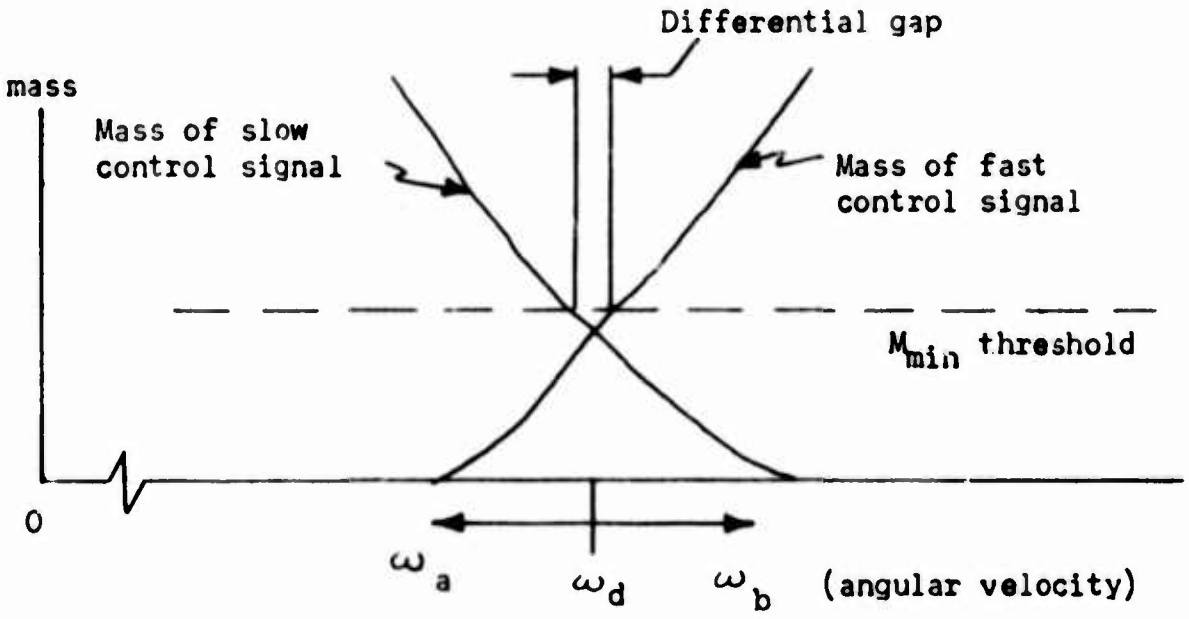

Figure 7b: Reduced differential gap

FIGURE 7 : DIFFERENTIAL GAP OF THE CONTROL SYSTEM

between its two outputs.

2.2 Angular Velocity Sensor and Pulse Generator

A diagram of the angular velocity sensor used is shown in figure 4. The ends of all pipes and slots are shaped as sectors of circular rings which have centers on the axis of rotation. As previously stated, air flows into the delay lines when slots in the disk permit, and continues into the collectors when arrival of the pulses and slots coincide. The transit time τ that a pulse requires to traverse a delay line may be expressed as

$$\tau = \frac{L}{v} \quad , \tag{3}$$

where L = length of delay line

v = velocity of fluid pulse.

During the interval τ the turbine is turning through an angle θ,

$$\theta = \omega\tau \quad , \tag{4}$$

where ω is the angular velocity.

Equations (3) and (4) can be combined to give the angular velocity as a function of θ, v, and L:

$$\omega = \frac{\theta v}{L} \quad . \tag{5}$$

In order to introduce the greatest possible mass into the collectors for any given angular velocity ω_f or ω_s, the total pressures of gas emanating from the emitters should be at 35 psig or slightly

higher. Therefore, the velocity of the outputs of the emitters $v = v(p^+)$ cannot be used as the main variable effecting a change in ω_f or ω_s; only L and θ may be used to obtain pulses at these angular velocities.

For a constant supply pressure, the magnitude and duration of the fluid signal depends upon the difference between the actual angular velocity and the ω_f or ω_s as the case may be. The mass flow into the collectors at any time is expressed as

$$\dot{m} = \rho\, A(t)\, v(t) , \qquad (6)$$

where $A(t)$ is the collector area exposed to the pulse as a function of time and $v(t)$ is the velocity of the pulse at the end of the delay line as a function of time, (see sec. 2.3) and ρ is the density.

It is convenient to express equation (6) in normalized form as

$$\frac{\dot{m}}{\dot{m}_m} = \frac{A(t)}{A_m} \quad \frac{v(t)}{v_m} , \qquad (7)$$

where it is assumed that the change in density is negligible, and where the subscript m indicates the maximum value.

2.3 Characteristics of Pulses in Delay Lines

Initial Pulse Shape

The pulse mass flow profile is a function of the shapes (fig. 4) of the slot θ_A, the emitters θ_E, and the openings of the delay lines θ_E. The pulse rise time t_r is the time required for the slot θ_A to expose the opening θ_E of the delay line completely.

Thus, the rise time is given by

$$t_r = \frac{\theta_E}{\omega} \quad . \tag{8}$$

The pulse width t_p is the total time that slot θ_A allows air to pass from the emitters into the delay lines, i.e., the total time that slot θ_A uncovers (illuminates) the emitters. The maximum angular displacement of the disk during illumination of an emitter is the sum of the angle θ_A and angle θ_E. Then, the pulse width is given by

$$t_p = \frac{\theta_A + \theta_E}{\omega} \quad . \tag{9}$$

The pulse falls off in amplitude during the same time interval as the rise time t_r (equation (8)); hence the initial pulse shape is trapezoidal.

As the pulse is transmitted through the delay line, its shape changes as a function of distance. The manner in which this change occurs may be seen as follows. The slot illuminates the emitter gradually and the delay line is also gradually filled by the flow of air (fig. 8). However, there is a rapid entrainment of air in a short distance along the delay line. Entrainment of the air into a flow completely filling the cross section of the delay line is accompanied by a reduction of dynamic pressure, and hence, a reduced velocity. When the slot illumination is complete, the flow velocity increases, and the cross section of the pipe becomes increasingly

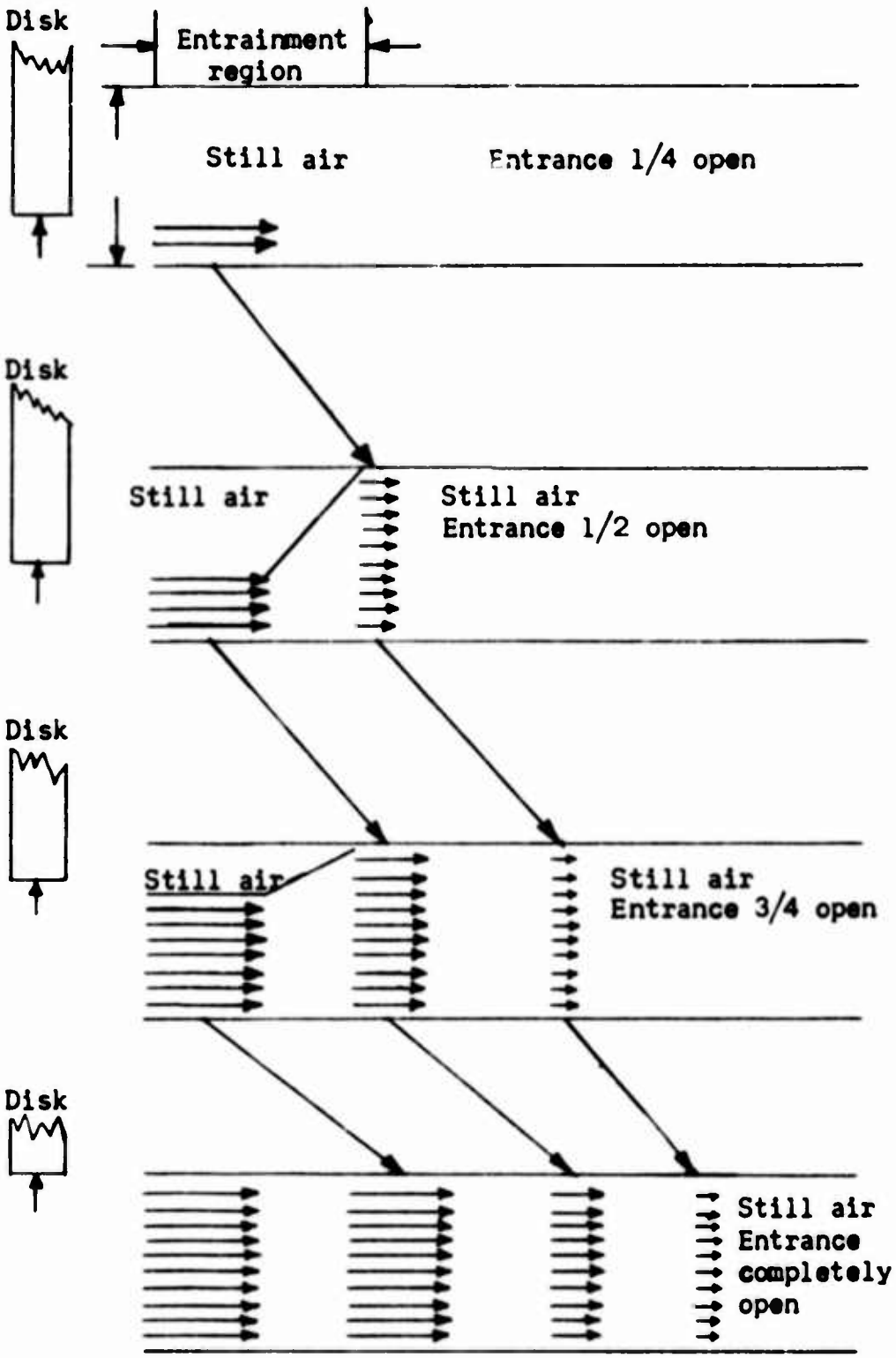

FIGURE 8 FORMATION OF A VELOCITY DISTRIBUTION IN THE DELAY LINES

filled with flow at maximum velocity. Since the higher velocity flow tends to overtake the lower velocity flow, the velocity profile of the front end of the pulse becomes steeper as it proceeds through the delay line.

Along the tail end of the pulse, there is a negative slope because the flow is gradually cut off, and the cross section becomes decreasingly filled. Therefore the velocity along the negative slope of the pulse decreases from a maximum value (when the emitter is fully illuminated) to zero (when there is no flow from the emitter into the delay line). Thus, the lower velocity air will lag an increasing distance behind the higher velocity air, extending the velocity profile of the rear end of the pulse.

Pulse Propagation Velocity

In evaluating v, the velocity of propagation of the pulses in the delay line, it should be noted that before slot θ_A starts to uncover the entrance to the delay line, the pressure in the delay line is much lower than the pressure in the emitter. When slot θ_A begins to uncover the delay line, the result is a pressure (shock) wave with a mean velocity of propagation (slightly supersonic) which precedes the mass flow of the pulse through the delay lines. The velocity c_s of the shock front in a shock tube may be calculated from equation (3.2) of reference 1

$$c_s = a\left[\frac{\gamma - 1}{2\gamma} \quad \frac{\gamma + 1}{2\gamma} \frac{p_\infty}{p_1 + p_\infty}\right]^{1/2}, \qquad (10)$$

where $p_\infty/(p_1 + p_\infty)$ is the absolute pressure ratio across the shock front, a is the sonic velocity under the test conditions (1128 ft/sec) and γ is the ratio of specific heats. Taking $p_\infty/(p_1 + p_\infty) = (25 \text{ psia}/15 \text{ psia})^* = 5/3$ gives a predicted result that the velocity of propagation of the shock front is 1421 ft/sec. The latter result agrees closely with a measured value of 1450 ft/sec.

It should be noted that the velocity of the flow behind the shock front is slower than that at the shock front. By equation (3.25a) of reference 1, the velocity v of the flow may be calculated

$$v = a \frac{p_\infty}{p_1 + p_\infty} - 1 \sqrt{\frac{2 - \gamma}{\left[(\gamma + 1) p_\infty/(p_1 + p_\infty)\right] + (\gamma - 1)}} . \qquad (11)$$

The velocity of the flow is 421 ft/sec. Therefore, for each foot of delay line, the flow will lag the shock front by approximately 2.3 msec.

2.4 Characteristics of the Collector Pulse

The velocity pulse shape emanating from the delay line is a function of the length of the delay line, and the illumination of the collector area is a function of the angular velocity of the disk.. These two functions are convoluted as given in equation (7) to give the pulse shape in the collector. The pulses in the fast

---

* The p^+ of 35 psi drops to approximately 10 psig when the flow traverses the first gap between the emitters and the delay line. Actually any gap of 1/4 in. causes a pressure drop of about 2/3.

and slow collectors may be computed as follows.

The pulse shape at the end of the delay lines is assumed to be as described in the previous sections. However, in calculating the pulse shape in the collector, two assumptions are made: (1) the rise time is assumed to be instantaneous; and (2) the trailing edge is taken to be of duration θ_E/ω.

Slow Signal Pulse Shape

If the disk is turning at or less than the slow threshold rate ω_s, the pulse of threshold-or-greater magnitude passes through slot θ_s (fig. 4) into the collector θ_C. Also if the turbine is turning faster than the slow threshold ω_s, the flow entering θ_C is insufficient for switching; i.e.

$$\begin{aligned} &\text{for} \quad \omega > \omega_s, \quad && \int \dot{m}\, dt < M_{min} \\ &\text{and for} \quad \omega \leq \omega_s, \quad && \int \dot{m}\, dt \geq M_{min} \end{aligned} \qquad (12)$$

where M_{min} is the mass needed to switch the amplifier.

Figure 9 shows that the leading edge of the slow error pulse is used as a reference for $\omega > \omega_s$ because it arrives at a constant time (each cycle) while the disk moves through the angle θ_1 in a time proportional to ω. The relationship of θ_1 to ω is given by a modified form of equation (5) as

$$\frac{\theta_1}{\omega} = \frac{L_s}{v} \qquad (13)$$

where as seen in figure 4, θ_1 is the angle swept by the turbine

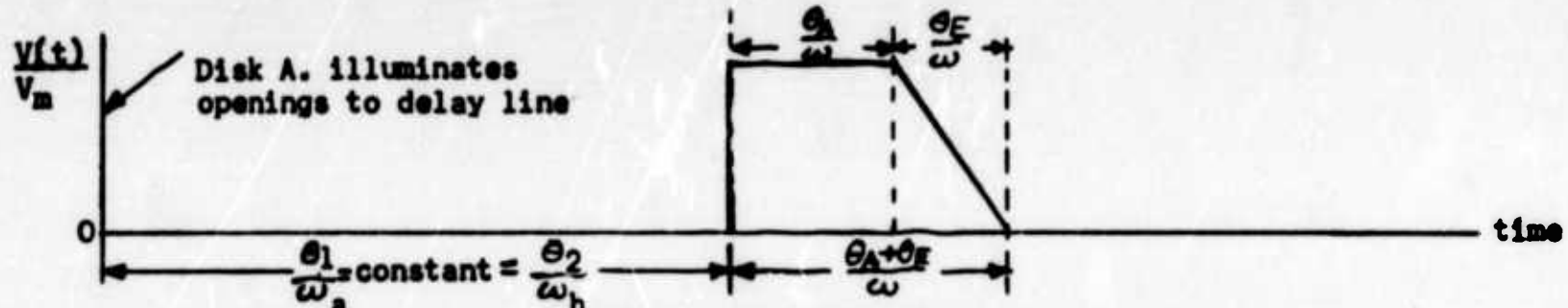

Figure 9a) Velocity pulse

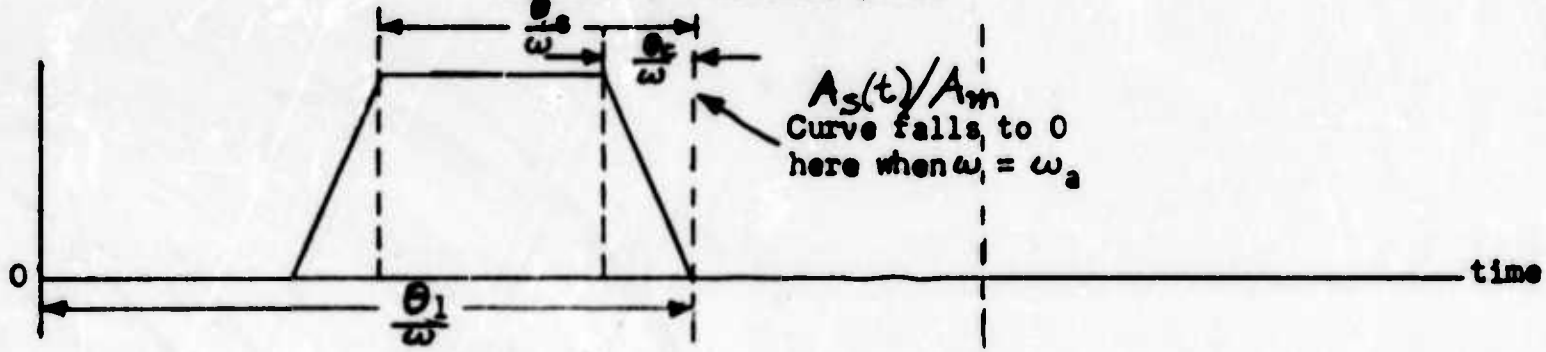

Figure 9b) Slow illuminated area

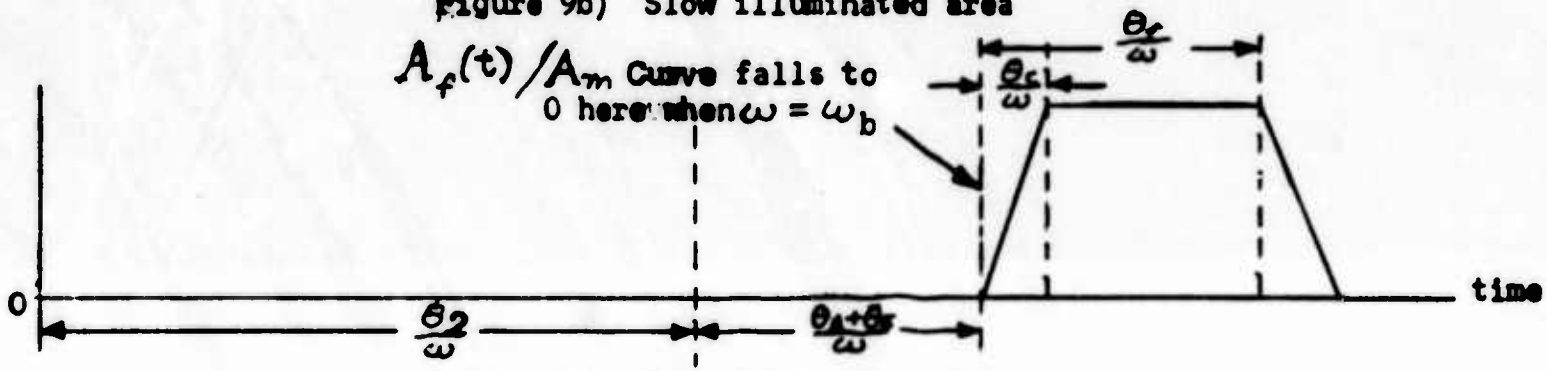

Figure 9c) Fast illuminated area

FIGURE 9: PROFILES OF THE VELOCITY PULSE AND ILLUMINATED AREAS

at ω_a between the time slot θ_A starts illuminating the delay line and the time slot θ_s stops illuminating the slow collector. L_s is the length of the delay line, and v is the velocity of propagation of the pulse down the delay line (see sec. 2.3).

Let the zero of the time base start when the slow indicating slot θ_A first starts to open the barrier between the emitter and the slow pulse delay line. Since the angular velocity ω changes only slightly during the fraction of a cycle that the pulse propagates through the delay line, we let ω = constant. Let us denote the angular width of the slow collector by θ_C and the angular width of the slow slot θ_s as θ_s, then, as shown by figure 9, the normalized illuminated area is

$$\begin{aligned}
&\frac{A_s(t)}{A_m} = 0 && \text{for} \quad t > \frac{\theta_s}{\omega_a} \\
&\frac{A_s(t)}{A_m} = \frac{\theta_1 - \omega t}{\theta_C} && \text{for} \quad \frac{\theta_1 - \theta_C}{\omega} \le t \le \frac{\theta_1}{\omega} \\
&\frac{A_s(t)}{A_m} = 1 && \text{for} \quad \frac{\theta_1 - \theta_s}{\omega} \le t \le \frac{\theta_1 - \theta_C}{\omega}
\end{aligned} \qquad (14)$$

where ω_a is the angular velocity at which no flow enters the collector.

The velocity term $[\, v_s(t)/v_m \,]$ of equation (7) is evaluated from the wave form of the pulse at the end of the delay line. Using the assumption that the leading edge of the pulse from the delay line is a step, the normalized velocity of the slow pulse is shown in figure 9 to be:

$$\frac{v_s(t)}{v_m} = 0 \qquad \text{for} \qquad t < \frac{\theta_1}{\omega_a}$$

$$\frac{v_s(t)}{v_m} = 1 \qquad \text{for} \qquad \frac{\theta_1}{\omega_a} \le t \le \frac{\theta_1}{\omega_a} + \frac{\theta_A}{\omega} \quad . \qquad (15)$$

For a computation of the function given in equation (7) see Appendix A. In Appendix A the shape of the pulse in the slow collector is shown to vary from a triangle to a trapezoid as the angular rate decreases from ω_d for the given geometrical configuration.

Fast Signal Pulse Shape

If the turbine is turning at or greater than the fast threshold rate ω_f, a switching pulse will pass through the fast slot θ_f into the fast collector; i.e.

$$\text{for} \quad \omega < \omega_f; \qquad \int \dot{m}\, dt < M_{min}$$

$$\text{and for} \quad \omega \ge \omega_f; \qquad \int \dot{m}\, dt \ge M_{min}, \qquad (16)$$

where M_{min} is the mass threshold needed to switch the amplifier.

Figure 9 shows that the trailing edge of the fast pulse is used as a reference for $\omega < \omega_f$ because it arrives at almost a constant time*

---

* In figure 9, the trailing edge of the pulse is referenced by quantity

$$t = \frac{\theta_2}{\omega_b} + \frac{\theta_A + \theta_E}{\omega} \qquad (17)$$

The second term of the latter is the pulse width which is a function of the angular velocity. Therefore the trailing edge of the pulse arrives at the end of the delay line at approximately a constant time.

(each cycle) while the angle θ_2 is swept out by the disk in a time proportional to ω. The relationship of θ_2 to ω is given by a modified form of equation (5) as

$$\frac{\theta_2}{\omega} = \frac{L_f}{v} \quad , \tag{18}$$

where θ_2 refers to the angle swept between the time slot θ_A has completed its illumination of θ_E to the time that slot θ_f begins illuminating θ_C. L_f is the length of the delay line, v is the velocity of propagation of the pulse down the delay line (see sec. 2.3).

The zero of the time base is the same as in the slow signal case. Again we assume that since the angular velocity ω changes slowly during the fraction of a cycle that the pulse propagates through the delay line, ω may be considered a constant. Let us denote the angular width of the fast collector θ_C by ϑ_C and the angular width of the fast slot θ_f by ϑ_f. Then as shown by figure 9, the normalized illuminated area of the fast collector is

$$\frac{A_f(t)}{A_m} = 1 \qquad \text{for} \quad \frac{\theta_2+\theta_A+\theta_E+\theta_C}{\omega} \leq t \leq \frac{\theta_2+\theta_A+\theta_E+\theta_C+\vartheta_f}{\omega}$$

$$\frac{A_f(t)}{A_m} = 0 \qquad \text{for} \quad t < \frac{\theta_2+\theta_A+\theta_E}{\omega}$$

$$\frac{A_f(t)}{A_m} = \frac{\omega t - (\theta_2+\theta_A+\theta_E)}{\vartheta_C} \quad \text{for} \quad \frac{\theta_2+\theta_A+\theta_E}{\omega} \leq t \leq \frac{\theta_2+\theta_A+\theta_E+\theta_C}{\omega} . \tag{19}$$

The velocity term $[A_f(t)/A_m]$ of equation (19) is evaluated from the wave from of the pulse at the end of the delay line. Here again it has been assumed that the trailing edge of the pulse emanating from the delay line is unchanged in shape or length within the delay line. Then from figure 9 the normalized velocity of the fast error pulse is

$$\frac{v_f(t)}{v_m} = 0 \qquad \text{for } t > \frac{\theta_2}{\omega_b} + \frac{\theta_A + \theta_E}{\omega}$$

$$\frac{v_f(t)}{v_m} = \frac{\theta_2 \frac{\omega}{\omega_b} (\theta_A + \theta_E) - \omega t}{\theta_E} \qquad \text{for } \frac{\theta_2}{\omega_b} + \frac{\theta_A}{\omega} \leq t \leq \frac{\theta_2}{\omega_b} + \frac{\theta_A + \theta_E}{\omega}$$

$$\frac{v_f(t)}{v_m} = 1 \qquad \text{for } \frac{\theta_2}{\omega_b} \leq t \leq \frac{\theta_2}{\omega_b} + \frac{\theta_A}{\omega} \quad . \tag{20}$$

For a computation of the function given in equation (7), see Appendix B. Appendix B also shows that in order to produce high mass flow signals for small angular velocity deviations from the set point, $1/\theta_C$, $1/\theta_E$, and $1/(\theta_C\theta_E)$ should be large. Thus θ_E and θ_C should be small. Higher mass flows may also be obtained by increasing the supply pressure, p^+.

3. EXPERIMENTS

A schematic diagram of the system constructed and tested is shown in figure 10. The angular velocity of the model was regulated at two set points, 910 and 1500 rpm, by using delay lines of different

lengths. At both settings, the control system maintained the turbine speed within ±2 percent with loads that would otherwise have caused a variation of ±20 percent.

The test set up consists of (fig. 10):

(1) A turbine wheel (3 in. in diameter) attached rigidly to a rotatable shaft mounted in a bracket.

(2) A control system made up of a slotted disk fixed rigidly to the turbine wheel shaft, a bistable fluid amplifier, a compressed air supply with input pipes to the control system, air lines to delay a fluid pulse for a known interval of time, and air pipes into the control channels of the bistable amplifier.

(3) Air supplies to drive the turbine wheel, to drive the wheel at an error velocity, to power the bistable amplifier, and to activate electronic measuring equipment.

(4) Electronic measuring equipment, made up of a stroboscope, a piezoelectric pressure transducer, an amplifier, and an oscilloscope.

The bistable fluid amplifier used had the following design characteristics: Nozzle width is 0.050 in.; splitter position is 0.2 in. (4 w) downstream; attachment wall angles are 12-1/2 deg; splitter included angle is 13 deg; control nozzle width is 0.0375 in. (3/4 w); wall setback is 0.0125 in. (1/4 w); and aspect ratio is 4:1.

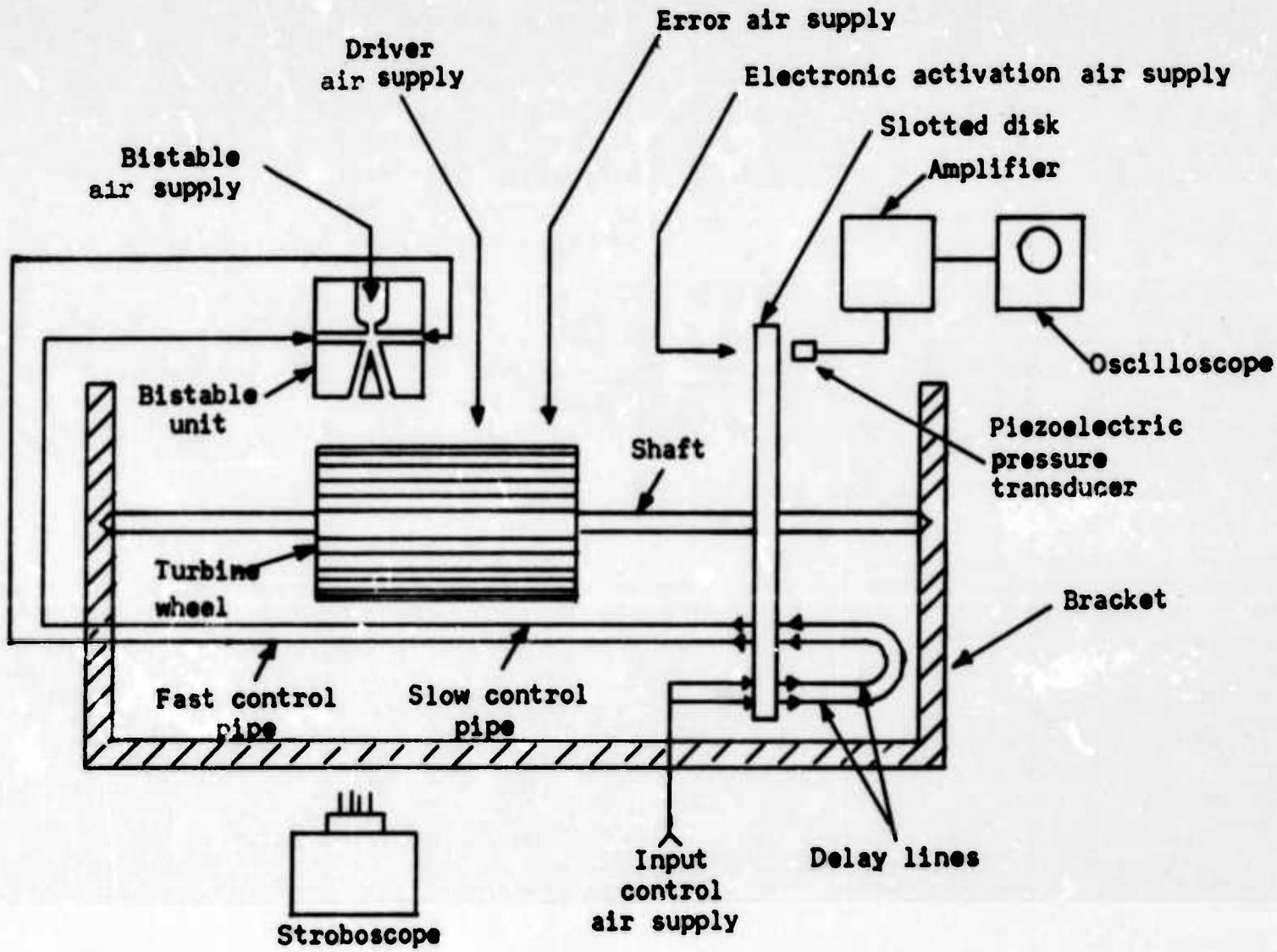

FIGURE 10: SCHEMATIC OF LABORATORY APPARATUS

The angular velocity sensor had the following design characteristics: $\theta_E = 4$ deg; $\theta_C = 1.6$ deg; θ_A 20 deg; $\theta_s = 17$ deg; $\theta_f > 40$ deg; $\theta_2 = 11$ deg; $L_s = L_f = 26$ in. for regulation at 910 rpm.

Both emitters were operated with a regulated pressure of 35 psig; the pulse flow velocity in the delay lines was measured to be 421 ft/sec. The value of L_f/θ_2 has been calculated from equation (18) to be

$$\frac{L_f}{\theta_2} = \frac{v}{\omega} \quad , \tag{21}$$

where $v = 1450$ ft/sec. In sec. 2.3 this supersonic velocity is discussed. It is the pressure pulse propagation velocity.

Test 1 - Changes in Pulse Pressure Profile

The change in the pressure profile of a pulse as it travels through the delay line was determined by measuring the profile at the end of the delay lines of three lengths. These measurements are plotted in figure 11a. While the amplitude of the pressure pulse remains unchanged, the waveform and pulse width change as expected. For increasing lengths of delay line, the upswing of the pulse approaches a step; the downswing decreases in steepness; and the pulse width increases. Figure 11b shows that the width of the pulse downswing is approximately a linear function of the length of the delay line.

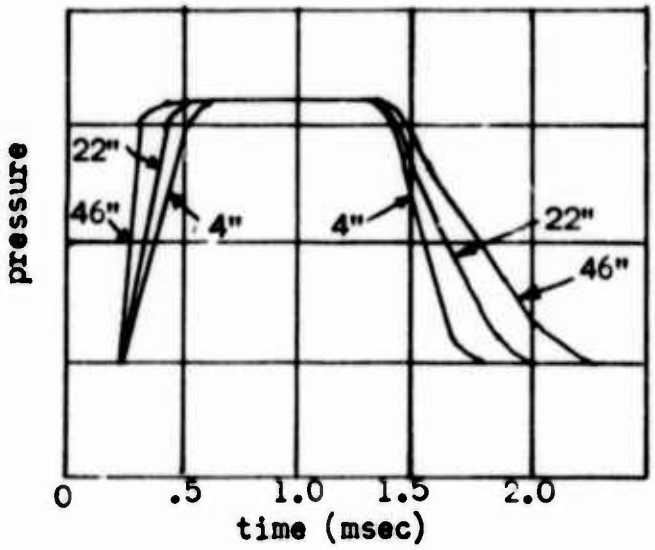

Figure 11a: Pressure pulse shapes for three lengths of delay lines (from oscilloscope photos)

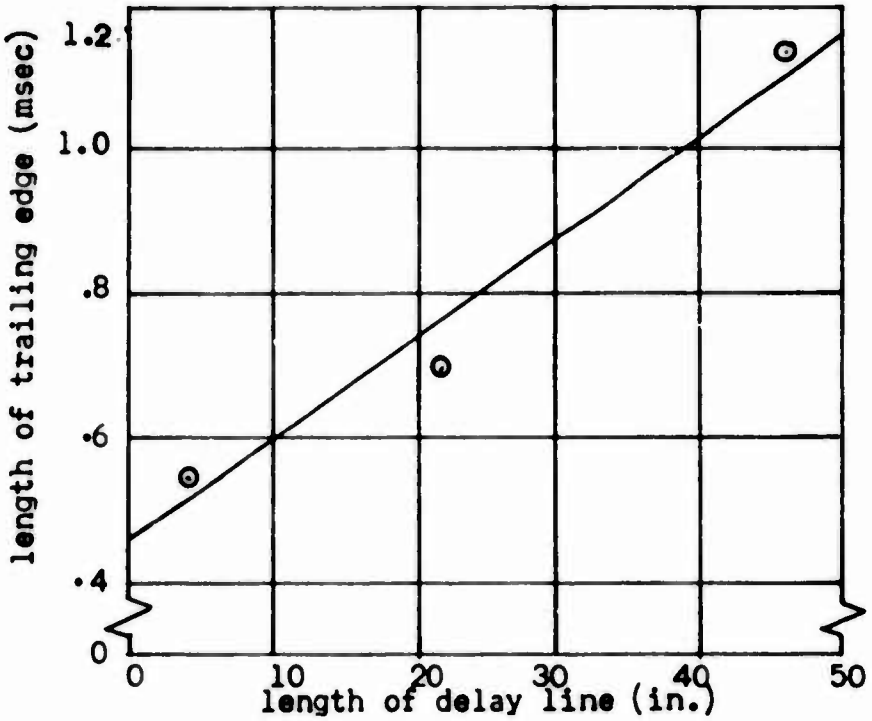

Figure 11b Length of trailing edge versus length of delay line

FIGURE 11: PRESSURE PULSE VARIATIONS IN THE DELAY LINE

Test 2 - Dynamic Switching of Bistable Amplifier

An investigation was made of the transient mass flow per pulse required to switch the bistable amplifier. As shown in figure 6, the mass flow versus time (duration of the mass flow) is a hyperbola, having asymptotes parallel to the coordinate axes. Signals falling in the region to the right and above the experimental curve should produce reliable switching. Signals in the region below and to the left of the curve have insufficient mass to switch the amplifier.

Making the simplifying assumption that the pulse shape is rectangular changes equation (2) to:

$$M_{min} = \dot{m}t = \text{constant} \quad . \qquad (22)$$

The discrepancy at low mass flows shown in figure 6 results primarily from the assumption that there is no change in bubble volume or length.

Test 3 - Mass Flow in Pulse

The set of equations (B-2, B-3, B-4, B-5, B-6) in Appendix B for the signal in the fast collector are compared with experimental data in figure 12 and are seen to correlate reasonably well. At angular rates between 1.05 ω_b and 1.65 ω_b in increments of 0.05 ω_b the pulses supplied to the fast collector are sensed at the stagnation pressure p_o as they impinge upon the face of a crystal force transducer installed in the collector. The measured stagnation pressure p_o is proportional to the square of the mass flow as

$$p_o \sim v^2 \sim \dot{m}_f^2 \quad . \qquad (23)$$

A comparison of the curves plotted from equations (B-2) through (B-6) and the curves which have been photographed from the display on an oscilloscope (fig. 12) demonstrates that the down-swing of the fast control signals in the experimental curves is considerably expanded over the calculated curves because the expansion of the mass flow pulses in the fast delay line has been neglected in the calculations. Equations (B-2) through (B-6) could be easily modified to take into account the effect of the delay lines.

4. CONCLUSIONS

The control system described, consisting of a turbine wheel regulated at rates of either 910 or 1500 rpm, can be maintained within ±2 percent of the desired speed. The average speed over many correction cycles is within a mean error of much less than 2 percent.

It is believed that a control system using the method described in this report can be made to control the angular velocity closer than ±2 percent since the control variation of the present system was attained without difficulty. However, this system has several problem areas that must be resolved before practical applications are possible. They may be summarized as follows:

(1) The bistable amplifier must be able to work into a load. In the present application the dynamic pressure of the amplifier output produces the corrective action. Amplifiers

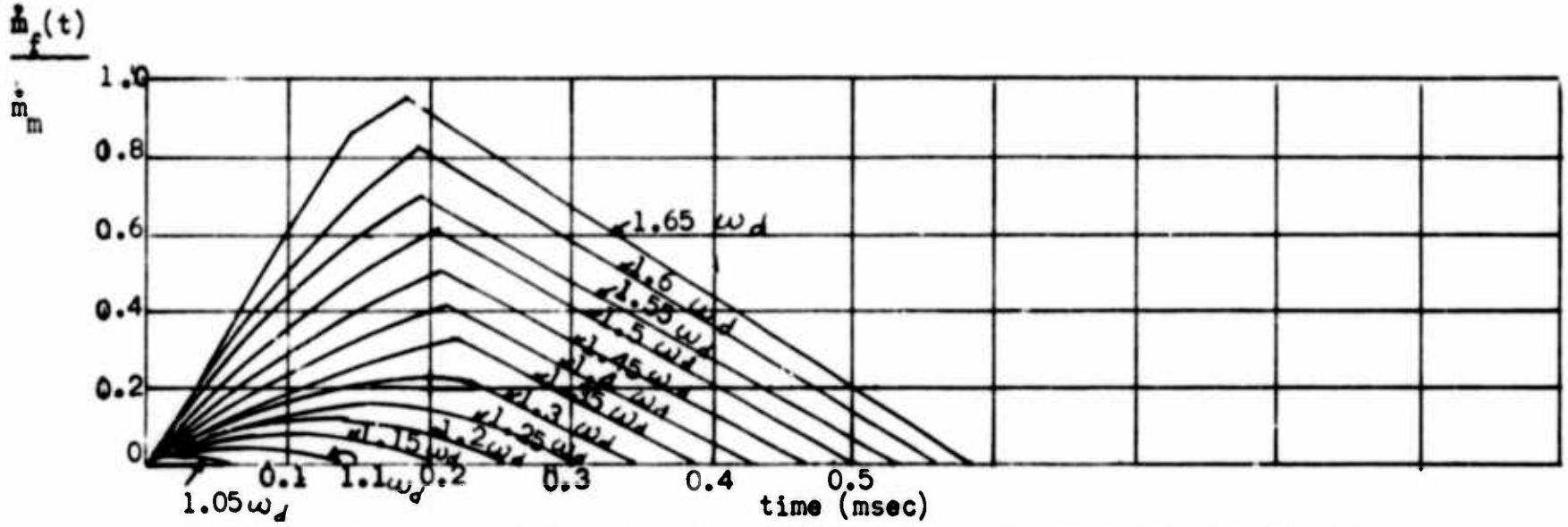

Figure 12a) Calculated mass flow signals to fast control for $\omega > \omega_d$

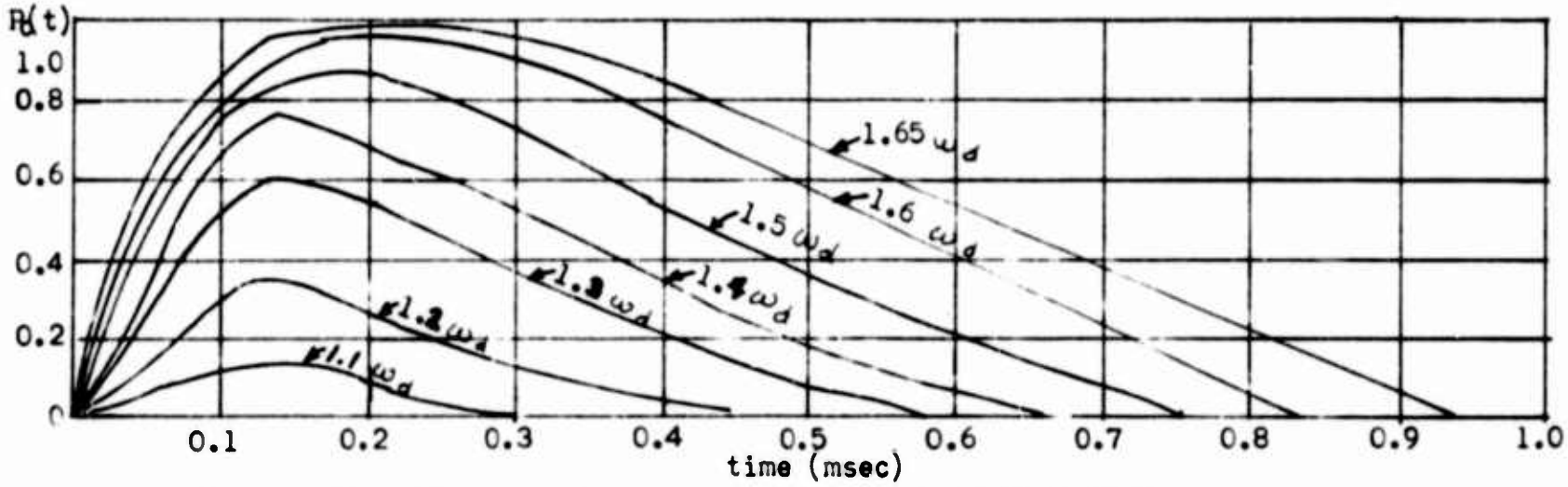

Figure 12b) Experimental Pressure Signals to Fast Control

FIGURE 12: CALCULATED MASS FLOW AND EXPERIMENTAL PRESSURE SIGNALS IN THE FAST COLLECTOR

utilizing bleeds may be the solution or staging of amplifiers may be required.

(2) The system requires a regulated source of pressure. The propagating velocity and mass flow or the signal pulse depends upon this pressure.

(3) The dynamic switching characteristics of the bistable amplifier must be accurately known.

(4) Should the final sensing rate for the system be about 15 cps or greater, the dynamic frequency response for pipes to a-c flows should be more fully investigated.

(5) A constant temperature air supply or a temperature compensating system is required. Both the pulse propagation velocity and amplifier switching characteristics are influenced by changes in temperatures.

5. REFERENCE

(1) Liepmann, H. W., and Roshko, A., Elements of Gasdynamics, Wiley, 1957.

6. APPENDICES

Section 2.3 developed expressions for calculating the pulse shape in the collectors as given in equation (7). The velocity and area functions are given in equations (14), (15) (19) and (20). The appropriate convolutions are performed as follows:

APPENDIX A

CONVOLUTION OF SLOW SIGNAL PULSE

The convolution of the functions given in equation (7) for the "slow" case,

$$\frac{\dot{m}_s}{\dot{m}_m} = \frac{A_s(t)}{A_m} \cdot \frac{v_s(t)}{v_m} , \qquad \text{(A-1)}$$

is calculated from equations (14) and (15)

$$\frac{A_s(t)}{A_m} = 0 \qquad \text{for } t > \frac{\theta_1}{\omega}$$

$$\frac{A_s(t)}{A_m} = \frac{\theta_1 - \omega t}{\theta_c} \qquad \text{for } \frac{\theta_1 - \theta_c}{\omega} \leq t \leq \frac{\theta_1}{\omega}$$

$$\frac{A_s(t)}{A_m} = 1 \qquad \text{for } \frac{\theta_1 - \theta_s}{\omega} \leq t \leq \frac{\theta_1 - \theta_c}{\omega} \qquad \text{(14)}$$

$$\frac{v_s(t)}{v_m} = 0 \qquad \text{for} \quad t < \frac{\theta_1}{\omega_a}$$

$$\frac{v_s(t)}{v_m} = 1 \qquad \text{for} \quad \frac{\theta_1}{\omega_a} \leq t \leq \frac{\theta_1}{\omega_a} + \frac{\theta_A}{\omega} \,. \tag{15}$$

This convolution has the two limiting cases shown in figure 13.

Limit S1: The zero points of the velocity and area functions coincide (figure 13 b).

Limit S2: The maximum value of the area function and the zero point of the velocity function coincide (figure 13 d).

When the area function $[A_s(t)/A_m]$ occurs earlier in time (to the left of limit S1 (figure 13 a)) equation (23) becomes zero everywhere,

$$\frac{\dot{m}_s}{\dot{m}_m} = 0. \tag{A-2}$$

Between limits S1 and S2, equation (A-1) becomes

$$\frac{\dot{m}_s}{\dot{m}_m} = \frac{\theta_1 - \omega t}{\theta_c} \qquad \text{for} \quad \frac{\theta_1 - \theta_c}{\omega} \leq t \leq \frac{\theta_1}{\omega} \,. \tag{A-3}$$

The latter expression, a first degree function of ω, describes a straight line for t within the above bounds. Therefore, the function is a triangular wave form (figure 13c).

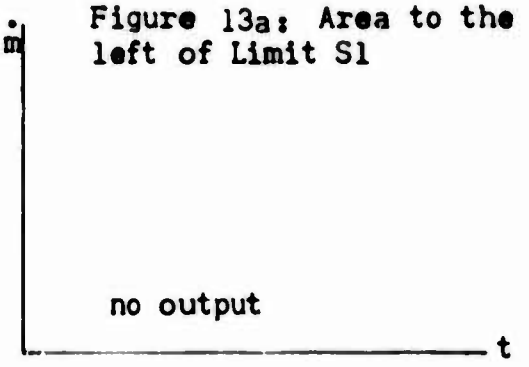

Figure 13a: Area to the left of Limit S1

Figure 13b: Limit S1

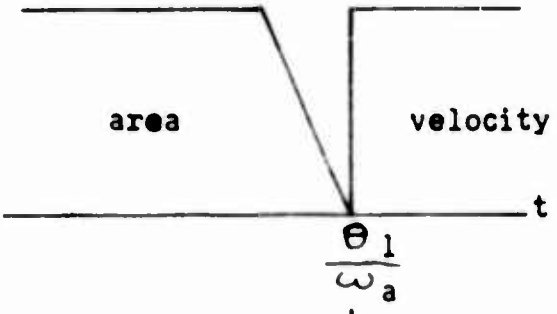

Figure 13c: Area between Limit S1 and Limit S2

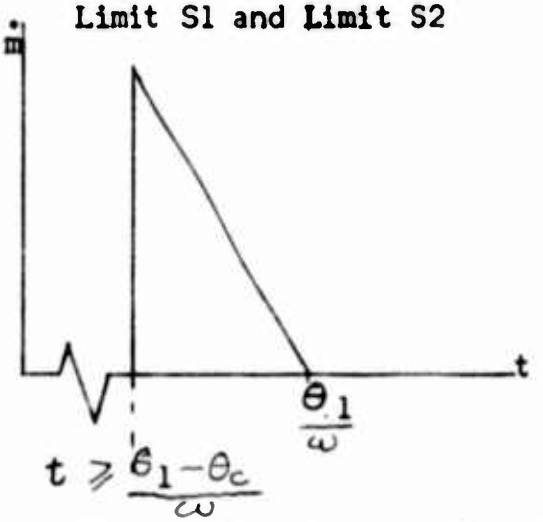

Figure 13d: Limit S2

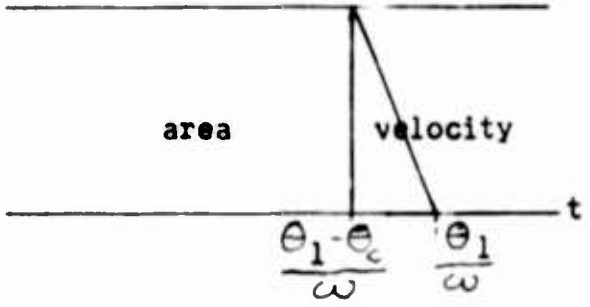

Figure 13e: Area to the right of Limit S2

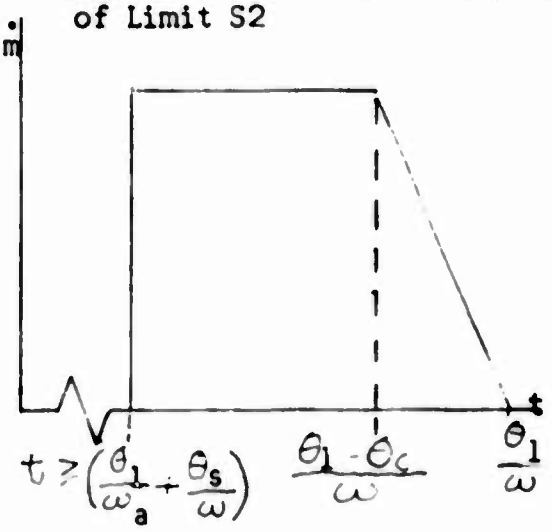

FIGURE 13: WAVE FORM GENERATION AND SHAPE IN THE SLOW COLLECTOR

When the area function occurs to the right of limit S2, equation (A-1) becomes equation (A-3) for $\frac{\theta_1 - \theta_c}{\omega} \leq t \leq \frac{\theta_1}{\omega}$

and $\frac{\dot{m}_s}{\dot{m}_m} = 1$ for $\frac{\theta_1}{\omega_a} + \frac{\theta_A}{\omega} \leq t \leq \frac{\theta_1 - \theta_c}{\omega}$. (A-4)

When the rectangular function of equation (A-4) is combined with the sawtooth to express the function occuring to the right of limit S2, the combined function is a trapezoid (figure 13e).

APPENDIX B

CONVOLUTION OF FAST SIGNAL PULSE

The convolution of the function given in equation (7) for the fast case

$$\frac{\dot{m}_f}{\dot{m}_m} = \frac{A_f(t)}{A_m} \cdot \frac{v_f(t)}{v_m} \qquad \text{(B-1)}$$

is calculated from equations (19) and (20)

$$\frac{A_f(t)}{A_m} = 0 \quad \text{for} \quad t < \frac{\theta_2 + \theta_A + \theta_E}{\omega}$$

$$\frac{A_f(t)}{A_m} = \frac{\omega t - (\theta_2 + \theta_A + \theta_E)}{\theta_C} \quad \text{for} \quad \frac{\theta_2+\theta_A+\theta_E}{\omega} \leq t \leq \frac{\theta_2+\theta_A+\theta_E+\theta_C}{\omega}$$

$$\frac{A_f(t)}{A_m} = 1 \qquad \text{for } \frac{\theta_2+\theta_A+\theta_E+\theta_C}{\omega} \leq t \leq \frac{\theta_2+\theta_A+\theta_E+\theta_C+\theta_f}{\omega} \tag{19}$$

$$\frac{v_f(t)}{v_m} = 0 \qquad \text{for } t > \frac{\theta_2}{\omega_b} + \frac{\theta_A + \theta_E}{\omega}$$

$$\frac{v_f(t)}{v_m} = \frac{\theta_2 \frac{\omega}{\omega_b} (\theta_A + \theta_E) - \omega t}{\theta_E} \quad \text{for } \frac{\theta_2}{\omega_b} + \frac{\theta_A}{\omega} \leq t \leq \frac{\theta_2}{\omega_b} + \frac{\theta_A + \theta_E}{\omega}$$

$$\frac{v_f(t)}{v_m} = 1 \qquad \text{for } \frac{\theta_2}{\omega_b} \leq t \leq \frac{\theta_2}{\omega_b} + \frac{\theta_A}{\omega} \; . \tag{20}$$

This convolution has the four limiting cases shown in Figure 14. The limits arise in this manner when it is assumed that $\theta_E > \theta_C$.

Limit F1: The zero points of the velocity and area function coincide (fig. 14b)

Limit F2: The zero point of the velocity function and the maximum value of the area function coincide (figure 14d).

Limit F3: The zero point of the area function and maximum value of the velocity function coincide (figure 14f).

Limit F4: The maximum values of both the velocity and area functions coincide (figure 14i).

Figure 14a:

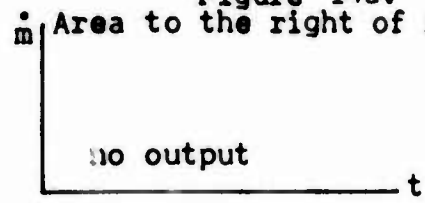

Figure 14b:

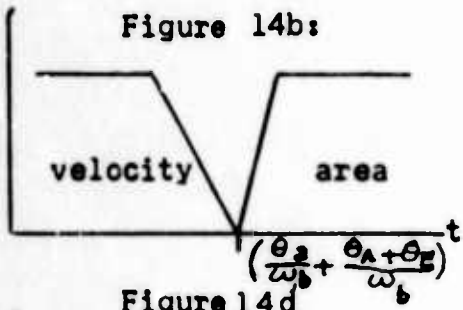

Figure 14c:

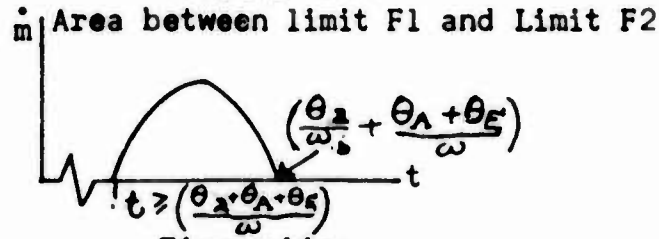

Figure 14d

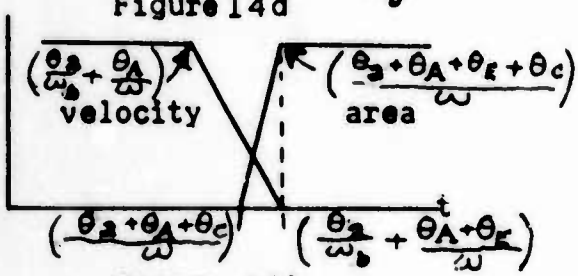

Figure 14e:

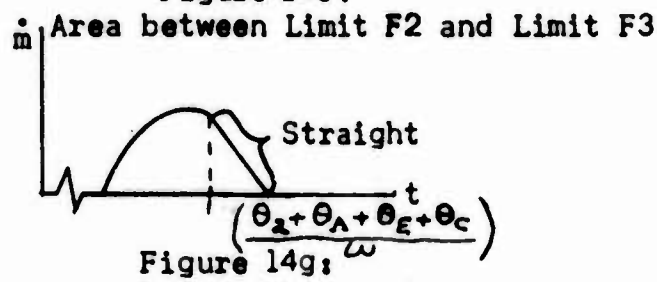

Figure 14f:

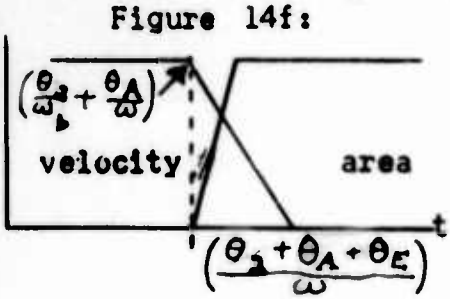

Figure 14g:

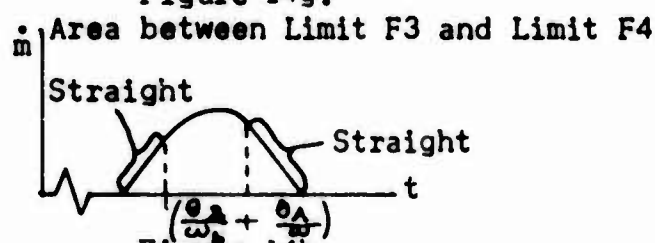

Figure 14h:

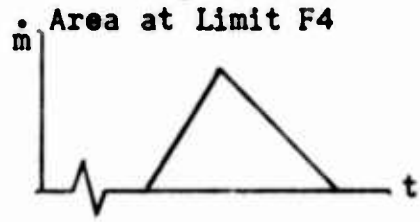

Figure 14i:

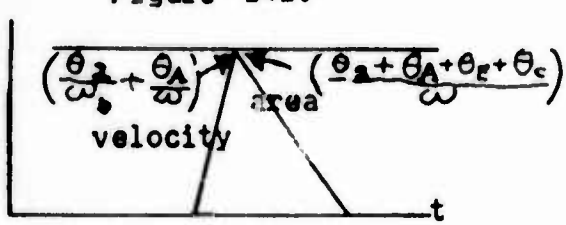

Figure 14j:

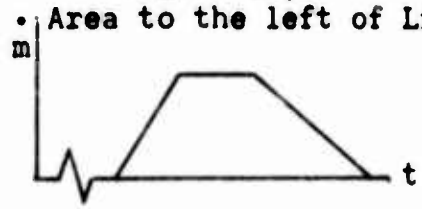

FIGURE 14: WAVE FORM GENERATION AND SHAPE IN THE FAST COLLECTOR ($\theta_C < \theta_E$)

Then the area function $[A_p(t)/A_m]$ occurs later in time (to the right of limit F1), equation (B-1) becomes zero everywhere (figure 14a)

$$\frac{\dot{m}_f}{\dot{m}_m} = 0 \quad . \tag{B-2}$$

Between limits F1 and F2, equation (B-1) becomes

$$\frac{\dot{m}_f}{\dot{m}_m} = \frac{1}{\theta_E \theta_C} \left[\theta_2 \frac{\omega}{\omega_b} + (\theta_A + \theta_E) - \omega t \right] \left[\omega t - (\theta_2 + \theta_A + \theta_E) \right] \tag{B-3}$$

$$\text{for } \frac{\theta_2 + \theta_A + \theta_E}{\omega} \leq t \leq \frac{\theta_2}{\omega_b} + \frac{\theta_A + \theta_E}{\omega} \quad .$$

Equation (B-3) is a quadratic function of ω, and describes a parabola for t within the above bounds (figure 14c).

Between the limits F2 and F3, equation (B-1) is the sum of equation (31) which describes a parabola

$$\text{for } \frac{\theta_2 + \theta_A + \theta_E}{\omega} \leq t \leq \frac{\theta_2 + \theta_A + \theta_E + \theta_C}{\omega}$$

$$\text{and } \frac{\dot{m}_f}{\dot{m}_m} = \frac{\theta_2 \omega / \omega_b + (\theta_A + \theta_E) - \omega t}{\theta_E} \tag{B-4}$$

$$\text{for } \frac{\theta_2 + \theta_A + \theta_E + \theta_C}{\omega} \leq t \leq \frac{\theta_2}{\omega_b} + \frac{\theta_A + \theta_E}{\omega} \quad .$$

Equation (B-4) is a first degree function of ω, and describes a straight line for t within the above bounds. The function between the limits F2 and F3 is a parabola with a straight line segment (figure 14e).

Between the limits F3 and F4, equation (B-1) becomes

$$\frac{\dot{m}_f}{\dot{m}_m} = \frac{\omega t-(\theta_2 + \theta_A + \theta_E)}{\theta_C} \quad \text{for} \quad \frac{\theta_2+\theta_A+\theta_E+\theta_C}{\omega} \leq t \leq \frac{\theta_2}{\omega_b} + \frac{\theta_A+\theta_E+\theta_C}{\omega} \qquad \text{(B-5)}$$

and by equation (B-4) which describes a straight line for

$$\frac{\theta_2 + \theta_A + \theta_E}{\omega} \leq t \leq \frac{\theta_2}{\omega_b} + \frac{\theta_A}{\omega}$$

and by equation (B-3) which describes a parabola for

$$\frac{\theta_2}{\omega_b} + \frac{\theta_A}{\omega} \leq t \leq \frac{\theta_2}{\omega_B} + \frac{\theta_A + \theta_E}{\omega} .$$

The function between the limits F3 and F4 is a parabola with straight line segments (figure 14g). At the limit F3 the function is a triangular shape (figure 14h).

When the area function occurs to the left of limit F4, equation (B-1) becomes

$$\frac{\dot{m}_f}{\dot{m}_m} = 1 \qquad \text{for } \frac{\theta_2+\theta_A+\theta_E+\theta_C}{\omega} \leq t \leq \frac{\theta_2}{\omega_b} + \frac{\theta_A}{\omega} \text{ ,} \tag{B-6}$$

where equation (B-6) is a rectangular wave form, and by equation (B-5) which is a straight line for

$$\frac{\theta_2 + \theta_A + \theta_B}{\omega} \leq t \leq \frac{\theta_2 + \theta_A + \theta_E + \theta_C}{\omega}$$

and by equation (B-4) which is a straight line for

$$\frac{\theta_2}{\omega_B} + \frac{\theta_A}{\omega} \leq t \leq \frac{\theta_2}{\omega_b} + \frac{\theta_A + \theta_E}{\omega} \text{ .}$$

Thus the entire wave form for the function occuring to the left of limit F4 is a trapezoid (figure 14j).

HARRY DIAMOND LABORATORIES

Washington 25, D. C.

FLUID AMPLIFICATION TECHNOLOGY:

A BIBLIOGRAPHY OF DIRECT CONTRIBUTIONS

by

Vondell Carter

Jonathan Fine

Department of the Army

Army Materiel Command

ABSTRACT

Contained in this bibliography are 143 citations of publications and patents considered contributory to the technology of "pure fluid amplifiers", that is, those fluid devices containing no moving parts and exemplified by the disclosures of Horton, Bowles, and Warren during the first half of 1959. Included are:

1. Reports (industry and government)
2. Theses
3. Papers
4. Articles (journals and periodicals)
5. Patents

Approximately 80% of the material cited has been abstracted.

TABLE OF CONTENTS

GLOSSARY

AIAA-American Institute of Aeronautics and Astronautics

ASTIA-Armed Services Technical Information Agency
(Changed to DDC, March 1963)

DDC-Defense Documentation Center
(For Scientific and Technical Information)

FSTC-Foreign Science and Technology Center

JPRS-Joint Publications Research Service

NASA-National Aeronautics and Space Administration

OSTI-Office of Scientific and Technical Information, NASA

OTIA-Ordnance Technical Information Agency (Now FSTC)

OTS-Office of Technical Services, U. S. Department of Commerce

USING THE BIBLIOGRAPHY

Contained in this bibliography are 143 citations of publications and patents considered contributory to the technology of "pure fluid amplifiers", that is, those fluid devices containing no moving parts and exemplified by the disclosures of Horton, Bowles, and Warren during the first half of 1959. Included are:

1. Reports (industry and government).
2. Theses.
3. Papers.
4. Articles (journal and periodical).
5. Patents.

Approximately 80% of the material cited has been abstracted.

Of the 3000 or so items reviewed, only those evaluated as directly applicable to fluid amplification and either adding to or utilizing the knowledge of their function were included in this document. This should not be construed to mean that work not cited has been negatively evaluated, or even reviewed. The scope of this effort was necessarily limited by such factors as personnel, time and the size of this volume. A much more comprehensive bibliography is intended for publication in the near future.

The bibliography is arranged according to subject matter.

Within each subject category, the arrangement is chronological, beginning with the oldest publications.

Each item has been serially numbered within each section (subject category), which facilitates cross referencing. An index of authors, which cites these serial numbers, has been included.

It will be found that three sections of the bibliography were included that contain no citations, and are so annotated. This was necessary to allow a sequential numbering of the sections to correspond to the previously mentioned comprehensive bibliography. This later publication will contain material pertinent to all of the sections listed.

A citation format consisting of four elements has been employed throughout the bibliography. The elements are, in order of appearance:

1. Title - (All upper case characters)
2. Personal Author - (Not applicable or available in some cases)
3. Source Information - Gives the name of the organization responsible for publishing the article, paper or report. In the case of articles, theses, and patents, the information is self-explanatory; for reports or papers, the number immediately following the name of the government agency, private

firm, or symposium is the original identification number assigned to that publication by the publishing organization.

Other identification numbers will appear in parentheses at or near the end of the "source information" element of the citation. Where available, one or more of the following forms will appear: (1) AD-xxx xxx, (2) Nxx-xxxxx, and (3) Axx-xxxxx, where "x" represents a digit. These numbers are the accession (or filing) numbers of the Defense Documentation Center, the NASA Office of Scientific and Technical Information, and the AIAA Technical Information Service, respectively. Accession numbers for other information facilities are identified. Finally, contract or project numbers may be cited to aid in researching documents otherwide not easily identifiable.

4. Abstract - Attempts to reveal the content of the reference with sufficient clarity to allow the user (of this bibliography) to determine applicability and extent of usefulness. Abstracts annotated "(A)" (in the right extremity of the last line of text, or the following line) are essentially those of the authors of the references. Others were generated by the authors of this bibliography.

THE BIBLIOGRAPHY

I - 1 BASIC RESEARCH AND DEVELOPMENT IN FLUID POWER CONTROL FOR THE UNITED STATES AIR FORCE. [NINTH PROGRESS REPORT.]

J. Lowen Shearer, F. T. Brown, R. S. Crossley, D. H. Marcus, K. N. Reid, and R. S. Scher

Wright-Patterson AFB, Ohio, Flight Control Lab. ASD-TDR-62-3, Jan 1962. 68 p. 21 refs. (N62-13871) (Contract AF 33-616-6120)

This report describes continuing applied research and development work on problems vital to the design and development of high performance hydraulic and pneumatic control equipment for advanced systems. Increased emphasis on high pressure pneumatic components and systems reflects the approach to an ultimate objective of employing hot gas power to operate such systems. Control valves, servomotors, fluid power and signal transmission, and techniques of control are the major items discussed in this report. Transient and frequency response studies of a reaction jet servosystem are described, and recent work on experimental determination of windage losses of reaction jet servomotor rotors is described. Basic investigations of jet relay devices have proceeded with the study of input impedance of a first stage device, study of jet reattachment to a downstream wall, and attachment to a downstream obstruction such as a knife edge. A recently completed thesis on flow induced forces in hydraulic jet-pipe valves is also summarized. Recently completed papers and theses are also listed. (A)

I - 2 FLUID JET RELAY DEVICES: A PARTIALLY ANNOTATED BIBLIOGRAPHY

Barbara Ann Bryce

Autonetics (Div. of North American Aviation), Downey, Calif. Report No. EM-1162-114, 21 March 1962. 80 p. 280 refs. (AD-276 419)

The subject of this report is fluid control devices which contain no moving parts and are referred to variously as "fluid amplifiers," "pure fluid systems" and fluid binary logic elements." The supporting theory referenced includes fluid mechanics in general, and more specifically the laminar boundary layer, the two-dimensional flow of gases, and the Coanda Effect.

The references are arranged according to the following categories: Theory and Analysis; Experiments and Methods; Types of Devices in Research and Development; Tangent References (closely related material). Indexes (by author and source) are included.

I - 3 FLUID AMPLIFIERS FOR AEROSPACE SYSTEMS

W. G. Wadey

National Aerospace Electronics Conference, 1962 Proceedings 14-16 May 1962, Dayton, Ohio, p. 353-358. (Sponsored by IRE with participation by IAS and ASME.)

The development of the various types of fluid amplifiers is reviewed. No-moving-parts devices are compared with those using diaphragms, balls and spool valves. Russian effort is covered. The advantages for military applications (within security limitations) as well as commercial applications are presented along with present developmental problems.

I - 4 THE ROLE OF NEW DEVELOPMENT IN FLUID POWER CONTROL FOR AEROSPACE SYSTEMS

J. Lowen Shearer

Society of Automotive Engineers, National Aeronautic and Space Engineering and Manufacturing Meeting, Los Angeles, Calif., Oct. 8-12, 1962. Paper 593B. 8 p. 17 refs. (Contract Nos. AF 33(616)-6120 and AF 33(657)-7535.

I - 5 PROCEEDINGS OF THE FLUID AMPLIFICATION SYMPOSIUM, VOLUME I, 2-4 OCTOBER 1962.

Diamond Ordnance Fuze Labs., Wash., D. C. Published 15 Nov 1962. 472 p. (N63-13380) (AD-297 935)

CONTENTS:

1. Wall Effect and Binary Devices by R. W. Warren (N63-13381)
2. An Introduction to Proportional Fluid Control by S. Katz (N63-13382)
3. Fluid Amplifier Demonstration Vehicle by R. R. Palmisano (N63-13383)
4. The Hydraulic Analogy by R. G. Barclay (N63-13384)
5. Pulse Duration Modulation by R. W. Warren (N63-13385)
6. A Three Stage Digital Amplifier by C. J. Campagnuolo (N63-13386)
7. Rocket Thrust Vectoring by A. B. Holmes (N63-13387)
8. A Fluid-Amplifier Artificial Heart Pump by T. G. Barila and D. E. Nunn; K. E. Woodward, G. Mon, and H. H. Straub
9. Survey on Coanda Flow by P. K. Chang (N63-13389)
10. Flow Visualization by J. R. Keto (N63-13390)
11. Flow Visualization and Experimental Studies of a Proportional Fluid Amplifier by R. J. Reilly and J. A. Kallevig (N63-13391)
12. Production of Fluid Amplifiers by Optical Fabrication Techniques by R. W. Van Tilburg (N63-13392)
13. "Optiform", Optical Machining of Pure Fluid Systems in Plastics by Ronald E. Bowles and John R. Colston (N63-13393)
14. Instrumentation for Research and Development in Pure Fluid Systems by Ronald L. Humprey and Eric E. Metzer (N63-13394)
15. Characteristics of Two-Dimensional Compressible Attached Jets by R. E. Olson (N63-13395)
16. The Application of Free Jet Mixing Theories to Fluid Amplifier Elements by Glen W. Zumwalt (N63-13396)
17. Interaction of Transversely Impinging Jets by Darshan S. Dosanjh and William J. Sheeran (N63-13397)
18. An Analytical and Experimental Study of Two-Dimensional Compressible Submerged Jets by R. E. Olson (N63-13398)
19. A Solution of the Two-Dimensional Turbulent Viscous Curved Jet Using the IBM 7090 Computer by G. D. Boehler (Abstract only)
20. Characteristics and Control of Free Laminar Jets by Alan Powell (N63-13399)

21. Pneumatic Linear Circuits by Beatrice A. Hicks and Evelyn S. Jetter (N63-13400)
22. Gain Analysis of the Proportional Fluid Amplifier by S. J. Peperone, S. Katz, and J. M. Goto (N63-13401)
23. Turbulence Amplifier Design and Application by R. N. Auger (N63-13402)
24. On the Inherent Limitations in Fluid-Jet Modulators by F. T. Brown (N63-13403)
25. Proportional Power Stages for Impedance Matching Pure Fluid Devices by T. J. Lechner and Martin W. Wambsganss (N63-13404)
26. Pure Fluid Digital Logic With a Single Switching Element by P. Bauer (N63-13405)
27. High Speed Pneumatic Digital Operations With Moving Elements by H. E. Riordan (N63-13406)
28. A Suggested System of Schematic Symbols for Fluid Amplifier Circuitry by W. A. Boothe and J. N. Shinn (N63-13407)
29. A Technique for Matching Pure Fluid Components Applied to the Design of a Shift Register by E. M. Dexter (N63-13408)
30. A Comparison of the Reliability of Electronic Components and Pure Fluid Amplifiers by H. L. Fox (N63-13409)

Volume I includes all unclassified presentations; Volume II includes all classified presentations.

I - 6 A COMPARISON OF THE RELIABILITY OF ELECTRONIC COMPONENTS AND PURE FLUID AMPLIFIERS

Harold L. Fox

Diamond Ordnance Fuze Labs., Wash., D. C. Proc. of the Fluid Amplification Symp., Vol. I, Oct. 2-4, 1962. Dated Nov. 15, 1962. p. 455-469. 6 refs. (N63-13409)

Current achievements in attaining high reliability for electronic components are compared to the predicted reliability of pure fluid amplifiers. Figures for electronic components are presented for various environmental regimes which may be encountered in industrial, field, and aerospace applications. A lack of data on fluid devices made necessary certain assumptions; these are discussed.

The reliability of pure fluid amplifiers under severe conditions of temperature, vibration, shock, and radiation is predicted. The results of the comparisons of the reli-

ability of electronic components and pure fluid amplifiers are applied to a typical system problem. Predicted system failure rates are given for both electronic and fluid systems. (A)

I - 7 STATE OF THE ART OF PURE FLUID SYSTEMS

R. E. Bowles

American Society of Mechanical Engineers, Hydraulic and Automatic Control Divisions, Winter Annual Meeting and Symposium on Fluid Jet Control Devices, New York, N.Y., Nov. 28, 1962. In: Fluid Jet Control Devices, New York, N. Y., 1962, p. 7-22. 348 refs. (A63-13667)

Presentation of a brief discussion and an extensive bibliography on the significant progress made in all phases of pure-fluid systems. The following topics are covered: (1) hardware (2) variables, such as power level, supply-pressure level, Reynolds number, power-nozzle width, gain, and frequency; (3) problem areas, including sealing, system power consumption, aspect ratio, coupling, interface, creep, definition of acceptable tolerances, SNR, and drift; (4) instrumentation; and (5) manufacturing. In addition, an account is given of the several flow visualization techniques, such as the water table, the smoke tunnel, hydrogen-bubble technique, interferometers, fiber-optic monitor, and hot-wire anemometry.

I - 8 FLUID JET CONTROL DEVICES

Edited by Forbes T. Brown

American Society of Mechanical Engineers, Hydraulic and Automatic Control Divisions, Winter Annual Meeting and Symposium on Fluid Jet Control Devices, New York, N. Y. Nov. 28, 1962. New York, ASME, 1962. 90 p. (A63-13665)

Collection of 10 papers which present detailed technical information on fluid-jet modulators or control devices which have no moving mechanical parts. In addition, a general state-of-the-art survey is attempted. Continuous and bistable amplifiers are discussed in detail.

I - 9 SCIENTIFIC SEMINAR ON PNEUMATIC-HYDRAULIC AUTOMATION

A. I. Semikova

Automation and Remote Control. Translation: Vol. 23, No. 12, Aug 1963. p. 1615-1619. (Russian Original: Vol. 23, No. 12, Dec 1962. p. 1720-1723.)

A relatively brief summary is given of the Fifth Session of the All-Union Seminar on Pneumo-Hydraulic Automation held in Leningrad, 11-13 June 1962. Approximately 380 persons contributed more than 50 reports and communications. One paper, presented by Berezovets and Tatarko, reports a detailed investigation of schemes for jet devices which do not contain moving parts.

I - 10 NO MOVING PARTS NEEDED! - FLUID AMPLIFIERS PERFORM ELECTRON-LIKE FUNCTIONS

Jeffrey N. Shinn

SAE Journal, Vol. 71, No. 8, Aug 1963. p. 38-43. (Based on "Fluid Amplifiers - Their Status and Some Applications", a report to SAE Subcommittee A-6C, 6 May 1963, Miami, Fla.)

Describes the characteristics of fluid amplifiers; gives developmental status and identification of some present and planned applications of fluid amplifier systems.

I - 11 FLUID COMPUTATION AND CONTROL SYMPOSIUM

W. T. Rauch, H. Stern

General Electric Co. GEL Report 63GL115, August 12, 1963.

I - 12 NEW DEVELOPMENTS IN PNEUMOAUTOMATION

M. Aizerman, A. Tal'

International Federation on Automatic Control. Presented September 1963, Zurich, Switzerland

I - 13 FLUID AMPLIFIER STATE OF THE ART, VOLUME I

General Electric Co., Advanced Technology Labs, and Light Military Electronics Dept. Phase I Report, Research and Development ____ Fluid Amplifiers and Logic; 3 Dec 1963. (Prepared for George C. Marshall S. F. C. under Contract NAS805408.)

The report is issued in four volumes. Volumes III and IV contain the classified material not contained in Volumes I and II, respectively.

This volume reports a survey of the current state-of-the-art of fluid amplifiers including both theoretical and practical aspects of devices having no mechanical moving parts. Specific areas covered are design techniques (analytical and experimental), typical elements and assemblies, applications, fabrication techniques, and instrumentation.

I - 14 FLUID AMPLIFIER STATE OF THE ART, VOLUME II - BIBLIOGRAPHY

General Electric Co., Advanced Technology Labs, and Light Military Electronics Dept. Phase I Report, Research and Development ____ Fluid Amplifiers and Logic; 3 Dec 1963. (Prepared for George C. Marshall S. F. C. under Contract NAS805408)

The report is issued in four volumes. Volumes III and IV contain the classified material not contained in Volumes I and II, respectively.

This volume, a bibliography, contains 317 references of which 210 are annotated. Material presented pertains to no-moving-parts devices, some closely related moving-parts devices, as well as some of the supporting technology.

I - 15 FROM THE INSTITUTE OF AUTOMATION AND REMOTE CONTROL: JET DEVICES FOR REGULATION AND CONTROL AND THE TECHNOLOGY OF PNEUMATIC PRINTED CIRCUITS

Automation and Remote Control. Translation: Vol. 24, No. 8, Jan 1964. p. 1050-1057. (Russian Original: Vol. 24, No. 8, Aug 1963. p. 1155ff.)

This article discusses research conducted at the Pneumatic Hydraulic Automation Laboratory of the Institute of Automation and Remote Control (IAT). The development of "jet stream technology" and "pneumonics" in the USSR is described. Several basic fluid elements, including logic devices, are illustrated and the principles underlying their function presented. Graphic representations of some basic element characteristics are also given. Other pictorials show a printed circuit, a circuit element, and a method of preparation. The article concludes with comments on the present state of "fluid technology" in the Institute of Automation and Remote Control.

Patents in several countries are cited in the bibliography of this article.

SECTION II —— BASIC FLUID THEORY

II - 1 REMARKS ON THE PURE FLUID AMPLIFIER

H. H. Glättli

IBM, Zurich Research Laboratory. Research Note RZ - 2.

II - 2 REATTACHMENT OF SEPARATED BOUNDARY LAYERS AND THEIR EFFECTS IN FLUID SWITCHING DEVICES

A. E. Mitchell

IBM, Zurich Research Laboratory, Adlisiwil - Zurich, Switzerland. Research Report No. RZ-81, 19 February 1962.

II - 3 THE APPLICATION OF FREE JET MIXING THEORIES TO FLUID AMPLIFIER ELEMENTS

Glen W. Zumwalt

Diamond Ordnance Fuze Laboratories, Washington, D. C. Proc. of the Fluid Amplification Symp., Oct. 2-4, 1962. Dated Nov. 15, 1962. p. 201-216. 21 refs. (N63-13396)

Korst's turbulent free-jet mixing theory and Champman's laminar free-jet mixing theory were investigated in order to (1) make immediate application where possible, (2) delineate inherent limitations, and (3) suggest profitable extensions of the theoretical treatments. The investigation was limited to two-dimensional, perfect gas jet-flows, where the jet "core"

is supersonic. Results indicate that the two jet mixing theories investigated can be applied immediately with confidence to many plane flow fluid amplifier problems.

II - 4 A THEORETICAL MODEL FOR SEPARATION IN THE FLUID JET AMPLIFIER

Yih-O Tu and H. Cohen

IBM Journal of Research and Development, Vol. 7, No. 4, October 1963. p. 288-296.

A theoretical study, based on the re-entrant jet model, is made of the growth of the separation region in the fluid jet amplifier. The flow is taken to be inviscid, but dissipation of momentum is obtained by means of the re-entrant jet. The effect of control port pressure and wall angle on the size of the separation region is calculated. Several other versions of the model are suggested. (A)

SECTION III — JETS

III - 1 JET INTERACTION IN A DEFINED REGION

Francis M. Manion

Catholic University, Dept. of Mech -Aero. Eng'g. Thesis, M. M. E., March 1962.

The problem presented deals with the interaction of two jet streams in a defined interaction region. The deflection of a power jet by the normal addition of a control jet is investigated. A two dimensional analysis is developed which relates the direction of the resultant stream to the input momentum ratio and the geometry of the interaction region.

(A)

III - 2 INTERACTION OF TRANSVERSELY IMPINGING JETS

Darshan S. Dosanjh and William J. Sheeran

Diamond Ordnance Fuze Labs., Washington D. C. Proceedings of the Fluid Amplification Symp., Vol 1, Oct 2-4, 1962. Dated Nov 15, 1962. p. 217-265. 15 refs.

Experiments on the interaction of transversely impinging jet flows were performed in which a low-pressure control-jet flow interacted with a relatively high-pressure power-jet flow. The ratio of the control-jet to the power-jet supply-chamber gage stagnation pressure was varied. Both two-dimensional and axisymmetric jets were used. Shadowgraphs of the power jet alone as well as of the corresponding interaction jet flows were recorded to establish the nature of, and changes in, the shock structure. The two-dimensional jet flows were traversed by a pitot tube to record pitot pressure at various locations downstream of the power jet exit. It was observed that the impingement of only two percent control jet flow was sufficient to change the normal shock front of the highly underexpanded two-dimensional jet flow to a repetitive oblique shock structure. A considerable increase in the corresponding maximum pitot pressure downstream of the previous location of the normal shock was

recorded. Possible importance of this phenomenon to fluid amplifiers using such highly underexpanded power-jet flows is pointed out. (A)

III - 3 AN ANALYTICAL AND EXPERIMENTAL STUDY OF TWO-DIMENSIONAL COMPRESSIBLE SUBMERGED JETS

R. E. Olson

Diamond Ordnance Fuze Labs., Washington D. C. Proceedings of the Fluid Amplification Symp., Vol 1, Oct 2-4, 1962. Dated Nov 15 1962. P 267-286. 3 refs. (N63 - 13398)

Analytical and experimental studies of compressible, two-dimensional, turbulent submerged jets were conducted with air as the working fluid. A theoretical flow model is presented and a momentum integral analysis is developed based on this flow model. The analysis employs constant exchange coefficient mixing theory to express the turbulent shear stress, and assumes a Gaussian velocity distribution in the mixing zone. Relationships are presented for the length of the inviscid core and the centerline velocity decay in the fully developed portion of the jet in terms of an empirical shear stress constant. Experimental results obtained for jet Mach numbers between 0.66 and 2.0 are discussed and employed to evaluate the shear stress constant which appears in the analysis. These values of shear stress constant are correlated with jet Mach number, and the significance of this correlation is discussed.

III - 4 CHARACTERISTICS OF TWO-DIMENSIONAL COMPRESSIBLE ATTACHED JETS

R. E. Olson

Diamond Ordnance Fuze Labs., Washington, D. C. Proceedings of the Fluid Amplification Symp., Vol 1, Oct. 2-4, 1962. Dated Nov. 15, 1962. P. 179-200 6 refs. (N63-13395)

Analytical and experimental studies of the characteristics of two-dimensional, compressible jets attached to an adjacent blundary wall were conducted with air as the working fluid. A theoretical flow model is presented and

methods for predicting the jet characteristics based on this model are discussed. Experimental measurements of the flow profiles within the jet at various axial stations both upstream and downstream of the reattachment location for Mach numbers of 0.90 and 2.0 are presented. Corrlations of the experimental results on the basis of the analytical concepts are made for certain regions of the jet. Measurements of pressure-recovery characteristics of a diffuser located downstream of reattachment are presented and compared with pressure recoveries calculcated on the basis of average conditions at the diffuser inlet. (A)

III - 5 CHARACTERISTICS AND CONTROL OF FREE LAMINAR JETS

Alan Powell

Diamond Ordnance Fuze Labs., Washington, D. C. Proceedings of the Fluid Amplification Symp., Vol. 1, Oct 2-4, 1962. Dated Nov 15, 1962. P. 289-299. 7 refs. (N63 - 13399)

A description is presented of some relevant basic features of laminar incompressible jet flows as a separate element free of the effects of adjacent solid walls. The characteristics of the steady flow are well established, theoretically and experimentally. Results are given showing how the main jet is deflected by side jets, the deflection angle being dependent upon the geometry. Classical instability theory of periodically disturbed "pseudo-laminar" jets has been supplemented by recent experimental work.

This work is now extended to the case of the main jet being disturbed by periodic (modulated) side jets. The classical oscillatory feedback of edgetones, from a wedge-like

obstruction lying in the jet, is discussed, as is also the case when a resonating element is in the feedback path. (A)

III - 6 FLUID AMPLIFICATION. 5. JET ATTACHMENT DISTANCE AS A FUNCTION OF ADJACENT WALL OFFSET AND ANGLE

Sheldon Levin and Francis M. Manion

Harry Diamond Labs., Washington D. C. TR - 1087, 31 Dec 1962. 32 p. 6 refs.
(N63 - 13624) (AD-297 895)

Attachment of a submerged, incompressible, two-dimensional, turbulent jet to an adjacent straight wall (Coanda)effect) is analyzed. Parametric equations are developed that predict the point at which the jet attaches as a function of wall angle and offset distance. Computer solutions were obtained for several sets of conditions. Experiments were conducted with both air and water jets at Mach 0.5 equivalent, and results agree well with correspondiing computer solutions when the spread parameter is also treated as a function of offset distance and wall angle. The equations provide an analytic method, independent of the particular fluid, for predicting the attachment distance, and should be helpful in designing elements based on the Coanda effect, e. g., the fluid flip-flops or bistable elements. (A)

III - 7 EXPERIMENTS WITH TWO-DIMENSIONAL, TRANSVERSELY IMPINGING JETS

D. S. Dosanjh and W. J. Sheeran

AIAA Journal, Vol. 1, No. 2, February 1963, p. 329-335.

Experiments on the interaction of transversely impinging two-dimensional jet flows were performed in which a low pressure control jet flow interacted with a relatively high pressure power jet flow. The ratio of the control jet to the power jet supply chamber gauge stagnation pressure was adjusted at 0, 10 and 15%. Shadowgraphs of the power jet alone, as well as the corresponding interacting jet flows, were recorded to establish the nature of and changes in the shock structure.

III - 8 INTERACTING JET FLOW INVESTIGATIONS PART I. FURTHER EXPERIMENTS WITH TWO-DIMENSIONAL UNDEREXPANDED, TRANSVERSELY IMPINGING JET FLOWS

D. S. Dosanjh and W. J. Sheeran

Syracuse University Research Institute, Dept. of ME, Report No. ME1058-63091, February 1963.

III - 9 FLUID AMPLIFICATION 6. AERODYNAMIC STUDIES OF FREE AND ATTACHED JETS

Robert E. Olson and David P. Miller

United Aircraft Corp., Research Laboratories. Report A-1771-24, 14 Oct 1963. 185 p. (Prepared for Army Materiel Command, Harry Diamond Laboratories under Contract DA-49-186-ORD-912; includes Interim Reports.)

Theoretical and experimental investigations were conducted to provide information regarding the aerodynamic characteristics of two-dimensional turbulent compressible jets. The investigations included studies of free jets, wall jets, and reattaching jets. The theoretical investigations provided analytical models for the three types of jet flows, procedures for predicting the velocity profile development characteristics for free jets and wall jets, and a procedure for predicting the reattachment location and mean pressure in the separation bubble for reattaching jets. The experimental studies which were conducted provided data to substantiate the analyses and to evaluate empirical constants. These data included measurements of the flow profiles at various stations downstream of the nozzle exit for the three types of jet flows. For the reattaching jets, additional measurements were made of wall static pressure distributions, reattachment locations, and the pressure recovery and weight-flow characteristics of diffusion systems located downstream of the reattachment point.

A correlation between theory and experiment was found for the free jet and wall jets in both the core and developed regions by using constant exchange coefficient mixing theory and by assuming velocity profile similarity within the fully developed mixing zones. For the reattaching jets, it was found that the analytical procedure, which assumed the jet characteristics upstream of reattachment were similar to the free jet, could be employed to predict the location of the reattachment point. Tests with a diffuser installed downstream of the reattachment point showed that the diffuser pressure recovery for the case of no spillage flow could be predicted by using average flow properties obtained from measured profiles in the jet without the diffuser installed.

(A)

SECTION IV —— NOZZLES AND DIFFUSERS

(No Citations)

V - 1 VORTEX VALVE DEVELOPMENT

E. M. Dexter

General Electric Co., General Engineering Lab. G. E. L.
Report, 17 April 1961. 7 p. 13 figs.

VI - 1 A VIBRATORY ACOUSTIC GYROSCOPE

Richard Swerdlow and John G. Whitman, Jr.

MIT, Electronic Systems Lab., Cambridge, Mass. ESL-TM-162, Dec 1963. 29 p. 8 refs. (DSR-8836; Avail. OTS) (N63-13603) (NASA grant NsG - 149-61)

SECTION VII —— THERMODYNAMICS

(No Citations)

VIII - 1 SOME EFFECTS OF GEOMETRY IN A FLUID AMPLIFIER

R. A. Comparin

IBM, Zurich Research Laboratory. IBM Research Note NZ-4.

VIII - 2 VALVULAR CONDUIT

N. Tesla

U. S. Patent No. 1,329,559; February 3, 1920.

This patent consists in the employment of a peculiar channel or conduit characterized by valvular action. This invention can be embodied in many constructions greatly varied in detail, but for the explanation of the underlying principle, it is stated by Tesla that the interior of the conduit is provided with enlargements, recesses, projections, baffles, or buckets which, while offering virtually no resistance to the passage of the fluid in one direction, other than surface friction, constitute an almost impossible barrier to its flow in the opposite sense by reason of the more or less sudden expansions, contractions, deflections, reversals of direction, stops and starts and attendant rapidly succeeding transformations of the pressure and velocity energies.

VIII - 3 DEVICE FOR DEFLECTING A STREAM OF ELASTIC FLUID PROJECTED INTO AN ELASTIC FLUID

Henri Coanda

U. S. Patent No. 2,052,869; September 1, 1936.

A device is described in which, by allowing a "suitable checking" of the surrounding fluid on one side of an orifice from which a fluid stream or sheet is discharged at high velocity, it is possible to act indirectly to control the direction of the issuing stream or sheet.

VIII - 4 MECHANICAL RELAY OF THE FLUID JET TYPE

R. C. Braithwaite and K. Wilcox

U. S. Patent No. 2,408,603; 1 October 1946.

This invention relates to mechanical relays of the fluid jet type and has for its object to reduce the reaction imposed upon the controlling member of the relay. According to the present invention the reaction of the fluid jet issuing from the supply nozzle upon the controlling member is reduced to a very small value without loss of controlling accuracy by deflecting said jet from alignment with the receiving orifice by means of another jet which is supplied from a deflecting or controlling nozzle and so mounted as to impinge upon the main jet of fluid issuing from the supply nozzle.

Although a mechanical means of varying impingment is mentioned, graduated control of the main jet may also be attained either by shaping the deflecting or controlling nozzle so that it gives a fantail flow (a flattened or slit-like orifice), or by using two jets impinging upon one another in the manner used in certain forms of acetylene gas burners.

VIII - 5 AERODYNAMIC CHECK VALVE

E. T. Linderoth

U. S. Patent No. 2,727,535; December 20, 1955.

VIII - 6 APPARATUS AND METHODS OF FILING MEASURED AMOUNTS OF VISCOUS OR FINELY DIVIDED SOLIDS

R. M. Magnuson

U. S. Patent No. 2,889,956; 9 June 1959.

This invention employs the basic principles of fluid stream interaction in an apparatus for placing accurately measured amounts of fluent material into a container. Toward this end, a means, comprised of a gaseous jet, is provided for starting or interrupting a flow of fluent material through space and directing it along a passageway other than the original path of flow.

VIII - 7 SUCTION AMPLIFIER

H. Hurvitz

U. S. Patent No. 3,001,539; 26 Sept 1961.

This invention concerns a type of fluid amplifier utilizing no moving parts, in which boundary layer lock-on effects are employed by controlled reduction of pressure in a boundary layer lock-on region, rather than by a control jet. This reduction is effected by means of a channel communicating between the boundary layer interaction region and a region of lower pressure that exists in the power stream itself.

VIII - 8 FLUID PULSE CONVERTER

R. W. Warren

Patent No. 3,001,698; 26 September 1961

It is an object of this invention to provide a fluid pulse converter capable of converting sequential fluid pulses received thereby into alternating fluid pulses without the need of moving parts, other than the fluid required for the operation thereof.

According to this invention, a pair of substantially opposed control nozzles of a fluid amplifier are connected to a novel tube system so that a pressure differential is created in the tube system when a power jet flowing between the nozzles more closely approaches one control nozzle than the other. This pressure differential is used to steer sequential pulses conveyed to the tube system into the one control nozzle so that the fluid flowing between the nozzles will be deflected by the one control nozzle towards the other control nozzle. Sequential fluid pulses can thusly be converted into alternating fluid pulses.

VIII - 9 FINAL REPORT ON THE DEVELOPMENT PROGRAM OF THE ADVANCED CONTROL COMPONENTS UNIT

S. F. Hemmenway and A. L. Spivak

General Electric Co. Report APEX-666, Part II, January 1962. [USAF Contract AF (600) 38062 and AEC Contract AT (11-1)-171]

VIII - 10 FLUID VALVE

George F. Hausmann

U. S. Patent No. 3,061,063; 9 January 1962.

It is the object of this invention to provide a fluid deflection type valve in which the control jets consist of ejectors which pump fluid from an area opposite the control jet to reduce the pressure on the opposite side of the main stream and thereby improve the effectiveness of the control jet in deflecting the main stream.

VIII - 11 FLUID OSCILLATOR

R. W. Warren

U. S. Patent No. 3,016,066; 9 January 1962.

Specifically the object of this invention is to provide a fluid oscillator which utilizes a jet of air which is made to oscillate back and forth between two passages in such a manner that it can be used for timing and other purposes where an alternating air stream is desired. The principle of boundary layer control is utilized in a system which has no moving parts.

VIII - 12 NEGATIVE FEEDBACK FLUID AMPLIFIER

B. M. Horton

U. S. Patent No. 3,024,805; 13 March 1962.

The invention claims a negative feedback fluid amplifier adapted to provide a substantially constant fluid flow therefrom, comprising a fluid feedback path having an opening for receiving and feeding back a portion of said main fluid stream into said amplifier, said fluid feedback path being constructed and arranged such that fluid fed back to said amplifier deflects said main stream so that less fluid flows into said opening, and means in said feedback path adapted to smooth out any variations of fluid flow therein.

VIII - 13 INDUCTION FLUID AMPLIFIER

R. J. Reilly

U. S. Patent No. 3,030,979; 24 April 1962.

This invention is directed to a type of induction fluid amplifier or element that utilizes the viscous forces existing between flowing fluids and associated fluids or fixed partitions. More specifically, the present invention is directed to a fluid flow element or system that utilizes no moving parts in control of a main fluid stream by the use of an inducing controlled fluid stream.

VIII - 14 AN EXPERIMENTAL STUDY OF THE CHARACTERISTICS OF A PNEUMATIC VALVE WITH NO MOVING MECHANICAL PARTS

W. J. Hastings

MIT, Department of Mechanical Engineering. Thesis, B. S., June 1962.

The thesis investigates,experimentally, the pressure-flow characteristics of a pneumatic valve with no moving mechanical parts, and having a main jet, a fluid dynamical means of deflecting the jet, and a pair of receivers which are connected to the load. The test valve allowed the variation of the following parameters: the receiver opening, the deflection of th e main jet, the spacing between the main jet and the receiver, and the spacing between the receivers. (A)

VIII - 15 CYLINDRICAL FLUID AMPLIFIER

William L. Carlson

U. S. Patent No. 3,039,490; 19 June 1962.

The present invention is directed to a fluid amplifier having a cylindrical configuration as opposed to the usual flat configuration. The principles of the fluid amplifiers developed by Horton, et al, are used, and the basic control theory used by either Horton or Reilly can be applied.

A primary object of the present invention is to disclose a fluid amplifier of cylindrical configuration that has reduced the turbulence generating corners of the conventional types of fluid amplifiers, and that can utilize conventional construction techniques and existing tubular members and parts.

VIII - 16 EXPERIMENTAL LOAD CHARACTERISTICS OF FLUID-JET AMPLIFIERS

A. R. Van Koevering

MIT, Dept. of Mechanical Engineering. Thesis, M. S., August 1962.

The experimental load-flow characteristics of fluid jet amplifiers with both single-control ports and double-control ports are presented. A pneumatic model was used and the effects of a supersonic jet at various supply pressures, a subsonic incompressible jet, and the position of the attachment wall or walls were investigated. It was concluded that these effects should be negligible with the proper design. The graphical techniques of matching source and load characteristics are illustrated and their usefulness in the design of fluid jet amplifiers is emphasized. (A)

VIII - 17 FLUID AMPLIFICATION. 1. BASIC PRINCIPLES

R. W. Warren and S. J. Peperone

Diamond Ordnance Fuze Labs., Washington, D. C. TR-1039, 15 Aug 1962. 24 p. (N62- 17222) (AD-286 256)

Studies made on pure fluid amplification have resulted in an overall program for design and development of fluid amplifiers, both bistable and proportional, with no moving parts. Both flow and pressure at the receiving apertures of the proportional-type device depend on the power jet strength and flow direction. Since the flow direction is controlled by a low-energy jet, the output from the apertures is an amplified version of the control jet input. The energy controlled in the amplifier is an order of magnitude larger than the controlling energy. If the walls are relatively close to the interaction region, the stream has a marked tendency to attach to one of the walls. This wall-attachment phenomenon causes the fluid stream to shift completely from one output to the other in response to a control jet pulse, thereby permitting bistable operation. For a proportional unit, the walls are positioned much farther out to minimize the wall effect. Specifically covered in this report are the effects of the wall and splitter positions in bistable operation, and an analysis of the gain for proportional operation. (A)

VIII - 18 FLUID AMPLIFICATION. 4. GAIN ANALYSIS OF THE PROPORTIONAL FLUID AMPLIFIER

S. J. Peperone, Silas Katz, and John M. Goto

Diamond Ordnance Fuze Labs., Washington, D. C. TR-1073, 30 Oct 1962. 43 p. 4 refs. (N63 - 12764) (AD-296 513)

A theoretical analysis of signal gain using principles of fluid stream interaction is presented. This analysis is applied to predict pressure, flow, and power gains of a fluid amplifier and to determine optimum operating conditions and geometry. Comparison of theory and measurements shows agreement within the experimental error. (A)

VIII - 19 FLUID OSCILLATOR

A. E. Mitchell

IBM Technical Disclosure Bulletin, Vol. 5, No. 6, Nov 1962. p. 25.

This fluid oscillator is built of a single-sided, monostable fluid amplifier by providing a single feedback connection from its stable outlet to the control channel.

VIII - 20 TURBULENCE AMPLIFIER DESIGN AND APPLICATION

Raymond N. Auger

Diamond Ordnance Fuze Labs., Washington, D. C. Proc. of the Fluid Amplification Symp., Vol. 1, Oct 2-4, 1962. Dated Nov. 15, 1962. P. 357-366. (N63-13402)

The turbulence amplifier is a pneumatic or hydraulic no-moving-parts fluid amplifier with many unique properties which make it suitable for use in logic circuits and as a primary sensor of low velocity fluid streams and low acoustic waves. The turbulence amplifier produces signal amplification by the disturbance of a laminar flow in a submerged jet. The turbulence amplifier has a number of advantages when used as a switching element in logic circuits. It is a major convenience in constructing such circuits to use an element which is free of impedance-matching problems and which exhibits the large fan-out ratio (1:10) of these units. The complete isolation of turbulence amplification inputs and the fact that a single amplifier can have an almost unlimited number of inputs is a major advantage in many practical circuits.

A third major advantage presented by the author is the fact that each amplifier performs the logical NOR function, which can be used as the basis for all other logic functions, such as AND, OR, MEMORY (flip-flop), and counting circuits.

VIII - 21 ON THE INHERENT LIMITATIONS IN FLUID-JET MODULATORS

F. T. Brown

Diamond Ordnance Fuze Labs., Washington, D. C. Proc. of the Fluid Amplification Symp., Vol. 1, Oct. 2-4, 1962. Dated Nov. 15, 1962. P. 367-279. 10 refs. (N63-13403)

The manner in which wave motion, energy dissipation, and gross jet turbulence produce inherent limitations in fluid-jet modulators is qualitatively discussed. Topics include surge impedance matching at input and load ports, the possibility of nearly infinite pressure and power gains of "momentum-controlled" and "pressure-controlled" jet amplifiers, and the effect of nozzle design on jet noise with implications on the signal-to-noise ratio and other operating conditions. (A)

VIII - 22 AN INTRODUCTION TO PROPORTIONAL FLUID CONTROL

Silas Katz

Diamond Ordnance Fuze Labs., Washington, D. C. Proc. of the Fluid Amplification Symp., Vol. 1, Oct. 2-4, 1962. Dated Nov 15, 1962. P. 21-26. (N63-13382)

A basic description of the proportional fluid amplifier and its function, is given. Some examples of geometry are shown. Passive components (those not requiring a separate power supply) and their general characteristics are also discussed.

VIII - 23 GAIN OF THE PROPORTIONAL FLUID AMPLIFIER

S. J. Peperone, Silas Katz, and John M. Goto

Diamond Ordnance Fuze Labs., Washington, D. C. Proc. of the Fluid Amplification Symp., Vol. 1, Oct. 2-4, 1962.

Dated Nov 15, 1962. P. 319-356. 4 refs. (N63-13401)

A theoretical analysis was made of the gains in pressure, volume flow, and power of a proportional amplifier. Predictions were compared with experimental data. Incompressible flow was assumed in this analysis, and the measurements were made for power-jet pressures of less than 5 psig. The theory indicates that a power gain of about 100 is easily achievable with pressure and flow gains of about 10. All gains are at maximum when the power stream is evenly divided by the two output apertures. The gains decrease with deflection angle and become zero when the stream is approximately centered in one of the apertures. The power gain maximizes at about 11 power-jet-nozzle widths downstream with aperture widths 1.5 times the power-jet nozzle width. Comparison of those aspects of the theory that could be checked on a single laboratory model showed good agreement within the experimental error. On this model, the pressure gain was calculated to be 9.1 and measured 8.4; the flow gain was calculated to be 10.5 and measured 9.4.

VIII - 24 WALL EFFECT AND BINARY DEVICES

R. W. Warren

Diamond Ordnance Fuze Labs., Washington, D. C. Proc of the Fluid Amplification Symp., Vol. 1, Oct 2-4, 1962. Dated Nov. 15, 1962. P. 11-20. (N63-13381)

Discussion of a bistable fluid amplifier using entrainment characteristics of a power stream and boundary walls to effect stream deflection is presented. Includes: initial and final fluid flows between parallel walls; methods of switching the stream; control of completely filled bistable elements; a flow model for interaction and profile adjustment regions; memory characteristics which are functions of the divider within the element; adjustment of an overexpanded stream by means of an oblique shock wave; and the effects of increasing the parameter dimensions of a bistable element.

VIII - 25 PERFORMANCE EVALUATION OF A HIGH-PRESSURE-RECOVERY BISTABLE FLUID AMPLIFIER

W. A. Boothe

American Society of Mechanical Engineers. Hydraulic and Automatic Control Division. Winter Annual Meeting and Symposium on Fluid Jet Control Devices. N. Y., N.Y., Nov. 28, 1962. IN: Fluid Jet Control Devices. P. 83-90. (A63-13675)

Description of the characteristics of a form of fluid amplifier that has both a high pressure recovery and a low sensitivity to output loading. A generalized configuration of the amplifier is graphically represented. The amplifier is designed to drive an air cylinder load. It must be capable of developing a high differential pressure across the piston under the blocked load conditions encountered during breakaway, and again at the end of the cylinder stroke. The high pressure recovery is obtained by use of an indented receiver spike which produces a "latching vortex" that presses the jet against the sidewall to which it is attached. This increases stability of the jet attachment and affects pressure levels and jet entrainment on the unattached side of the jet. The two load outputs are effectively "decoupled" by the use of vents placed in the high-velocity region of the receivers. This also allows simplification of the presentation of the amplifier's static characteristics.

VIII - 26 A COMBINED ANALYTICAL AND EXPERIMENTAL APPROACH TO THE DEVELOPMENT OF FLUID JET AMPLIFIERS.

Forbes T. Brown

American Society of Mechanical Engineers, Hydraulic and Automatic Control Division, Winter Annual Meeting and Symposium on Fluid Jet Control Devices, N.Y., N.Y. Nov 28, 1962. IN: Fluid Jet Control Devices. ASME, 1962. P. 1-5. (Abridged) (A63-13666)

Discussion of an approach to the development of "pressure-controlled" fluid jet relays and amplifiers. The technique, based on experiments of a jet attaching to a flat wall, combines theoretical reasoning, experi-

mental data, and graphical source-load matching. Single-control and symmetrical double-control amplifiers of a particular "knife-edge" design are used in the illustrations of the approach; typical data are given. Static and dynamic stability of the jet is emphasized, including the criteria for oscillations. (A)

VIII - 27 ON THE LIMITATIONS AND SPECIAL EFFECTS IN FLUID JET AMPLIFIERS

R. A. Comparin, H. H. Glättli, A. E. Mitchell, and H. R. Müller

American Society of Mechanical Engineers, Hydraulic and Automatic Control Divisions, Winter Annual Meeting and Symposium on Fluid Jet Control Devices, N.Y., N.Y. Nov 28, 1962. IN: Fluid Jet Control Devices, N.Y., ASME 1962, P. 65-73. (A63-13673)

Description of the effect of variation of the Reynolds number on the flow pattern in a fluid amplifier. A minimum Reynolds number is observed below which monostable or bistable flow does not occur, and the effect of variation of shape of the element on this minimum value is given. A maximum jet velocity is discussed which depends primarily upon whether the fluid is a liquid or a gas. The response time and power consumption of an element are shown to be dependent on thefluid, the jet velocity, and the linear size of the element. An estimate of response time and power is given as a function of the linear size of the element and the Reynolds number.

A discussion by F. R. Goldschmied is presented on page 73.

VIII - 28 AN ANALOG PURE FLUID AMPLIFIER.

E.M. Dexter

American Society of Mechanical Engineers, Hydraulic and Automatic Control Divisions, Winter Annual Meeting and Symposium on Fluid Jet Control Devices, N.Y., N.Y., Nov 28, 1962. IN: Fluid Jet Control Devices. N.Y., ASME, 1962, P. 41-49. (A63-13670)

Description of a vented-type pure-fluid amplifier in which the power jet issuing from the power nozzle enters a cavity that is vented to the ambient pressure before being recovered in the receivers. The analog amplifier theory presented establishes approximate receiver locations for a maximum gain and some considerations for receiver nozzle sizing in staged systems. The calculations given show that the receivers for a general-purpose amplifier should be located somewhere between 6 and 9 power-nozzle diameters downstream. For staging, it is desirable to have receivers and control nozzles of the same area. The model investigations provide information on noise attenuation, size and location of the vent areas, and the desirability of providing a cross vent under the power jet. The models of art board and laminated phenolic are modified to test the effects of geometry changes. It is found that the observations hold true in 4 to 1 reduction to an amplifier with a 0.025-in.nozzle. A three-stage amplifier has been utilized in a feedback system and the frequency response measured to 200 cps without detection of any appreciable attenuation or phase shift.

VIII - 29 A PERFORMANCE CRITERION FOR FLUID JET AMPLIFIERS.

R. E. Norwood

American Society of Mechanical Engineers, Hydraulic and Automatic Control Divisions, Winter Annual Meeting and Symposium on Fluid Jet Control Devices, N.Y., N.Y., Nov 28, 1962. IN: Fluid Jet Control Devices. N.Y., ASME, 1962, P. 59-63. (A63-13672)

An examination of a bistable-type fluid amplifier in which the jet has two stable positions. The problem considered is that of evaluating the performance of a fluid jet amplifier in order that the elements can be properly interconnected. The performance criterion selected is the input impedance of the device. It is indicated that by using this concept, the switching behavior can be more clearly understood and the type of operation desired can be chosen. Some experimental data are shown to illustrate the method.

VIII - 30 NOTES ON A PROPORTIONAL FLUID AMPLIFIER

R. J. Reilly and F. A. Moynihan

American Society of Mechanical Engineers, Hydraulic and Automatic Control Divisions, Winter Annual Meeting and Symposium on Fluid Jet Control Devices, N.Y., N.Y., Nov 28, 1962. IN: Fluid Jet Control Devices, N.Y., ASME, 1962, P. 51-57. (A63-13671)

Analytical investigation of a proportional, beam-deflection fluid amplifier, involving the mixing process of three impinging jets.

On the basis of flow visualization studies, an inviscid analytical model, which assumes no mixing, is postulated. A submerged jet formulation is also presented; however, it has been extended to include numerical integration of the velocity profile. The two mathematical models are analyzed, and the results are compared with experimental data taken on a specific type of momentum-controlled proportional fluid amplifier. The following conclusions are reached: (1) the experimental output vs input, the experimentally derived velocity profiles, and the visualization studies all detract from the validity of the submerged jet analogy as applied to the fluid amplifier configuration tested; (2) the inviscid model does not adequately predict the performance of the fluid amplifier, and the change in amplification with changing mass ratio predicted by the inviscid model does not appear in experimental measurements; and (3) a modification of the inviscid model to account for the contraction of the power stream should be examined.

VIII - 31 SOME PARAMETERS AFFECTING THE DESIGN OF BISTABLE FLUID AMPLIFIERS.

R. W. Warren

American Society of Mechanical Engineers, Hydraulic and Automatic Control Divisions, Winter Annual Meeting and Symposium on Fluid Jet Control Devices, N.Y., N.Y., Nov 28, 1962. IN: Fluid Jet Control Devices, N.Y., ASME, 1962, P. 75-82. (A63-13674)

A description of the characteristics of two bistable fluid amplifiers, which represent the two extremes affecting the design of a fluid amplification system. One is a low-gain bistable fluid amplifier which is very stable. The other is a high-gain bistable amplifier which tends to oscillate.

VIII - 32 PNEUMATIC TO ELECTRIC TRANSDUCERS

I. G. Akmenkalns, E. Pasternak, and R. R. Schaffer

IBM Technical Disclosure Bulletin, Vol. 5, No. 7, Dec 1962

These transducers provide electrical output signals denoting the logic state of a fluid amplifier type logic device. The transducing system employs either temperature-sensitive diodes or pressure-sensitive resistors.

VIII - 33 PNEUMATIC DIODE

H. E. Riordan

U. S. Patent No. 3,068,880; 18 Dec 1962.

This invention utilizes the phenomenon of critical flow to produce diode-like properties in a simple orifice arrangement which can be used to instrument digital logic functions pneumatically. One object is to produce a pneumatic diode which is simple in operating principle and construction, has no moving parts, and has very high response speed.

VIII - 34 EXPERIMENTAL DESIGN OF A FLUID-CONTROLLED HOT GAS VALVE

Kenneth C. Evans, Carroll Godwin, J. C. Dunaway, W. E. Lane and Vernon Ayre

Army Missile Command, Huntsville, Ala. Electromagnetic Laboratory. RE - TR - 62 - 9, 21 Dec 1962. 27 p. (N63-19598)

This report describes an effort toward development of a hot-gas-jet reaction valve utilizing boundary-layer techniques to control a high-temperature gas stream. The result of this work has been the successful design of a hot-gas valve in a reaction control system, utilizing fluid-controlled bistable amplifier principles and requiring no moving parts in the gas stream. This preliminary status report on the work gives the experimental design approach and results achieved with no particular attempt being made to develop the theory. Valves have been fabricated and successfully tested to control gas at pressures to 1200 psi and temperatures to 2350°F with flow rates as high as 0.16 lb/sec at the highest temperatures. Efficiencies comparable to standard valving techniques have been realized. (A)

VIII - 35 A COMBINED ANALYTICAL AND EXPERIMENTAL APPROACH TO THE DEVELOPMENT OF FLUID-JET AMPLIFIERS

F. T. Brown

American Society of Mechanical Engineers. Paper No. 62-WA-154, 30 July 1962. (Unabridged)

An approach to the development of "pressure-controlled" fluid-jet relays and amplifiers is proposed. The technique, based on experiments of a jet attaching to a flat wall, combines theoretical reasoning, experimental data, and graphical source - load matching. Single-control and symmetrical double-control amplifiers of a particular "knife-edge" design are used in the illustrations of the approach; typical data are given. Static and dynamic stability of the jet is emphasized, including the criteria for oscillators. (A)

VIII - 36 ELECTRO-PNEUMATIC FLUID AMPLIFIER

N. A. Cargill and T. D. Reader

U. S. Patent No. 2,071,154; 1 January 1963

This invention pertains to an electrical means for controlling a fluid amplifier without the need for an intermediate transducer. The device has only one fluid input stream called the power stream. The object is to provide

a means responsive to small power electrical signals, for producing larger power fluid signals; also to provide multistable switches responsive to electrical signals for producing fluid output signals.

VIII - 37 THE USE OF SEPARATED CURVED FLOW FOR PROPORTIONAL FLUID STATE AMPLIFICATION

M. B. Zisfein and H. A. Curtiss

Giannini Controls Corp. Report. No. ARD - 06 - 009, March 1963.

VIII - 38 FLUID AMPLIFIER

A. M. Severson

U. S. Patent No. 3,080,886; 12 March 1963.

The object of this invention is to disclose a novel type of fluid amplifier that is capable of controlling the flow of a fluid in a manner which distributes the fluid in one or more of a plurality of outlets; also, to disclose a fluid amplifier that can be used to create turbulence of flow between the inlet and outlet to thoroughly mix one or more fluids fed into an inlet manifold or to separate inlets. A device which can be step controlled, so that fluid can be directed into a plurality of paths from a single inlet, is also an objective.

VIII - 39 FLUID INDICATOR

D. J. Truslove

IBM Technical Disclosure Bulletin, Vol. 6, No. 1, June 1963. P. 26

A tube and reservoir arrangement utilizes the high surface tension forces of a liquid (such as mercury) to produce a visual indication. The liquid is forced from the reservoir into the tube as a result of pressure applied to the reservoir, and returns to the reservoir when the pressure is removed as a result of the surface tension forces. The tube can have various shapes.

VIII - 40 A THEORETICAL STUDY OF THE DESIGN PARAMETERS OF SUBSONIC, PRESSURE CONTROLLED, FLUID JET AMPLIFIERS

A. K. Simson

MIT, Dept. of Mechanical Engineering. Thesis, Ph. D., 15 July 1963.

VIII - 41 SELF-LOCKING FLUID SENSING-STATION

A. E. Mitchell and H. R. Müller

IBM Technical Disclosure Bulletin, Vol. 6, No. 3, August 1963. P 31.

Inventor uses a nozzle-shaped sensing channel, a monostable fluid amplifier, and a bistable fluid amplifier in such an arrangement as to effect a device which does not react to input manipulations when in the "self-locking state," until it is released by applying a reset pulse.

VIII - 42 PNEUMATIC DIODE

D. J. Truslove

IBM Technical Disclosure Bulletin, Vol. 6, No. 3, August 1963. P. 30

This device uses a globule of high-surface-tension liquid (within a tapered cylindrical cavity) in much the same manner as a conventional check valve uses a ball or poppet. The pressure of the fluid tending to flow in one direction causes the "globule" to seal off the potential flow path, while the pressure of fluid tending to flow in the opposite direction "unseats" the "globule" and allows the fluid to flow through a channel by-passing the "globule".

VIII - 43 DISPLAY DEVICE

J. E. R. Young

IBM Technical Disclosure Bulletin, Vol. 6, No. 3, August 1963. P. 22.

The display device has a transparent solid substrate which carries a rough-surfaced shape of the object, e.g., a character, to be displayed. With side illumination, light is scattered by the rough surface. The object is visible if the refractive indexes of the substrate and the surrounding transparent fluid medium differ considerably from each other. If their refractive indexes are either the same or nearly the same, there is no scattering of light and the object remains invisible.

The display device is controlled by displacement of the surrounding fluid medium having the same refractive index as that of the substrate by another with a different refractive index.

VIII - 44 FLUID CONTROL DEVICE

J. E. R. Young

IBM Technical Disclosure Bulletin, Vol. 6, No. 3, August 1963. P. 23.

An otherwise conventional fluid amplifier is controlled on the principle of the ion drag pump, by electrical signals. Ions injected into a fluid are transported through the fluid by application of a high electrical field. The viscous drag on the ions produces a pressure gradient in the fluid. This effect is used to control the switch-over of the main jet of the amplifier.

VIII - 45 RESEARCH STUDIES IN PROPORTIONAL FLUID STATE CONTROL COMPONENTS

H. A. Curtiss and D. J. Lequornik

Giannini Controls Corp., Astromechanics Research Division, Malvern, Pa. ARD - TR - 013 - 01, Sep 1963. 53 p., 34 illustrations. (Prepared under contract DA-36-034-ORD-37-22-RD for Army Missile Command, Guidance and Control Laboratory.)

Results of experimental research in high-gain fluid-state proportional amplification techniques are presented. In particular, the Giannini Controls Corp. Double Leg Elbow Amplifier (DLEA) concept was partially optimized.

This included experimental studies of steady state performance plus the effects of dynamic and transient inputs, output loading, variable input flows, and differing element sizes.

Tests were also conducted to study the possible advantages of amplification obtainable by injecting a control flow at the throat of a converging-diverging nozzle (Aerodynamic Throat Modulation). (A)

VIII - 46 FLUID CONTROLLED DEVICE

B. J. Greenblott

IBM, Technical Disclosure Bulletin, Vol. 6, No. 5, October 1963. P. 15

VIII - 47 THE ANALYTICAL DESIGN AND OPTIMIZATION OF A PNEUMATIC RATE GYROSCOPE FOR HIGH TEMPERATURE APPLICATIONS

W. S. Griffin

MIT. Thesis, Sc.D., 3 October 1963.

SECTION IX --- LOGIC AND COMPUTATION

IX - 1 THE DESIGN AND DEVELOPMENT OF A FLUID LOGIC ELEMENT

J. R. Greenwood

MIT, Dept. of Mechanical Engineering. Thesis, B. S., May 1960.

IX - 2 HYDRAULIC SWITCHING DEVICES

A. P. Speiser

IBM Corp., (Zurich) Research Lab., Adlisiwil-Zurich, Switzerland. IBM Research Report RZ80, 31 Jan 1962. 21 p.

Two all-fluid logic systems are described, one using spool valves as switches, the other employing dynamic phenomena involving no moving (or deformable) solid parts. Both schemes may be operated with liquid or gas. Advantages in power consumption and speed are given for each.

IX - 3 FLUID AMPLIFICATION. 3. FLUID FLIP FLOPS AND A COUNTER

R. W. Warren

Diamond Ordnance Fuze Labs., Washington D. C. TR-1061, 25 August 1962. 25 p. (AD-285 572)

The operating principles of a single-input, fluid-operated flip flop which employs no moving mechanical parts are explained in detail. The principles of the dual-input flip flop are reviewed, and the discussion is extended to the single-input case. Staging is discussed and an example of cascaded staging in a fluid binary counter is given. (A)

IX - 4 FLUID LOGIC DEVICES AND CIRCUITS

A. E. Mitchell, H. H. Glättli and H. R. Müller

IBM, Zürich Research Lab., Ruschlikon, Zurich, Switzerland. Research Paper RZ-99, 20 September 1962. (Translated by Society of Instrument Technology, 26 February 1963).

IX - 5 MAKING PNEUMATIC LOGIC DEVICES

R. F. Langley

IBM Technical Disclosure Bulletin, Vol. 5, No. 5, October 1962. P 4.

This method of making pneumatic logic devices utilizes DYCRIL (trademark) printing plates developed by E. I. du Pont de Nemours and Co. The process suggested uses collimated ultra-violet light and metal backing plates with photosensitive plastic layers bonded on both sides. The object is to etch into the two plastic layers, circuits which would be oriented along axes displaced 90 degrees from each other. Holes would then be drilled through the metal backing plate to connect the "x-axis circuit" to the "y-axis circuit".

IX - 6 FLUID "AND" GATE

R. A. Comparin, A. E. Mitchell and H. R. Müller

IBM Technical Disclosure Bulletin, Vol. 5, No. 6, November 1962. P 30.

A combination of at least two single-sided, monostable, pure fluid amplifiers is described which performs the Boolean AND function of the input pressure signals, which are the controls of the monostable amplifiers. The control signals cause the stream to deviate from the stable mode and exhaust in the direction that a free jet would assume.

IX - 7 FLUID BINARY FULL ADDER

A. E. Mitchell

IBM Technical Disclosure Bulletin, Vol. 5, No. 6, November 1962. P. 26, 27.

IX - 8 PURE FLUID DIGITAL LOGIC WITH A SINGLE SWITCHING ELEMENT

Peter Bauer

Diamond Ordnance Fuze Lab., Washington D. C. Proc. of the Fluid Amplification Symp., Vol. 1, Oct 2-4, 1962. Dated Nov 15, 1962. P. 405-414. 2 refs. (N63-13405)

The principles of conventional electronic logic design (such as "NOR" logic) were employed as the basis for the development of one universal digital element to serve a multitude of logic functions, singly and in combinations. Definite and conclusive evidence was desired to prove the objective not only feasible but practical as well. The selection of the kind of element used in this study is discussed, and preliminary specifications are given. The design and operation of the fluid element selected are described, and pertinent performance characteristics are presented. The principles on which circuit and circuit assembly design were based are discussed, and examples of the main logic functions performed by this element, when used in digital circuits, are given. Circuits which were tested are described together with element interconnection characteristics obtained. Some results of in-circuit measurements, steady state as well as transient, are given. Conclusions are drawn from characteristics. The breadboard circuit assembly developed during this program, performing the principal logic operations including amplification, inversion, "OR", "NOR" and "AND" gating, is described. Fabrication techniques used and later advances made are mentioned. The feasibility as well as practicability, of employing one fluid element to provide most of the basic logic functions needed in digital systems is demonstrated, and the direction of future development is indicated. (A)

IX - 9 DELAY LINE MEMORY

H. B. Horton

U. S. Patent No. 3,075, 548; January 29, 1963.

This invention relates to information storage devices of the type commonly referred to as delay line memories.

The object is to provide a fluid delay line memory wherein the read, write and recirculate functions are all performed in response to fluid control signals.

IX - 10 CALCULATING WITH JETS

Dr. A. E. Mitchell

New Scientist, Vol. 17, No. 329, March 7, 1963.

IX - 11 FLUID AMPLIFICATION. 9. LOGIC ELEMENTS

E. V. Hobbs

Harry Diamond Labs., Washington, D. C. TR-1114, 8 March 1963. 4 p. 2 refs. (N63 - 14779) (AD-401 321)

Descriptions are given of the operation of various fluid logic elements--singly and in combination. (A)

IX - 12 FLUID LOGIC SHIFT REGISTER WITH INTERMEDIATE STAGES

H. R. Grubb

IBM Technical Disclosure Bulletin, Vol. 6, No. 1, June 1963. P. 24, 25.

In this disclosure, a shift register is described which uses bistable fluid logic devices as intermediate and mainstage latches, thus requiring two successive fluid shift pulses to shift information from one mainstage to the next mainstage.

IX - 13 FLUID LOGIC PARITY CHECKING

H. R. Grubb

IBM Technical Disclosure Bulletin, Vol. 6, No. 1, June 1963. P. 27, 28

A device is disclosed which employs a plurality of interconnected momentum-type jet fluid elements. In each element, a power stream is deflected into either

a left or right output when either a right or left control signal is present, respectively. The concurrent presence of the control signals gives a signal at the third (center) output. The checking of a six-bit code for the presence of an odd number of bits is demonstrated.

IX - 14 FLUID BINARY FULL-ADDER

H. R. Grubb

IBM Technical Disclosure Bulletin, Vol. 6, No. 1, June 1963. P. 29, 30.

Two full-adders are described, both operating on fluid jet momentum interchange principles. The first uses two interconnected half-adders having three outputs each, corresponding to "no-sum-no-carry", "sum", and "carry" outputs signals. The power stream is control biased to the "no-sum-no-carry" position. Either or the combination of the two control signals (double-input control) produces a "sum" or "carry" output signal, respectively.

The second device operates quite similarly except that four outputs, corresponding to "no-sum-no-carry", "sum-no-carry", "carry-no-sum", and "carry & sum", are used. The control is of the triple-input variety. The control biased power stream is deflected in proportion to the number of control signals simultaneously present.

IX - 15 FLUID BINARY FULL-ADDER

H. H. Glättli

IBM Technical Disclosure Bulletin, Vol. 6, No. 2, July 1963. P. 29.

The full-adder of this disclosure utilizes two fluid amplifiers (active elements) and two passive elements (AND and OR gates). The amplifiers each have three outputs and single-input controls. The stable position of the power jet (center output) requires equal control signals on the opposite sides of the power jet.

IX - 16 FLUID BINARY COUNTER

A. E. Mitchell

IBM Technical Disclosure Bulletin, Vol. 6, No. 2, July 1963, P. 30.

IX - 17 FLUID MATRIX

A. E. Mitchell

IBM Technical Disclosure Bulletin, Vol 6, No. 2, July 1963, P31.

Each cell of the matrix contains a passive element connected to an active element. One of the two inputs to the passive unit represents a column signal while the other represents a row signal. The simultaneous presence of the signals gives an output signal which indicates coincidence. Selecting either input signal singularly produces an output which is a control signal for the connected active element. The output signal thus effected in the active element is the input signal for the passive element of the next following cell, the input being column or row depending upon the input of the previous cell, respectively. Through this mechanism, a signal is transferred along a particular row and column of the matrix until coincidence occurs, thus indicating the selected cell.

IX - 18 FLUID COUNTER

D. J. Truslove

IBM Technical Disclosure Bulletin, Vol, 6, No. 3, August 1963. P. 24, 25.

In this device, globules of a high-surface-tension liquid are indexed around a closed path. The path is defined by a plurality of pairs of cavaties interconnected by restricted passages of a material which does not wet. The combination of a steady fluid bias stream and a counting fluid pressure pulse displaces the globule rightward in the right cavity or, using a different set of ducts, leftward in the left cavity. By a particular arrangement of ducts with respect to these cavities, both addition and subtraction are claimed for this disclosure.

IX - 19 FLUID DECIMAL COUNTER

D. J. Truslove

IBM Technical Disclosure Bulletin, Vol. 6, No. 3, August 1963. p. 26, 27.

IX - 20 HYDRAULIC MEMORY DEVICE

D. J. Truslove

IBM Technical Disclosure Bulletin, Vol. 6, No. 3, August 1963. p. 32, 33.

IX - 21 FLUID MEMORY DEVICE

D. J. Truslove

IBM Technical Disclosure Bulletin, Vol. 6, No. 3, August 1963. p. 80

IX - 22 BINARY LOGIC DEVICE

A. E. Mitchell

IBM Technical Disclosure Bulletin, Vol. 6, No. 4, Sep 1963. p. 91, 92.

IX - 23 BINARY FULL-ADDER

A. E. Mitchell

IBM Technical Disclosure Bulletin, Vol. 6, No. 4, Sep 1963. p. 93, 94.

This disclosure concerns fluid logic elements for performing the binary full-adder function. One of the two elements composing the device generates the "carry" and the "non-carry" functions, while the other generates the sum function. The elements are engraved on plates which can be stacked.

IX - 24 BINARY INFORMATION TRANSFERRING DEVICE

H. R. Müller

IBM Technical Disclosure Bulletin, Vol. 6, No. 4, September 1963. P. 89, 90.

The device is described as consisting of a main and an auxiliary cell, both engraved on a single plate. Each cell contains one bistable element and two monostable elements. Multi-stage systems are obtained by stacking several plates.

A decoupling of the main cell from the auxiliary cell during data transfer is cited as an advantageous separation of function between storage cell and transfer cell.

IX - 25 MODULAR PNEUMATIC LOGIC PACKAGE

R. F. Langley and P. B. Schulz

IBM Technical Disclosure Bulletin, Vol. 6. No. 5, October 1963. P. 3

IX - 26 FLUID LOGIC SUCTION CONTROL

A. E. Mitchell

IBM Technical Disclosure Bulletin, Vol. 6, No. 5, October 1963. P. 16.

IX - 27 TWO JET LOGIC USING WALLS

A. E. Mitchell

IBM Technical Disclosure Bulletin, Vol. 6, No. 5, October 1963. P. 17.

IX - 28 FLUID-OPERATED TIMER

R. W. Warren

U. S. Patent No. 3,093,306; October 22, 1963.

This invention relates to a fluid-operated timer which is capable of indicating predetermined time intervals. The fluid-operated timer of this invention incorporates the combination of a fluid-operated oscillator, a fluid-operated binary counter and a fluid-operated AND component. The fluid oscillator, counter and AND component require no moving parts other than the working fluid employed therein for their operation.

IX - 29 FLUID LOGIC COMPONENTS

R. W. Warren, Billy M. Horton

U. S. Patent No. 3,107,850; 22 Oct 1963

This invention is concerned with the AND-NOT, OR, and OR-NOR functions of fluid logic elements. One object of this invention is to provide, in combination, a fluid amplifier for amplifying a plurality of fluid signals supplied thereto and a fluid directing means for preventing a certain type of signal from issuing from the amplifier when there is an absence of the required number of fluid input signals.

IX - 30 FLUID COMPUTERS

O. Lew Wood and H. L. Fox

International Science and Technology, Nov. 1963.
p. 44-52.

A review of the early pure fluid device inventions is presented. Various configurations for "NOR," "AND" and "OR" gates are discussed and comparisons made with the equivalent electronic devices. A "universal" register circuit is also described. The effects of environment, and the problems of transients, speed of operation, and precision measuring equipment are presented as well as some predictions for the future of fluid computers.

IX - 31 FLUID DEVICES FOR COMPUTERS

H. H. Glättli

U. S. Patent No. 3,114,390; 17 Dec 1963

The inventor states that normally in the field of fluid operated computer devices, one would require three fluid controlling eells per stage of a series connected arrangement to allow information to proceed controllably from one stage to the other. This invention provides an arrangement of a plurality of fluid operated cells that requires only two cells per stage for shifting information in a given direction; and such arrangement requires only a single source of fluid that is pulsed for each stage.

SECTION X —— CONTROL SYSTEMS AND CIRCUITS

X - 1 JET PROPULSION UNITS

M. Kadosch, F. G. Paris, J. LeFoll and J. Bertin

U.S. Patent No. 2,825,204; 4 March 1958.

The interaction of auxiliary gas jets with a main propulsive jet is embodied in some of the systems described. One control configuration uses a pod-shaped device, located at the centerline of an axisymmetric main jet, from which a radially directed flow deflects the main jet toward the boundary walls of a diverging duct.

X - 2 PNEUMATIC PULSE TRANSMISSION WITH BISTABLE-JET RELAY RECEPTION AND AMPLIFICATION

F. T. Brown

MIT, Dept. of Mechanical Engineering. Thesis, Sc. D., May 1962.

A system is developed in which the command position of an output shaft is encoded into a pulse-position-modulated signal, converted to pneumatic pulses, transmitted along a line, received, amplified and integrated by a two-stage bistable jet relay without moving parts, and demodulated by the push-pull piston-cylinder load, which assumes the commanded position. Modulation periods are of the order of five milliseconds.

Theory is developed for the dispersion of transients in fluid lines. The propagation operator and characteristic impedance are derived, including the frequency-dependent effects of wall shear and heat transfer, from which impulse and step responses are calculated. Generalized plots allow the rapid solution of most problems of transients in liquid and air-filled lines. The step responses of tapered lines are determined approximately.

A combined theoretical and experimental approach to the development of fluid-jet modulators is proposed. The technique, founded on experiments of a jet attaching to an adjacent parallel wall with flow injected into the separated region, involves elaborations, performed graphically, of the source-load matching concept. Examples illustrated include continuous amplifiers, bistable relays, and oscillators, the operation of which is predicted from a separate determination of the characteristics of the jet "load" and control-line "source". Single and double control ports are considered. Proper static and surge impedance matching are emphasized. Some data is presented.

The two-stage pulse receiver operates in both continuous and bistable modes, depending on the jet-supply pressures. Power gains are as high as 60,000 in the bistable mode and 2,000 in the continuous mode. Although desired linearity can offer a limitation to the available gains of jet amplifiers, the fundamental limitation results from the relatively low-frequency noise inherent in nearly all fluid jets. (A)

X - 3 PNEUMATIC KEYBOARD

W. G. Wadey

U. S. Patent No. 3,034,628; May 15, 1962

The object of this invention is to provide a pure fluid system for inserting information into a fluid data processing device.

X - 4 HOW STREAMS OF WATER CAN BE USED TO CREATE ANALOGUES OF ELECTRONIC TUBES AND CIRCUITS

C. L. Strong

Scientific American, Vol. 207, NO. 2, August 1962
P. 128-138.

Article describes the work of Murray O. Meetze, a high-school student (then) in Heath Springs, S. C. Meetze designed and built a working model of the triode vacuum tube in which nothing moved except a fluid representing the electric current. He later constructed a fluid diode, a

fluid oscillator and a variety of hydraulic "circuits", including one that has no electronic counterpart.

X - 5 A FLUID-AMPLIFIER ARTIFICIAL HEART PUMP

Timothy G. Barila, Daniel E. Nunn, Kenneth E. Woodward, George Mon, and Henrik H. Straub

Diamond Ordnance Fuze Labs., Washington, D. C. Proc. of the Fluid Amplification Symp., Vol. 1, Oct 2-4, 1962. Dated Nov. 15, 1962 p 81-93 2 refs. (N63-13388)

Fluid amplification, a recent invention concerned with the control of flowing fluids without moving parts, has been applied to the powering and control of an extracorporeal heart pump. Except for an artificial ventricle, two artificial heart valves and a flapper to control suction, the fluid amplifier pump has neither moving control parts nor electronics. The output is pulsatile, and its average rate of flow varies directly with filling pressure and inversely with vascular and other resistances, to achieve flow regulation. High reliability, long life, and low cost are achieved. Early evaluation tests suggest its performance capabilities and hemolytic characteristcs are at least equal to those of the better available heart pumps. (A)

X - 6 A SUGGESTED SYSTEM OF SCHEMATIC SYMBOLS FOR FLUID AMPLIFIER CIRCUITRY

W. A. Boothe and J. N. Shinn

Diamond Ordnance Fuze Labs., Washington, D. C. Proc. of the Fluid Amplification Symp., Vol. 1, Oct. 2-4, 1962. Dated Nov. 15, 1962. p. 437-447. (N63-13407)

This paper proposes a system of shorthand symbols that effectively differentiates between analog and digital devices, beam deflector and vortex amplifiers and passive versus active types of valves. A means of designating the memory and no-memory digital amplifier is also provided. On this simple base it is possible to build symbols representing the more sophisticated logic and control components. Examples given include an operational amplifier, simple flip-flop, counter, half-adder (or exclusive OR), AND, OR, and NOT elements. Representation is also suggested for the commonly used circuit elements such as resistance, capacitance, and inductance. Some of the common pitfalls of electrical anal-

ogies to these elements are outlined. Examples of schematic circuits using these suggested symbols are also presented. (A)

X - 7 A THREE STAGE DIGITAL AMPLIFIER

Carl J. Campagnuolo

Proc. of the Fluid Amplification Symp., Vol. 1, Oct. 2-4, 1962. Dated Nov. 15, 1962. p. 47-72. (N63-13386)

This paper describes digital pneumatic elements, cascaded so as to obtain a high power output which can be controlled by means of a stream containing 10^{-3} of the output flow. A system consisting of three units in a cascade is discussed. (A)

X - 8 A TECHNIQUE FOR MATCHING PURE FLUID COMPONENTS APPLIED TO THE DESIGN OF A SHIFT REGISTER

Edwin M. Dexter

Diamond Ordnance Fuze Lab., Washington, D. C. Proc. of the Fluid Amplification Symp., Vol. 1, Oct. 2-4, 1962. Dated Nov. 15, 1962. p. 449-453. (N63-13408)

An approximate method is described which has proven useful in evaluating the matching possibilities of units, quality control, and circuit testing of a pure fluid circuit. The basis for this technique is in approximating the steady-state control input admittance of elements with an equivalent orifice which performs in the manner of the hydraulics square law, $Q = KP^{\frac{1}{2}}$. It is shown that the admittance characteristics, Q^2/P, can be used to select elements to perform a desired function as well as to establish the expected performance of elements in a circuit during trouble-shooting. Tests for quality control purposes can also be made effectively with this method to check performance at specific operating conditions.

X - 9 ROCKET THRUST VECTORING

Allen B. Holmes

Diamond Ordnance Fuze Labs., Washington, D. C. Proc. of the

Fluid Amplification Symposium, Vol. 1, Oct 2-4, 1962. Dated Nov 15, 1962. P. 73-80. (N63-13387)

An experimental program is being conducted at DOFL to investigate the characteristics of a supersonic fluid amplifier discharging air at high Mach numbers into the expansion cone of a rocket nozzle for thrust vector control. Preliminary static firings of a cold gas Mach 3.2 nozzle with fluid amplifier controls were made. Direct measurements were made of the amplifier input flow, induced lateral thrust, and switching levels. (A)

X - 10 PROPORTIONAL POWER STAGES FOR IMPEDANCE MATCHING PURE FLUID DEVICES

Thomas J. Lechner and Martin W. Wambsganss

Diamond Ordnance Fuze Labs., Washington, D. C.. Proc. of the Fluid Amplification Symp., Vol. 1, Oct 2-4, 1962. Dated Nov 15, 1962. P. 381-404. (N63-13404)

A study is made of the proportional power stages for impedance-matching pure-fluid amplifiers of the three-dimensional type (single output). This type amplifier is based on the interaction of two streams: a supply (or power) stream and a signal (or control) stream. The principle of operation of such a pure fluid amplifier is a transfer of momentum at the point of intersection of the two streams. The paper concludes that the equations presented, representing the flow ratios, are only approximate, but the results give direction and insight as to the compatibility of pure fluid devices. Even though restrictions were placed on the geometric parameters, these restrictions do not contradict the physically realizable range.

X - 11 FLUID AMPLIFIER DEMONSTRATION VEHICLE

R. R. Palmisano

Diamond Ordnance Fuze Labs., Proc. of the Fluid Amplification Symp., Vol. 1, Oct 2-4, 1962. Dated Nov 15, 1962. P. 27-36. (N63-13383)

A jet-propelled vehicle has been built which demonstrates the practicability of fluid amplification for

thrust vectoring. An account is also given of a 5-stage proportional fluid amplifier which is capable of amplifying control signals over 100,000 times. (A)

X - 12 PULSE DURATION MODULATION

R. W. Warren

Diamond Ordnance Fuze Labs., Washington D. C. Proc. of the Fluid Amplification Symp., Vol 1, Oct 2-4, 1962. Dated Nov 15, 1962. P. 41-45. (N63-13385)

An all-fluid pulse-duration modulation system, which accepts fluid signals proportional to missile error, is described. The system consists of a feedback-type oscillator driving a buffer amplifier which, in turn, drives the output bistable amplifier. All of the output of the bistable amplifier issues out of one output at a time, either the left or the right, and can be used as a reaction jet for purposes of control. If the error of the missile is sensed with a gyro, an air jet from the gyro can be divided between two adjacent orifices when the missile is on course, and as it deviates from the true course the flow will be more to one orifice than to the other. This variation can be fed into the left and right control inputs of the pulse duration modulation system. The control inputs are connected to the capacitors on the bistable amplifier. As the control signal on one side increases, the control signal on the other side will decrease.

X - 13 PROGRAM CONTROL DEVICES FOR FLUID APPARATUS

W. G. Wadey

U. S. Patent No. 3,076,473; February 5, 1963.

This invention relates to means for controlling and varying the internal operations of a fluid apparatus by changing fluid circuits external of the main body of the apparatus to be controlled. More particularly, the present invention provides program control devices for fluid apparatus. Quick and easy interchangeability is claimed.

X - 14 RESEARCH AND DEVELOPMENT OF PNEUMATIC JET RELAY SYSTEMS FOR PROPULSION SYSTEM CONTROL

W. B. Bails, F. T. Brown, K. N. Reid and R. J. Gurski

MIT, Dept. of Mechanical Engineering. Report No. DSR-9159-1, March 31, 1963

X - 15 A SURVEY OF FLUID DEVICES FOR AUTOMATIC CONTROL SYSTEMS

H. L. Fox and O. L. Wood

I. E. E. E. Technical Conference, 6th Region. Paper presented April 26, 1963. (Sperry Utah Co.)

X - 16 PURE FLUID CONTROL DEVICES AND THE DESIGN OF PRINTED PNEUMATIC CIRCUITS

Joint Publications Research Service, Washington D. C. JPRS-21085, 13 Sep 63. 18 p. 9 refs. (Translated from Avtomat. i Telemekh., Vol. 24, No. 8, Aug 1963. P. 1155-1162. Moscow) (OTS-63-31761) (N63-22100)

X- 17 FLUID AMPLIFICATION. 7. A THREE-STAGE DIGITAL AMPLIFIER

Carl J. Campagnuolo

Harry Diamond Labs., Washington D. C. TR-1106, Aug 1, 1963. 33 p. 12 refs. (N63-22095)

The design and performance of a three-stage digital amplifier system obtaining a high power output and flow gain are described. The design of the system was arrived at by taking measurements of single elements and matching the units with respect to input, output, and feedback performance. Flow gain in the system was obtained by increasing the nozzle widths by a factor of ten from stage to stage. Effects of loading on the stability of intermediate units were controlled by positioning the splitters further downstream than would be required for maximum efficiency. The system was operated with a common power-jet supply pressure of 1 to 15 psig. The system

was switched with flow at atmospheric pressure. The third-stage output was exhausted to atmosphere through a 12-deg diffuser. Flow gains up to 3000, pressure recovery of 50 to 67 percent, and power gains up to about 10,000 were obtained. (A)

X - 18 SYSTEM AND COMPONENT CONSIDERATIONS FOR AN ALL PNEUMATIC MISSILE ATTITUDE CONTROL SYSTEM

William A. Griffith and Joe L. Byrd

American Institute of Aeronautics and Astronautics, Guidance and Control Conference, Cambridge, Mass., August 12-14, 1963. Paper 63-330. 22 p. (A63-21593)

X- 19 FLUID AMPLIFICATION. 11. STAGING OF PROPORTIONAL AND BISTABLE FLUID AMPLIFIERS

Silas Katz and Robert J. Dockery

Harry Diamond Laboratories, Washington D. C. TR-1165, 30 August 1963. 59 p.

The generalized performance characteristics are examined in detail for both proportional and bistable (digital) fluid amplifiers with no moving parts. An approach leading to the solution of fluid systems design problems is given. Equations describing the pressure and flow variations are developed. Typical performance curves are drawn showing performance trends with several variables manipulated. Experimental curves are presented confirming the theoretical approach. A typical proportional unit, with principle dimensions, is shown with its characteristic curves. (A)

X - 20 A PNEUMATIC PURE FLUID SPEED CONTROL FOR A 500 KW STEAM TURBINE GENERATOR

J. R. Colston

Bowles Engineering Corp. Report dated September 1963. (Contract No. NR-4033-00) (Also, Bowles Engineering Corp., R-1-31-64)

A feasibility model of a pneumatic pure fluid speed control was designed and constructed for a 500 KW steam turbine generator. Its performance was demonstrated in a laboratory bench test on a scaled system. The unit met the specification for 1/2% speed control for a 10% load change. This report covers the selection of a suitable system, a description of the performance of each component, and a summary of the test results. (A)

X - 21 ANALOG FLUID STATE DEVICES AND THEIR APPLICATION IN CONTROL SYSTEMS

M. B. Zisfein

Giannini Controls Corp. Report No. ARD-06-010. (Presented at SAE Committee A-6, Symposium On Fluid Amplifiers, Kansas City, Missouri, Oct 3, 1963.)

X - 22 FLUID SERVO SYSTEM

Billy M. Horton

U. S. Patent No. 3,111,291; 19 November 1963

It is the object of this invention to provide a fluid-operated system, having no moving parts, which performs functions analogous to functions performed by existing electronic systems, such as a speed control for a vehicle as in this disclosure.

X - 23 MULTI-FREQUENCY FLUID OSCILLATOR

Edwin U. Sowers, III

U. S. Patent 3,117,593; 14 January 1964.

This invention relates to a pure fluid oscillator, and more particularly, to one having a plurality of stable non-simultaneous output frequencies. Any one of these frequencies may be selectively provided, depending upon which one of a plurality of feedback passageways is selected by control means.

X - 24 FLUID OPERATED SYSTEM

B. M. Horton

U. S. Patent 3,122,165; 25 Feb 1964.

The present invention relates to continuously variable pure fluid amplifiers, that is, those devices or systems for which the output signal is related by a proportionality factor to the input signal and boundary layer effects are not dominate. The application of these amplifiers to several systems is described. Specifically, the objectives of the invention are to provide:

(1) A fluid amplifier having no end wall losses, by virtue of utilization of toroidal or cylindrical geometry in stream forming, controlling and collecting components of the amplifier.

(2) A novel acoustic amplifier having no moving parts.

(3) A speed control device for a moving vehicle employing a fluid amplifier having no moving parts as a control element.

(4) A system for correcting the attitude of an aircraft in response to attitude sensors, by means of a pure fluid servo system.

In addition to a detailed discussion of the above cited applications, the patent gives an extensive description of the operating principles of various types of fluid amplifiers, including a categorization according to these operating principles.

SECTION XI INSTRUMENTATION

XI - 1 FLUID AMPLIFICATION. 2. FLOW VISUALIZATION-COMPRESSIBLE FLUIDS

Jorma R. Keto

Diamond Ordnance Fuze Labs., Wash., D.C. TR-1041, 20 Aug 1962. 45 p. (AD-286 666) (N62-17221)

A study has been made of the methods generally used in flow visualization and their applications to pure fluid systems. Comparison details of the shadowgraph, schlieren, and interferometer techniques are reported; also, a generalized equation is derived for the schlieren method, relating light intensity to gas density for two-dimensional flow. Construction details are presented on two schlieren-type systems, together with illustrated results of typical images obtained. Improved visualization techniques were realized, using helium, volatile liquids, and condensible vapor. In addition, a technique was developed for sealing interchangeable pure fluid elements to optical windows permitting repeated use without replacing the sealing materials or cleaning windows. (A)

XI - 2 INSTRUMENTATION FOR RESEARCH AND DEVELOPMENT IN PURE FLUID SYSTEMS

Ronald L. Humphrey, Eric E. Metzger

Diamond Ordnance Fuze Labs., Wash., D.C. Proc. of the Fluid Amplification Symp., Vol. I, Oct. 2-4, 1962. Dated Nov. 15, 1962. p. 169-177. (N63-13394)

Some instruments used for flow and pressure measurements in pure fluid systems are: (1) a thermistor anemometer, which is a visual indicator for quickly checking a large number of flow passageways; (2) a hot wire anemometer, which is an indicator used in conjunction with an

oscilloscope for displaying pneumatic waveforms; (3) a miniducer, which is a miniature piezoelectric pressure sensor for use in small channels; and (4) a fiber optics monitor, which is a system consisting of four channels containing light guides, photomultipliers, and amplifiers. This monitor combines high response with small sensors for the study of transients of density in the air flowing through pure fluid elements or systems and is used cooperatively with shadowgraph, schlieren, or interferometer systems.

XI - 3 FLOW VISUALIZATION

Jorma R. Keto

Diamond Ordnance Fuze Labs., Wash., D.C. Proc. of the Fluid Amplification Symp., Vol. I, Oct. 2-4, 1962. Dated Nov. 15, 1962. p. 109-123. 4 refs. (N63-13390)

Construction details are presented for two schlieren systems which have been used at DOFL, together with illustrated results of typical image studies. A method of sealing interchangeable pure-fluid elements to optical windows, permitting repeated use without renewal of materials or contamination of windows, is given. Techniques for aiding visualization in difficult situations are discussed. Motion pictures are presented to illustrate the various schlieren techniques and the use of high-speed photography in the visualization of transient phenomena. (A)

XI - 4 FLOW VISUALIZATION AND EXPERIMENTAL STUDIES OF A PROPORTIONAL FLUID AMPLIFIER

R. J. Reilly, J. A. Kallevig

Diamond Ordnance Fuze Labs., Wash., D.C. Proc. of the Fluid Amplification Symp., Vol. I, Oct. 2-4, 1962. Dated Nov. 15, 1962. p. 125-142. 3 refs. (N63-13391)

Experimental data taken on a particular type of closed, proportional fluid amplifier did not agree with analysis based on two mathematical models. Visualization studies and detailed measurements in the interaction region of 3 fluid jets show that the power stream is

accelerated after leaving the power nozzle. This fact is not predicted by either mathematical model. (A)

SECTION XII —— SIMULATION AND MATHEMATICAL TECHNIQUES

XII - 1 THE HYDRAULIC ANALOGY

Ralph Barclay

Diamond Ordnance Fuze Labs., Washington, D. C. Proceedings of Fluid Amplification Symposium, Vol. 1, 2-4 Oct 1962. Dated 15 Nov 1962. p. 37-40. (N 63-13384)

The basic phenomena of fluid amplifiers, as found in compressible flow, were investigated by using techniques of the hydraulic analogy, which is the analogy existing between two-dimensional compressible-gas flow and open-channel liquid flow. This technique provides a means of flow visualization. Complex flows can be observed through the use of models which are very easily made and changed. In this way the effect of various shapes can be quickly ascertained in a qualitative manner. Visualization is aided by the fact that the speed of flow in the liquid is approximately a thousand times slower than the corresponding flow in the compressible gas; thus, transient flow conditions can be observed by the naked eye. Results indicate that the ratio of the specific heats for the "analog gas" was 2. These results were based on inviscid flow conditions for both gas and liquid, with only negligible vertical accelerations allowed in the liquid.

XII - 2 PNEUMATIC LINEAR CIRCUITS

Beatrice A. Hicks and Evelyn S. Jetter

Diamond Ordnance Fuze Labs., Washington, D. C. Proc. of the Fluid Amplification Symp., Vol, 1, Oct 2-4, 1962. Dated Nov. 15, 1962. P. 301-318. 2 refs. (N63 - 13400)

Demonstrable analogies between pneumatic, electrical, and mechanical systems are applied to the same kinds of circuit theory so as to be able to predict the behaviour of a given pneumatic system and to design for desired performance characteristics. The flow rate of gases in pneumatic circuits

corresponds to current in electrical circuits or velocity in mechanical analysis. In a pneumatic circuit that is in temperature equilibrium, flow rate is the number of cubic inches of gas passing a given point in one second when that gas is measured at unit pressure. Flow rate may vary with time and be an alternating flow just as current or velocity. The authors state the point of view that the extension of the analysis to a pneumatic system including inductance will obviously result in more complex equations because it is necessary to consider the difference in pressure through the inductance as well as through the resistance of the orifice.

XII - 3 FLUID AMPLIFICATION. 10. USE OF THE HYDRAULIC ANALOGY IN THE STUDY OF FLUID-INTERACTION DEVICES.

Ralph G. Barclay, Allen A. Bowers, and John G. Moorhead

Harry Diamond Labs., Washington D. C. TR-1098, 15 April 1963. 48 p. 1 ref. (N63 - 16549) (AD - 405 867)

The advantages of using the hydraulic analogy to study compressible gas flow in fluid-interaction devices are discussed. The mathematical basis of the analogy is summarized, and limitations in its use are pointed out. Various practical aspects concerning operation of an analogy facility are reviewed.

Four hydraulic-analogy studies are briefly described: (1) subsonic diffuser performance, (2) three-stage closed-system bistable fluid-flow amplifier performance, (3) quantitative measurement of switching flow required by a bistable fluid amplifier, and (4) blocked-output-channel and stream-attachment characteristics in fixed and adjustable models of bistable elements. Abstracts of seventeen references regarding the theory and application of the hydraulic analogy are given. (A)

SECTION XIII-FABRICATION

XIII - 1 "OPTIFORM", OPTICAL MACHINING OF PURE FLUID SYSTEMS IN PLASTICS

Romald E. Bowles and John R. Colston

Diamond Ordnance Fuze Labs., Wash., D.C. Proc. of the Fluid Amplification Symp., Vol. I, Oct. 2-4, 1962. Dated Nov. 15, 1962. p. 157-168. 1 ref. (N63-13393)

Optiform is a low-cost, fast, production technique for machining constant-depth pure fluid systems in plastic. The optical machining is accomplished by using a master silhouette to define the areas of a conditioned sheet of plastic which are exposed to ultraviolet light and consequently polymerized. The unexposed areas remain soft and are washed away with a sodium hydroxide solution. From the standpoint of pure fluid systems, Optiform has limitations as to maximum temperature (150°F) and minimum size components which can be processed as a production-line product, i.e., with limited inspection. The basic circuit plate is assembled with a transfer plate and a manifold plate to provide a rugged package having a thick aluminum surface front and rear, and can be further protected by addition of an aluminum channel (like a picture frame) to protect the edges of the assembly where the plastic edge is exposed. Standard Clippard fittings tapped into the aluminum base plates provide an easy means for connecting the system inputs and outputs to auxiliary equipment. With Optiform and a file of silhouettes of components of known performance characteristics, one can assemble a pure fluid control system at the drawing board with high probability that the first of the resulting low-cost, short-lead-time production models will function properly. (A)

XIII - 2 PRODUCTION OF FLUID AMPLIFIERS BY OPTICAL FABRICATION TECHNIQUES

R. W. Van Tilburg

Diamond Ordnance Fuze Labs., Wash., D.C. Proc. of the Fluid Amplification Symp., Vol. I, Oct. 2-4, 1962. Dated Nov. 15, 1962. p. 143-156. (N63-13392)

A presentation is made of the results of a study of the applicability of optical fabrication techniques to the production of fluid amplifiers. Advantages and limitations of Fotoform materials as they are related to the fabrication of fluid systems are discussed, along with data relating process variables and performance. Results indicate that it is possible to fabricate the complex fluid amplifier designs rapidly and relatively inexpensively, and this can be done with a material which is dimensionally stable, capable of high-temperature operation, unaffected by nuclear radiation, and impervious to most corrosive liquids and gases. (A)

XIII - 3 FLUID AMPLIFICATION. 8. USE OF EPOXY CASTINGS FOR FLUID AMPLIFIER DESIGN

David S. Marsh, Edward V. Hobbs

Harry Diamond Labs., Wash., D.C. TR-1102, 11 Feb 1963. 14 p. (AD-401 319)

An adjustable master unit has been used to make a series of cast-epoxy fluid amplifiers that incorporate incremental dimensional changes. Subsequent unit testing identifies the best geometry for a given performance requirement. The process provides an inexpensive means of precisely producing the numerous units necessary for empirical design studies. The basic rubber mold and epoxy-casting process is described, as well as the adjustment of the master unit. Some other uses of epoxy castings in the fluid-amplifier field are also described. (A)

XIII - 4 APPLICATION OF OPTICAL TECHNIQUES TO THE FABRICATION AND DEVELOPMENT OF FLUID AMPLIFIERS

R. W. Van Tilburg, W. L. Cochran

Corning Electronic Components, Bradford, Pa. Report Covering Work of 10th-18th Month, Ending 31 Oct 63; Dated Nov. 1963. 63 p. (Under Contract DA-49-186-ORD-1076 with Harry Diamond Labs., USA, AMC)

Results from a program of design, fabrication, and evaluation of pressure proportional fluid amplifiers, gain blocks,,and circuits are presented. Included is a brief discussion of the development of a multi-stage, high amplification, gain block. From this gain block, a rudimentary pneumatic analog scale changer is developed which incorporates feedback and the matching of linear pneumatic resistances.

(A)

XIV — POWER SUPPLIES

XIV - 1 PRELIMINARY STUDY OF POWER SUPPLIES FOR PNEUMATIC SYSTEMS

D. J. Grant, A. Krasnick and S. Katz

Diamond Ordnance Fuze Labs., Washington D. C. TR-847, 30 June 1960. 5 p.

A preliminary study was made of power supplies for pure pneumatic systems. This included: (1) a survey of several representative methods of supplying gas for pneumatic system elements; (2) consideration of the thermodynamic relationships pertinent to their design; and (3) a comparison of representative power supplies on the basis of weight, size, and estimated cost for specific pressure and mass flow requirements. Other factors considered in the study are handling problems, reliability, safety, and container shape. Packaged power supplies, such as gas generators and compressed gas bottles, are recommended for further study.

(A)

SECTION XV —— ENVIRONMENT

(No Citations)

AUTHORS INDEX

A

B

C

D

E

F

G

H

J

K

L

M

N

O

P

R

S